# CORRALES REACH

## CORRALES FLOOD CHANNEL TO MONTANO BRIDGE

# HYDRAULIC MODELING ANALYSIS

# 1962-2001

---

## MIDDLE RIO GRANDE,
## NEW MEXICO
## AUGUST 2003

**PREPARED FOR:**

US BUREAU OF RECLAMATION

ALBUQUERQUE, NEW MEXICO


**PREPARED BY:**

JASON ALBERT

MIKE SIXTA

DR. CLAUDIA LEÓN

DR. PIERRE Y. JULIEN

COLORADO STATE UNIVERSITY

ENGINEERING RESEARCH CENTER

DEPARTMENT OF CIVIL ENGINEERING

FORT COLLINS, COLORADO 80523

## ABSTRACT

The Corrales Reach spans 10.3 miles downstream from the Corrales Flood Channel to the Montano Bridge. This reach is included in the habitat designation for two federally-listed endangered species, the Rio Grande silvery minnow and the southwestern willow flycatcher. Restoration efforts for these species require the understanding of historic, current and potential future geomorphic characteristics of the channel. Analysis of water and suspended sediment data at the USGS gaging stations, aerial photos, cross-section surveys and bed material size, reveal the temporal and spatial changes in the processes acting on the channel.

Geomorphic analyses indicate that the general trends of the Corrales Reach are a decrease in width, width-to-depth ratio, area, water surface slope, energy-grade line slope and wetted perimeter and an increase in mean flow velocity and depth during the 1962 to 2001 time period. Single-thread channels characterized the 1962 and 1972 channel planform. New islands and sediment bars developed after 1972 and are evident in the 1992 and 2001 planform at both low and high flows. Sinuosity has slightly increased throughout the entire period analyzed. However, it is lower than 1.2 for the entire reach. Changes in channel width during the 1962 to 2001 time period were not significant.

The entire reach aggraded approximately 0.1 feet between 1962 and 1972, with sand deposits of $D_{50}$ = 0.20 mm. Subsequently, the bed degraded between 1972 and 1992 by approximately 2.5 feet. From 1992 to 2001 subreach 1 degraded slightly while subreaches 2 and 3 aggraded, with a maximum aggradation of about 2.0 feet. Degradation resulted in a coarsening of the bed material from fine sand to medium sand to coarse gravel sized material of about $D_{10}$ = 0.28 mm and $D_{50}$ = 0.98 mm in 2001. From 1992 to 2001 however, the bed material in the reach became finer. During this time period, the $D_{10}$ value remained the same and the $D_{50}$ value went from 4.4 mm to 0.98 mm. This is indicative of the dates in which the data were collected; the 1992 bed material data was collected in the summer, while the 2001 bed material data was collected in the fall.

The Corrales Reach is close to equilibrium conditions as suggested by the 2001 low rate of change in channel width and the capacity of most of the channel to transport the incoming bed material load. According to the sediment transport and hydraulic geometry equation analyses, subreach 1 is the closest reach to a stable state. Conversely, subreach 3 is the farthest from a

state of equilibrium. Based on hydraulic geometry and empirical channel width analyses, the equilibrium width of the reach might be slightly narrower than the existing 2001 channel width.

A stable channel analysis (SAM®) suggests that the 2001 slope should be increased to attain equilibrium in the channel. This result is not in agreement with the historical trend of degradation observed from 1972 to 2001.

## *TABLE OF CONTENTS*

## *LIST OF FIGURES*

## *LIST OF TABLES*

# 1 INTRODUCTION

The hydrologic and sediment regime of the Middle Rio Grande, New Mexico has been altered in the last century through construction of several dams and channelization. The quantity and quality of habitat for native species, such as the silvery minnow (*Hybognathus amarus*), the southwestern willow flycatcher (*Empidonax traillii extimus*) and the southwestern cottonwood-willow riparian habitat has been significantly reduced.

The Rio Grande silvery minnow occurs in less than 10% of its original range (Bestgen 1996) and reaches its most upstream distribution in the Cochiti Reach (Platania 1999). Remaining populations of this species continue to decline primarily due to the lack of warm, slow-moving, silt-sand substrate pools, dewatering of the river and abundance of non-native and exotic fish species (Platania 1991, Bestgen et. al 1991, Burton 1997, Robinson 1995, Arritt 1996). The silvery minnow became a federally listed endangered species in July 1999, after the US Fish and Wildlife Service (USFWS) designated the Middle Rio Grande, New Mexico from just downstream of Cochiti Dam to the railroad bridge at San Marcial as critical habitat for this species.

In addition, deterioration of riparian bosque habitat has occurred (Taylor et. al 2001). The USFWS listed the southwestern willow flycatcher (*Empidonax traillii extimus*) as an endangered species in February 27, 1995. This species is a small, grayish-green migratory songbird found primarily in riparian habitats characterized by dense growths of willows, arrowweed and other species that provide foraging and nesting habitat (USFWS 2000). The loss of southwestern cottonwood-willow riparian habitat has been the main reason for the decline of the population of the southwestern willow flycatcher (USFWS 2000).

The Corrales Reach (Figure 1-1) in the Middle Rio Grande is included in both critical habitat designations. This reach begins at the Corrales Flood Channel and ends 10.3 miles downstream from the Flood Channel at the Montano Bridge. Corrales Reach is immediately downstream from the Bernalillo Bridge reach (León et. al 2000).

The objective of this work is to analyze historical data and estimate potential conditions of the river channel. Prediction of future equilibrium conditions of the Corrales Reach will facilitate the identification of sites that are more conducive to restoration efforts.

In order to achieve this objective, the following analyses were performed:

- Identification of spatial and temporal trends in channel geometry through the analysis of cross-section survey data.
- Planform classification through analysis of aerial photos and channel geometry data.
- Analysis of temporal trends in water and sediment discharge and sediment concentration using United States Geological Survey (USGS) gaging station data.
- Identification of temporal trends in bed material through the analysis of gradation curves and histograms.
- Evaluation of the equilibrium state of the river through the application of hydraulic geometry methods, empirical width-time relationships and sediment transport analyses.

This work consists of eight sections. The introduction is included in section 1. Description and background of the study site is in section 2. Geomorphic characterization of the reach, including planform classification, sinuosity computations, longitudinal profiles, channel geometry and bed material sediment characterizations are presented in section 3. Section 4 presents the sediment continuity analysis of the reach, including single and double discharge and suspended sediment mass curves. Section 5 contains the predicted equilibrium states of the channel based on sediment transport analyses, hydraulic geometry equations and minimum stream power methods. Section 6 presents the discussion of the results. Summary of the results is included in section 7 and the list of cited references is presented in section 8.

**Figure 1-1: Corrales Reach location map.**

## 2 SITE DESCRIPTION AND BACKGROUND

The Corrales Reach of the Middle Rio Grande spans 10.3 miles from the Corrales Flood Channel (agg/deg 351) to the Montano Bridge (agg/deg line 462) (Figure 1-1). The reach is generally straight with low sinuosity (≈1.2) and an average valley slope of 0.0011. The reach is characterized by a bimodal sediment size distribution, from very fine sand to coarse gravel.

Historically, the Middle Rio Grande was a relatively straight, braided channel (Baird 1996). In addition, the river bed was characterized by an aggradational trend, which might have started about 11,000 to 22,000 years ago (Sanchez et al. 1997). Increasing sedimentation of the river bed began after 1850 due to water shortage and increasing sediment input from tributaries and arroyos (Scurlock 1998). The aggradation of the river bed induced severe flooding, waterlogged lands and failing irrigation facilities (Scurlock 1998).

The Middle Rio Grande Conservancy District was organized in 1925 for the main purpose of improving drainage, irrigation and flood control in the middle valley (Woodson and Martin 1962). A floodway was constructed in the early 1930's to provide flood protection to the adjacent irrigated and urban areas (Woodson 1961). In addition, the Conservancy District built El Vado Dam on the Rio Chama in 1935, four diversion dams along the main stem, two canal headings and many miles of drainage and irrigation canals (Lagasse 1980).

Further aggradation and seepage induced deterioration of the floodway and suggested the need for regulation of floodflows, sediment retention and channel stabilization (Woodson and Martin 1962). A Comprehensive Plan of Improvement for the Rio Grande in New Mexico was recommended by the Corps of Engineers and the Bureau of Reclamation together with other Federal, State and local agencies in 1948 (Pemberton 1964). The plan consisted of constructing a system of reservoirs on the Rio Grande (Cochiti) and its tributaries (Abiquiu, Jemez, Galisteo) as well as the rehabilitation of the floodway constructed by the Rio Grande Conservancy District in 1935 (Woodson and Martin 1962).

Cochiti Dam, built on the Rio Grande, began impounding water and sediment in November 1973 (Lagasse 1980). Cochiti Dam was intended for flood and sediment control, preventing aggradation and inducing degradation of the main stem (Lagasse 1980). Additionally, other dams on the main tributaries (Jemez, Galisteo) and agricultural diversions (Angostura) in the main stem decrease the flow between Cochiti Dam and the Corrales reach.

Figure 2-1 shows a typical spring runoff hydrograph in the Middle Rio Grande. The Otowi stream gage station is located upstream of Cochiti Dam. Attenuation of the spring runoff peak between Otowi and the gages located downstream of the dam is evident in the hydrographs (Figure 2-1). Peak outflows from Cochiti can historically occur as much as 62 days after, or as much as 225 days prior to the peak inflows to the reservoir (Bullard and Lane 1993).

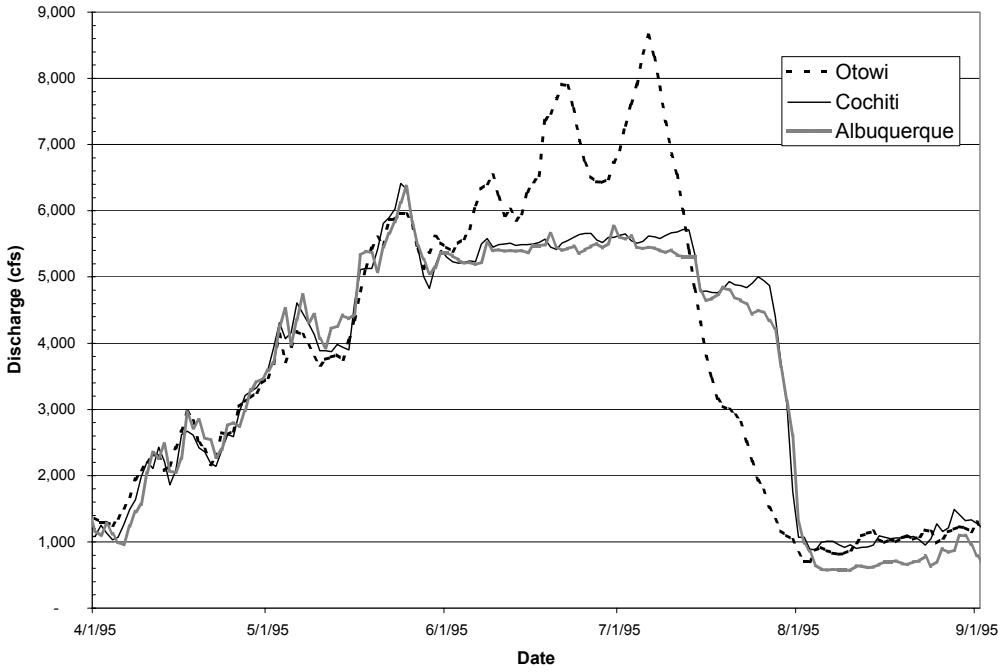


**Figure 2-1: 1995 Rio Grande spring runoff hydrograph.**

Cochiti Dam also traps virtually all (99%) of the sediment entering the reservoir from upstream. Figure 2-2 shows the change in annual suspended sediment yield from upstream of Cochiti Dam to downstream. Tributary input and erosion of the channel bed and banks are the major sources of sediment to the middle Rio Grande downstream from Cochiti Dam. Increase of sediment yield between Cochiti Dam and Albuquerque gaging station is evident in Figure 2-2.

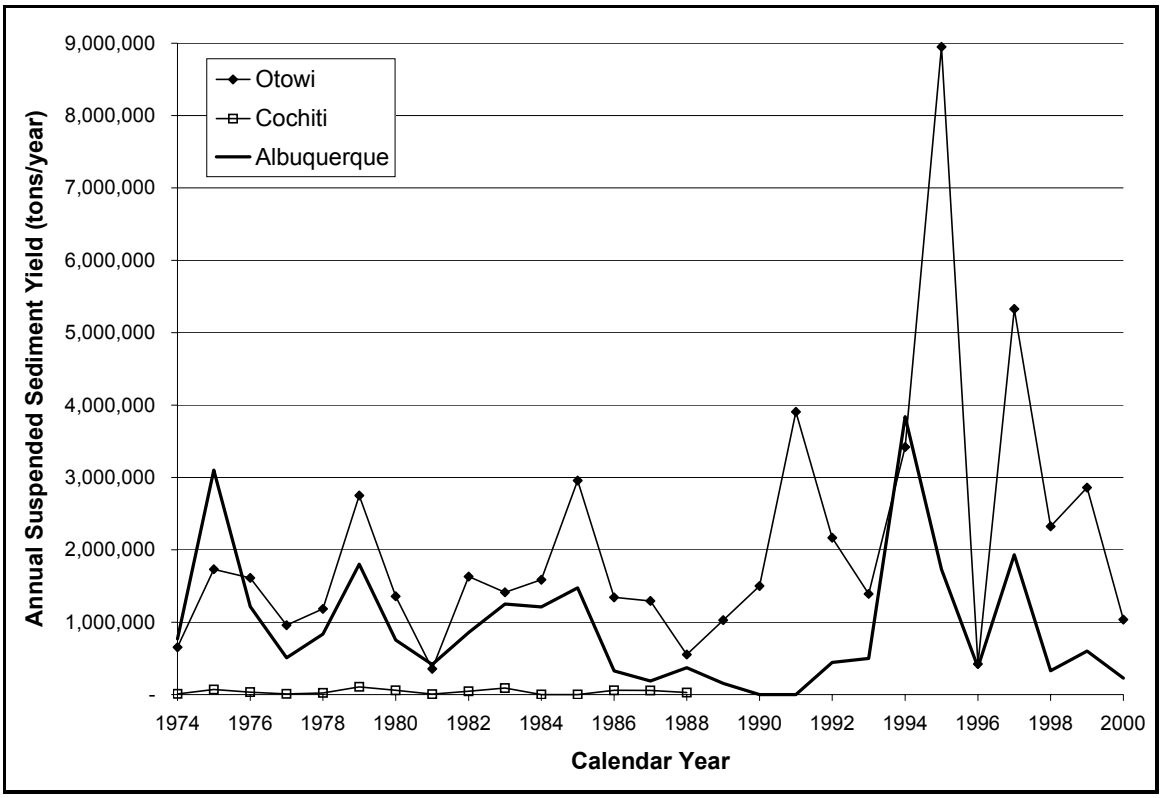


**Figure 2-2: Annual Suspended Sediment Yield in the Rio Grande at Otowi Gage (upstream of Cochiti Dam), Cochiti Gage (just downstream of Cochiti dam) and Albuquerque Gage (downstream of Cochiti Gage) from 1974 to 2000. Cochiti gage record ends in 1988.**

Two ephemeral tributaries, Arroyo de Las Lomitas Negras and Arroyo de Las Calabacillas, join the study reach from the west. The AMAFCA North Diversion Drain, enters the river from the east. The locations of these arroyos and the North Diversion Drain are indicated in the aerial photos in Figures 2-4 and 2-5.

## 2.1 SUBREACH DEFINITION

The Corrales Reach was subdivided into three subreaches to facilitate the characterization of the reach. The entire reach exhibits similar channel characteristics, such as width, planform and profile. Subreach delineation was based largely on water and sediment inputs to the reach from tributaries and diversion channels. The subreach definition is outlined in Table 2-1 and in Figures 2-3 and 2-4 to 2-6. Subreach 1 is 4.1 miles long and spans from cross section CO-33 (Agg/Deg 351) to the AMAFCA North Diversion Drain (Agg/Deg 397). Subreach 2 is 3.0 miles long and spans from the AMAFCA North Diversion Drain to Arroyo de las Calabacillas (Agg/Deg

428), just upstream from Paseo del Norte Bridge. Subreach 3 is 3.2 miles long and extends from the Arroyo de las Calabacillas to Montano Bridge (Agg/deg 462).

**Table 2-1: Corrales Reach subreach definition.**

| | Agg/Deg # | | Length (miles) |
|---|---|---|---|
| | From | To | |
| **Subreach 1** | 351 | 397 | 4.1 |
| **Subreach 2** | 397 | 428 | 3 |
| **Subreach 3** | 428 | 462 | 3.2 |

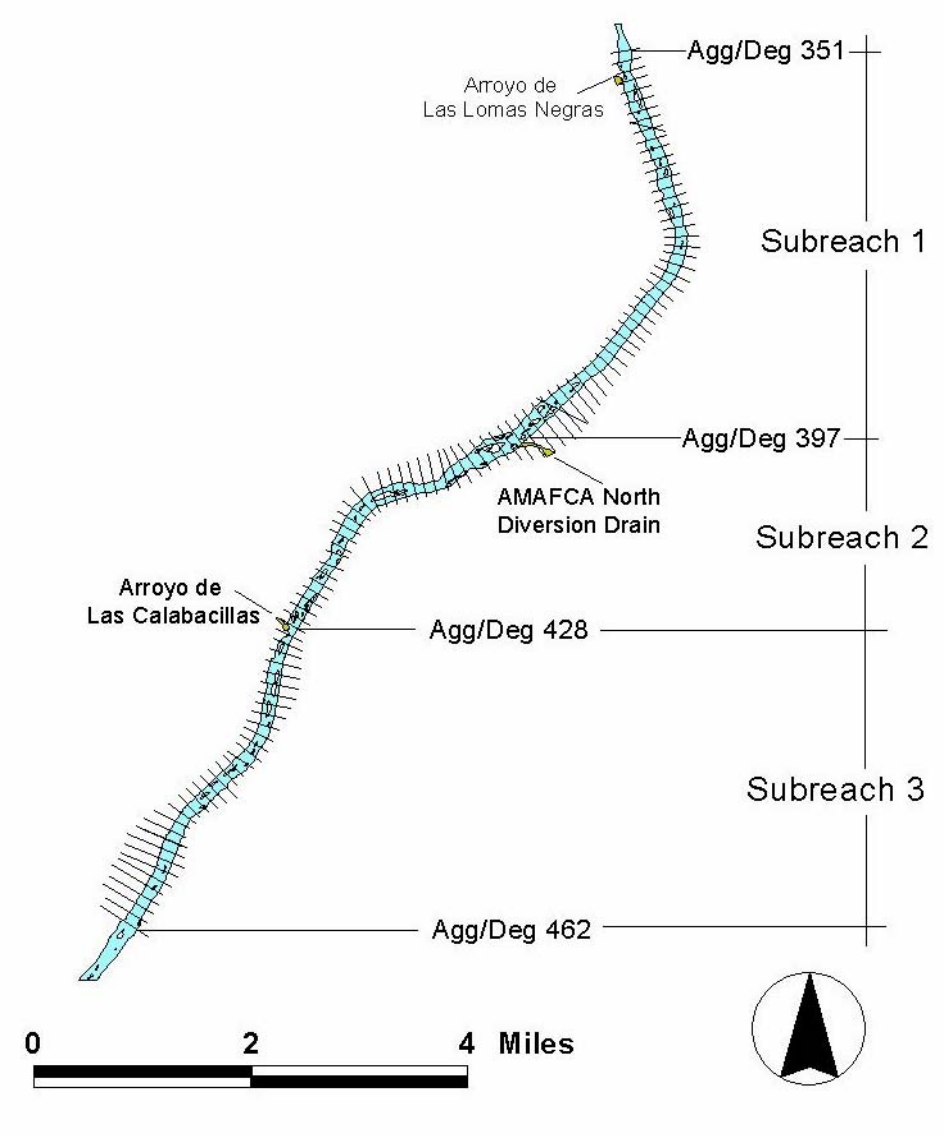


**Figure 2-3: Corrales Reach subreach definitions.**

**Figure 2-4: Aerial photo of subreach 1.**

**Figure 2-5: Aerial photo of subreach 2.**

**Figure 2-6: Aerial photo of subreach 3.**

## 2.2 AVAILABLE DATA

There is one U.S. Geological Survey (USGS) gaging station (Bernalillo - # 08329500) located about 1.8 miles upstream from Corrales Reach. In addition, there is a gaging station located downstream of the study reach. Rio Grande at Albuquerque (#08330000) gaging station is about 6.2 miles downstream from Montano Bridge. Both of these gaging stations were primarily utilized in this study. Table 2-2 summarizes the available water discharge and suspended sediment data from the USGS gages.

**Table 2-2: Periods of record for discharge and continuous suspended sediment data collection by the USGS.**

| ***Stations*** | ***Mean Daily Discharge*** | ***Continuous Suspended Sediment Discharge*** |
|---|---|---|
| | Period of Record | Period of Record |
| Rio Grande near Bernalillo | 1942-1968 | 1956-1969 |
| Rio Grande at Albuquerque | 1942-2001 | 1969-1989 1992-1999 |

Bed material particle size distribution data were collected at the USGS gaging stations at Bernalillo and Albuquerque. Table 2-3 summarizes the periods of record for the bed material data from the above-mentioned USGS gages. Additionally, bed material samples were collected at the CO, CR and CA-lines by the United States Bureau of Reclamation (USBR). Table 2-4 lists the bed material surveyed dates at the CO-lines, CA-lines and CR-lines.

**Table 2-3: Periods of record for bed material particle size distribution data collected by the USGS.**

| ***Stations*** | ***Bed Material Particle Size Distributions*** |
|---|---|
| | Period of Record |
| Rio Grande near Bernalillo | 1961, 1966 - 1969 |
| Rio Grande at Albuquerque | 1969 - 2001 |

**Table 2-4: Surveyed dates for bed material particle size distribution data at CO-Lines and CA-Lines.**

| ***Stations*** | ***Bed Material Particle Size Distributions*** |
|---|---|
| | Surveyed Date |
| CO-33 | 1970 - 1982, 1992, 1995, 2001 |
| CO-34 | 1970 - 1972, 1974, 1975, 2001 |
| CO-35 | 1970 - 1972, 1974, 1975,1992,1995,2001 |
| CA-1 | 1988-1993,1995,1996, 2001 |
| CA-6 and CA-12 | 1988-1996, 2001 |
| CA-2 to CA-5, CA-7 to CA-11 and CA-13 | 1988-1996 |
| CR-355, 361, 367, 372, 378, 382, 388, 394, 400, 413, 443, 448, 458, 462 | 2001 |

Reclamation's GIS and Remote Sensing group in Denver, CO digitized the aerial photos and topographic surveys of the study reach which are available for 1918, 1935, 1949, 1962, 1972, 1992 and 2001. Dates and scales of the aerial photos as well as the estimated mean daily discharges in the channel on the dates of the photos, according to USGS gaging stations, are summarized in Appendix A.

Aggradation/Degradation (agg/deg) line surveys, collected by the USBR, are available for 1962, 1972 and 1992. These cross section lines are photogrammetrically surveyed. The mean bed elevations were estimated by the USBR based on the water surface elevation, slope, channel roughness and discharge at the time of the survey. Agg/deg lines are approximately spaced every 500 feet apart.

Cochiti (CO) range lines were field surveyed in this reach for US Bureau of Reclamation. There are three lines located in this study reach (Figure 2-7). CO-33 is the first upstream cross section of the study reach (agg/deg 351). CO-34 is located in subreach 2 and coincides with agg/deg 407. CO-35 is in subreach 3 and corresponds to the agg/deg line 453. Calabacillas (CA) range lines were also field surveyed and established along subreaches 2 and 3, just upstream and downstream from Paseo del Norte Bridge (Figure 2-8).In addition to the CO and CA lines 14 Corrales (CR) range lines these lines are located in all of the subreaches. Table 2-5 summarizes the survey dates for the CO-lines and CA-lines; CR-lines were all surveyed in May of 2001. CO-lines and their correspondent agg/deg lines are plotted in Appendix B.

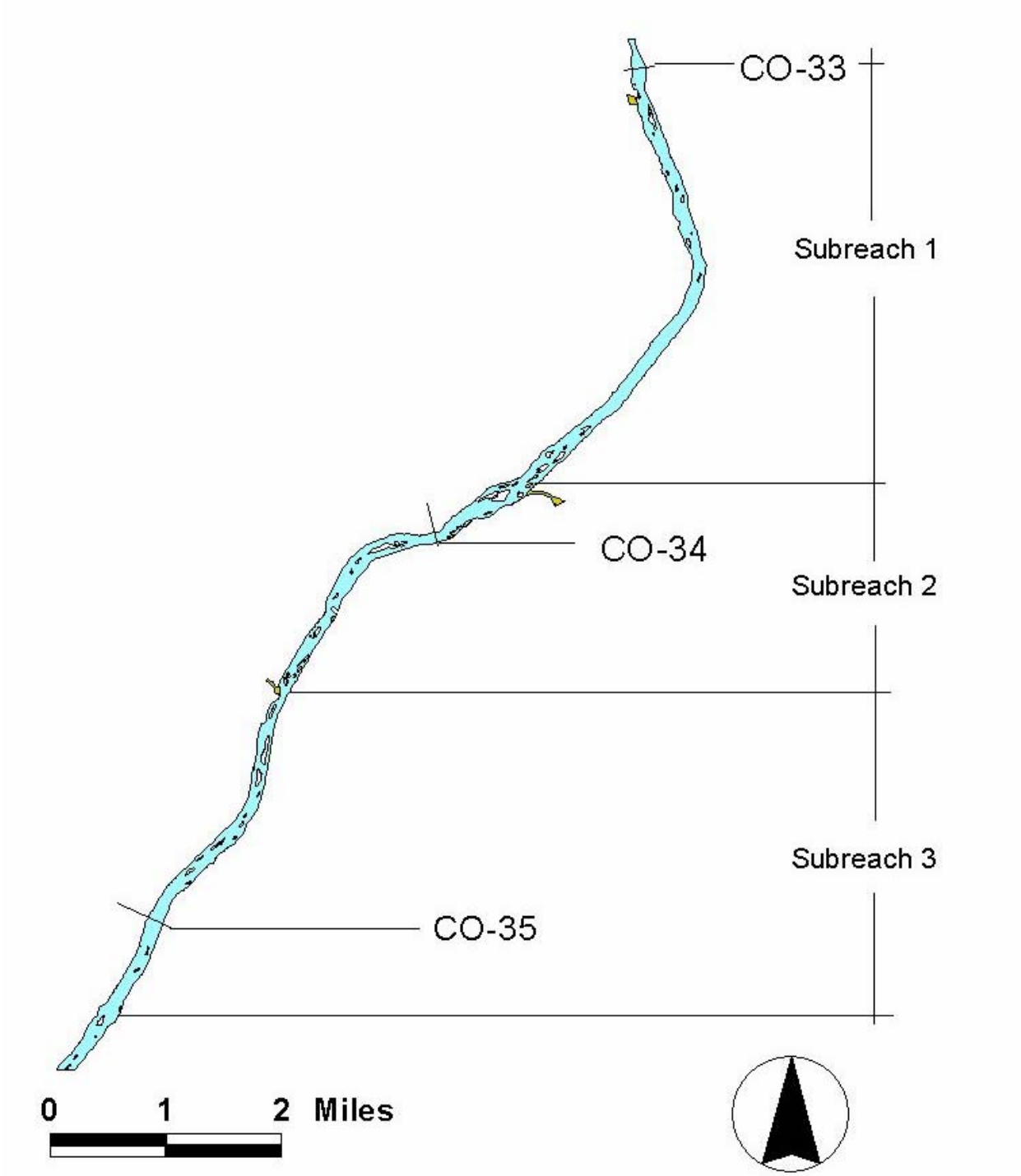


**Figure 2-7: 1992 River planform of the Corrales Reach indicating locations of CO-lines and subreaches.**

**Table 2-5: Surveyed dates for the CO and CA lines collected by the US Bureau of Reclamation.**

| | Cross section | | | | | | | | | | | | | | | |
|---|---|---|---|---|---|---|---|---|---|---|---|---|---|---|---|---|
| Date | CO-33 | CO-34 | CO-35 | CA-1 | CA-2 | CA-3 | CA-4 | CA-5 | CA-6 | CA-7 | CA-8 | CA-9 | CA-10 | CA-11 | CA-12 | CA-13 |
| May-70 | | | x | | | | | | | | | | | | | |
| May-71 | x | x | x | | | | | | | | | | | | | |
| Sep-71 | | x | x | | | | | | | | | | | | | |
| Mar-72 | x | x | x | | | | | | | | | | | | | |
| Nov-72 | x | x | x | | | | | | | | | | | | | |
| May-73 | | x | | | | | | | | | | | | | | |
| Jun-73 | x | x | x | | | | | | | | | | | | | |
| May-74 | x | x | x | | | | | | | | | | | | | |
| Sep-74 | x | x | x | | | | | | | | | | | | | |
| Nov-74 | x | | x | | | | | | | | | | | | | |
| May-75 | | | x | | | | | | | | | | | | | |
| Jul-75 | x | x | | | | | | | | | | | | | | |
| Nov-75 | x | x | x | | | | | | | | | | | | | |
| Apr-79 | x | x | x | | | | | | | | | | | | | |
| May-79 | x | | | | | | | | | | | | | | | |
| Jul-79 | x | x | x | | | | | | | | | | | | | |
| Jan-80 | x | x | x | | | | | | | | | | | | | |
| Oct-82 | | x | x | | | | | | | | | | | | | |
| Nov-83 | x | x | x | | | | | | | | | | | | | |
| Dec-86 | | x | x | | | | | | | | | | | | | |
| Nov-88 | | | | x | x | x | x | | | | | | | | | |
| Dec-88 | | | | | | | | x | x | x | x | x | x | x | x | x |
| Oct-89 | | | | x | x | x | x | x | x | x | x | x | x | x | x | x |
| Jul-90 | | | | x | x | x | x | x | x | x | x | x | x | x | x | x |
| Jun-91 | | | | x | x | x | x | x | x | x | x | x | x | x | x | x |
| Jun-92 | | | | x | x | x | x | x | x | x | x | x | x | x | x | x |
| Jul-92 | x | x | x | | | | | | | | | | | | | |
| Apr-93 | | | | x | x | x | x | x | x | x | x | x | x | x | x | x |
| Jun-93 A | | | | x | x | x | x | x | x | x | x | x | x | x | x | x |
| Jun-93 B | | | | x | x | x | x | x | x | x | x | x | x | x | x | x |
| May-94 A | | | | | x | x | x | x | x | x | x | x | x | x | x | x |
| May-94 B | | | | | x | x | x | x | x | x | x | | | | | |
| Jun-94 A | | | | | x | x | x | x | x | x | x | x | x | x | x | x |
| Jun-94 B | | | | | | | | | | | | x | x | x | x | x |
| May-95 | | | | | | x | x | x | x | x | x | x | x | x | x | x |
| Jun-95 | | | | x | x | x | x | x | x | x | x | x | x | x | x | x |
| Jul-95 | | | | x | x | x | x | x | x | x | x | x | x | x | x | x |
| Aug-95 | x | x | x | | | | | | | | | | | | | |
| Mar-96 | | | | x | x | x | x | x | x | x | x | x | x | x | x | x |
| May-96 A | | | | | x | | | | | | | | | | | |
| May-96 B | | | | | x | | | | | | | | | | | |
| Jun-96 | | | | x | x | x | x | x | x | x | x | x | x | x | x | x |
| Sep-98 | x | x | x | | | | | | | | | | | | | |
| Apr-01 | x | x | x | x | x | | x | | x | | | x | | | x | x |
| Aug-01 | x | x | x | | | | | | x | | | | | | x | |

**Figure 2-8: 1992 Aerial photo of downstream reach of subreach 2 and upstream reach of subreach 3 indicating locations of CA-lines and CO-34 and CO-35 lines.**

## 2.3 CHANNEL FORMING DISCHARGE

Reclamation's Albuquerque office determined the channel forming discharge from discharge/frequency analysis in the Santa Ana Reach. The Corrales reach is 5.10 miles downstream from the Santa Ana Restoration Project. The two year instantaneous peak discharge ($Q_{2y}$= 5,000 cfs) used as the channel maintenance discharge in the Santa Ana Geomorphic Analysis (Mosley and Boelman, 1998) is also utilized in this work.

Figure 2-9 shows the annual maximum daily mean discharges recorded by the USGS at the Albuquerque gaging station. Since 1958, there haven't been any flows recorded at Albuquerque exceeding 10,000 cfs. Since flow regulation began at the Abiquiu Dam on the Rio Chama in 1963 and at the Cochiti Dam on the Rio Grande in 1973, the regulated two-year flow has decreased to 5,650 cfs (Bullard and Lane, 1993). Figure 2-10 shows annual peak flow histograms before and after 1958. Most of the flows are between 3,000 cfs and 7,000 cfs after 1958. Annual peak daily-mean discharge plot at the Bernalillo Gage is included in Appendix C.

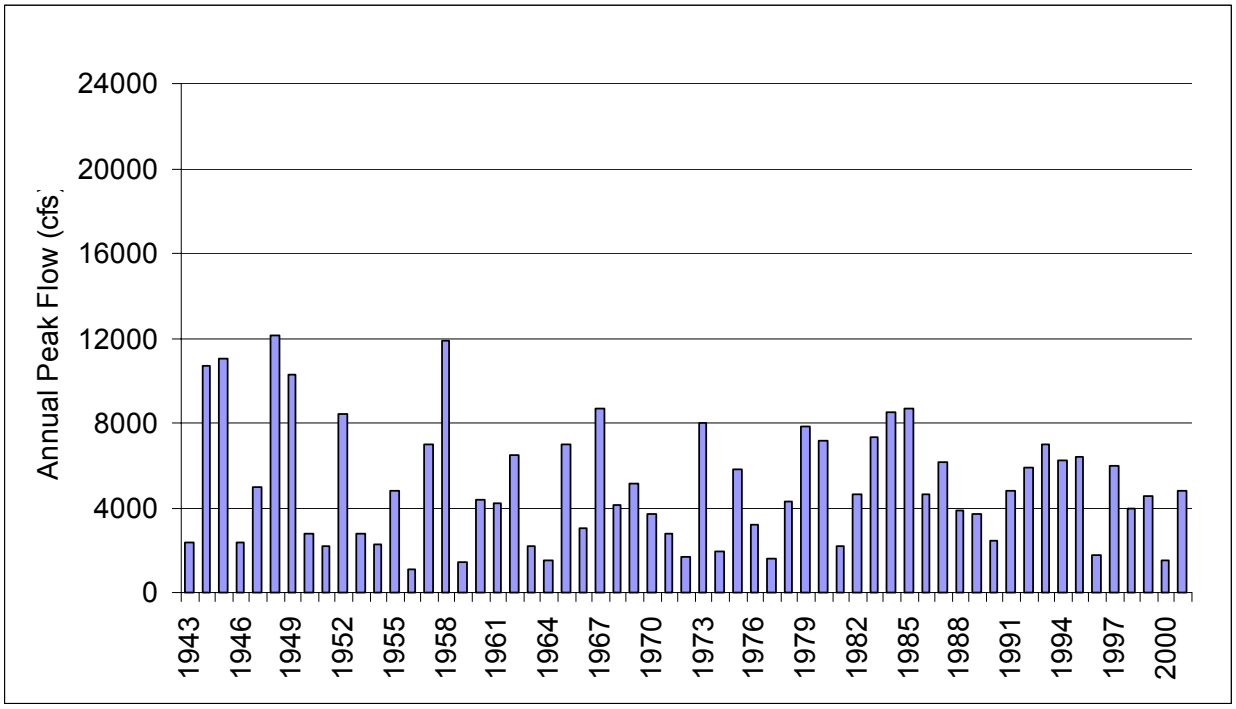


**Figure 2-9: Annual peak daily-mean discharge at Rio Grande at Albuquerque (1943 – 2001).**

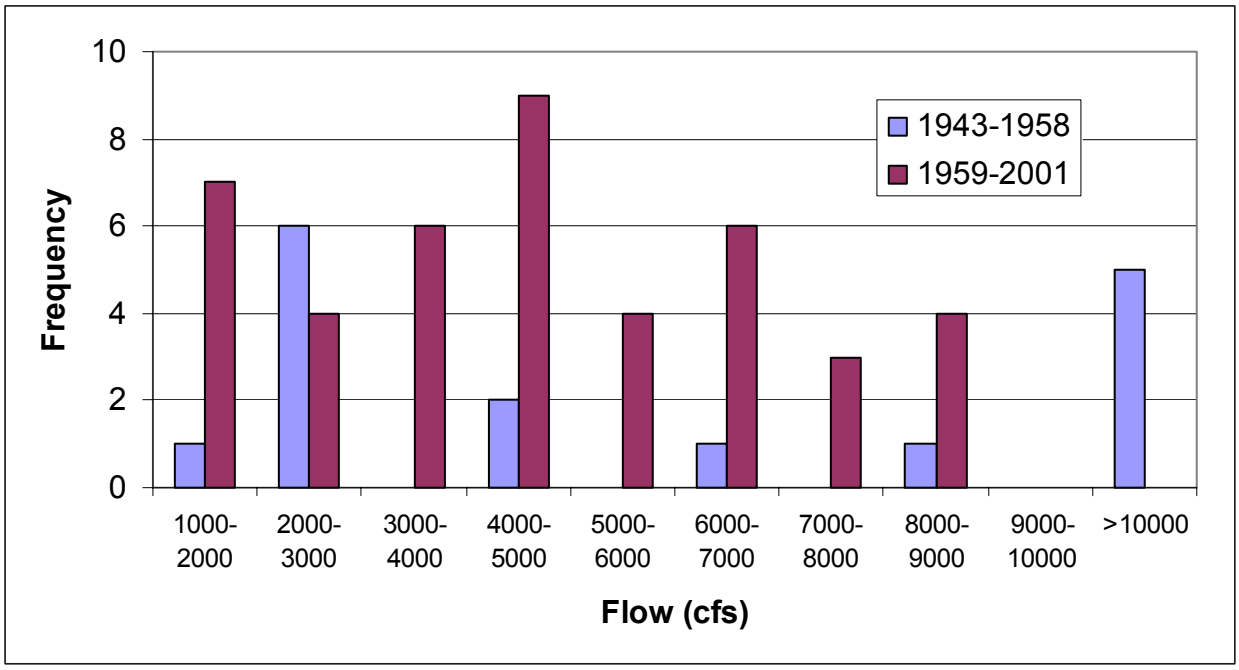


**Figure 2-10: Maximum mean daily annual discharge histograms on the Rio Grande at Albuquerque.**

Besides flood regulation, climate changes seem to have a strong influence in the flow regime of the Rio Grande. Richard (2001) observed that the magnitude of the annual peak flows at the Otowi and Cochiti Gages declined with time since 1895, prior to the construction of main dams in the Rio Grande system. Cochiti Gage data show a dry period from about 1942 to about 1978 (Richard 2001). Richard (2001) also determined that peak flows between 1943 and 1973 (pre-Cochiti Dam) are not statistically different from those between 1974 and 1996 (post-Cochiti Dam).

Molnár (2001) analyzed trends in precipitation and streamflow in the Rio Puerco, one of the largest tributary arroyos of the Rio Grande downstream from the Bernallilo Reach. He concluded that a statistically significant increasing trend in precipitation in the basin at the annual timescale occurred between 1948 and 1997. This increase is due to increases in non-summer precipitation, in particular in the frequency and intensity of moderate rainfall events (Molnár 2001). Molnár also concluded that there is a strong relationship between the long-term precipitation trends in the Rio Puerco Basin and the sea surface temperature anomalies in the Northern Pacific (Molnár 2001).

Also, annual maximum precipitation events seem to produce lower annual maximum runoff events in the last 50 years, most likely due to vegetation cover and the hydraulic characteristics

of the basin (Molnár 2001). Even though this type of analysis has not been performed in other sub-basins of the Rio Grande, it is likely that the same trends occur in nearby areas along the Rio Grande.

# 3 GEOMORPHIC CHARACTERIZATION

## 3.1 METHODS

### Channel Classification

Current channel pattern was qualitatively described from the 2001 set of aerial photos. In addition, qualitative descriptions of the non-vegetated channel planform were performed from the GIS coverages from 1918 to 2001.

Several channel classification methods were applied to the study reach to characterize the spatial and temporal trend of the channel planform. These methods are based on different concepts, such as slope-discharge relationships, channel morphology and unit stream power. The following methods were computed for the study reach: Leopold and Wolman (1957), Lane (1957, from Richardson et al. 1990), Henderson (1963, from Henderson 1966), Ackers and Charlton (1970, from Ackers 1982), Schumm and Khan (1972), Rosgen (1996), Parker (1976), Van den Berg (1995), Knighton and Nanson (1993) and Chang (1979).

The methods that incorporate slope-discharge relationships are as follows:

Leopold and Wolman (1957) classify channel planform as meandering, braided and straight based on a slope-discharge relationship. The criterion $S_o = 0.06\ Q^{-0.44}$ distinguishes between braided and meandering rivers. Q is the bankfull discharge in cfs and $S_o$ is the channel slope in ft/ft. Straight channels (sinuosity (thalweg length to valley length) < 1.5) have slopes above and below the discriminator. In other words, straight channels occur throughout the range of slopes. They define meandering as channels with sinuosity > 1.5. Braiding refers to channels with relatively stable alluvial islands.

Lane (1957, from Richardson et al. 1990) also proposed a slope-discharge relationship to discriminate meandering from braided channel patterns. The relationship between mean discharge in cfs and slope in ft/ft in sand bed rivers is $SQ^{0.25} = K$. When $SQ^{0.25} \leq 0.0017$ the sand bed channel is considered to be meandering and when $SQ^{0.25} \geq 0.010$ the sand bed channel is considered braided. Between these two values the channel is classified as intermediate sand bed stream.

Henderson (1963, from Henderson 1966) incorporated bed material into Leopold and Wolman's slope-discharge relationship to describe channel pattern. Plotting the ratio of $S/0.06Q^{-0.44}$ against median bed size d (in feet), the following discriminator was proposed:

$$S = 0.64d1^{.14}Q^{0.44}$$

Two-thirds of the data points representing straight or meandering channels fell close to the line of distinction. All braided channels had S values that were substantially greater than indicated by the equation.

Ackers and Charlton (1979, Ackers 1982) proposed slope-discharge relationships to distinguish straight channels from straight channels with alternating bars and meandering channels. These relationships are as follows:

- Straight channels:

  $S < 0.001Q^{-0.12}$
- Straight channels with alternating bars:

  $0.001Q^{-0.12} < S < 0.0014Q^{-0.12}$
- Meanders develop if:

  $S_v > 0.0014Q^{-0.12}$

In these relationships S is the water surface slope (m/m) along a straight axial line for straight channels and channels with prominent shoals, $S_v$ is the straight line slope (m/m) for meandered channels and Q is the water discharge ($m^3/s$).

It was later discovered by Ackers (1982) that a straight line of the form $S_v = 0.0008\ Q^{-0.21}$ separates the straight and meandered data of sand-bed rivers and canals.

Schumm and Khan (1972) proposed the following valley slope thresholds to define channel pattern:

- Straight $S < 0.0026$
- Meandering thalweg $0.0026 < S < 0.016$
- Braided $S > 0.016$

In these distinctions S is the valley slope (ft/ft).

The methods that are based on channel morphology are as follows:

Rosgen (1996) classified rivers based on channel morphology and sediment characteristics. Classification is determined from slope, entrenchment, sinuosity, width-depth ratio and bed material.

Parker (1976) indicates that rivers with sediment transport and depth to width ratio ($d_o/B$) << 1 at formative discharge have a tendency toward meandering or braiding. His classification is based on the relative magnitude of the depth-width ratio to the channel slope-Froude number ratio (S/F). Meandering occurs when S/F << $d_o/B$, braiding occurs for S/F >> $d_o/B$ and transition between the two occurs when S/F ~ $d_o/B$.

The methods based on the concept of stream power are as follows:

van den Berg (1995) proposed a discriminator between braided and single-thread channels with sinuosity larger than 1.3 that is based on potential specific stream power and bed material size. The discriminator is defined as:

$$\omega_{v,t} = 900 \cdot D_{50}^{0.42} \qquad \text{Eq. 1}$$

$\omega_{v,bf}$ = potential specific stream power, for sand-bed:

$$\omega_{v,bf} = 2.1 \cdot S_v \sqrt{Q_{bf}} \ \ (kW/m^2)$$

$\omega_{v,bf}$ = potential specific stream power, for gravel-bed:

$$\omega_{v,bf} = 3.3 \cdot S_v \sqrt{Q_{bf}} \ \ (kW/m^2)$$

In these relationships $Q_{bf}$ is the bankfull discharge ($m^3/s$), $D_{50}$ is the median grain size (mm) and $S_v$ is the Valley slope (m/m).

Straight, single-thread rivers with sinuosity < 1.3 plot on both sides of the discriminator. Low stream power straight channels generally have a much smaller width-depth ratio than high stream power channels. Plotting the ratio of measured to reference bankfull channel width ($w=aQ_{bf}^b$ (Eq. 2)) against the ratio of potential specific stream power to the value of the discriminating function straight single thread channels can be classified as high or low energy channels. From the developed relationships van den Berg established the following criteria:

- If $\frac{\omega_{v,bf}}{\omega_{v,t}} > 1$ the channel pattern corresponds to low sinuosity single-thread and multi-thread channel.
- If $\frac{\omega_{v,bf}}{\omega_{v,t}} < 1$ the river is a single-thread channel (see Figure 3-1).

- If measure to reference width ratio > 1 the river is a high energy wide channel (see Figure 3-1).
- If measure to reference width ratio < 1 the river is a low energy narrow channel (see Figure 3-1).

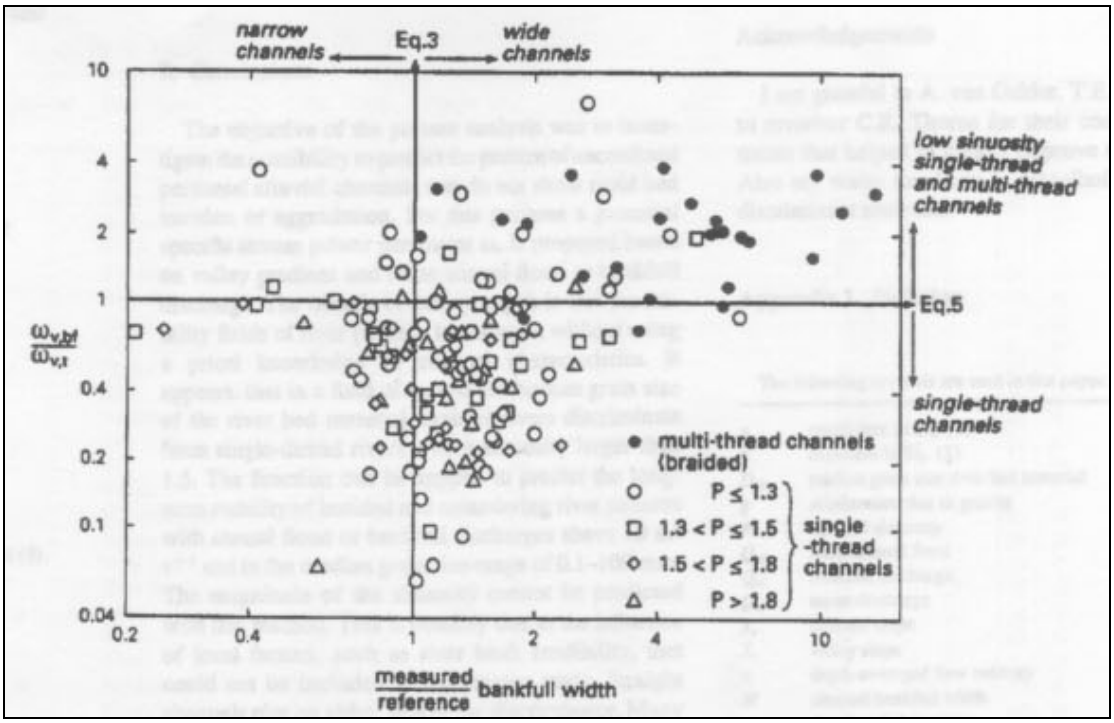


**Figure 3-1: Channel pattern, width/depth ratio and potential specific stream power relative to reference values, as defined by Eqs. 1 and 2 (after van den Berg 1995).**

Knighton and Nanson (1993) defined channel pattern in terms of the following three variables:

- Flow strength
- Bank erodibility
- Relative sediment supply: rate at which material is supplied either from bank erosion or from upstream relative to the rate it is transported downstream.

This classification is based on the continuum from straight to meandering to braided corresponding to increases in the three variables listed above. Flow strength can be defined through specific stream power, total power, or shear stress. Bank erodibility could be estimated by the silt-clay content of the bank material.

Knighton and Nanson (1993) do not quantify thresholds for these variables, but rather expressed the continuum concept on the following ordinal scale:

| | | |
|---|---|---|
| **LOW (L)** | **FLOW STRENGTH** | **HIGH (H)** |
| | ----------→ | |
| *Straight* | *Meandering* | *Braided* |
| **LOW (L)** | **BANK ERODIBILITY** | **HIGH (H)** |
| | ----------→ | |
| *Straight* | *Meandering* | *Braided* |
| **LOW (L)** | **RELATIVE SEDIMENT SUPPLY RATE** | **HIGH (H)** |
| | ----------→ | |
| *Straight* | *Meandering* | *Braided* |

In order to apply this method to the Corrales Reach, changes in flow strength were evaluated as changes in water discharge (Chapter 4). Changes in bank erodibility were considered as changes in channel width (Chapter 3) and changes in sediment supply rate as the changes in suspended sediment with time (Chapter 4).

Chang (1979) classifies channel patterns based on stream power and slope-discharge relationships. For a given water and sediment discharge, a stable channel geometry and slope correspond to a minimum stream power per unit channel length. For small values of water and sediment discharge a unique minimum exists and therefore a unique stable channel configuration and slope (Chang 1979). When this unique stable channel slope equals the valley slope, the channel pattern is straight (Chang 1979). Above a certain threshold valley slope the stream power has two minimums, indicating two possible stable channel configurations and slopes (Chang 1979). Highly sinuous rivers, with small width-depth ratios occur on flatter valley slopes and they become braided and less sinuous as the valley slope increases (Chang 1979).

Figure 3-2 shows Chang's (1979) channel pattern diagram.

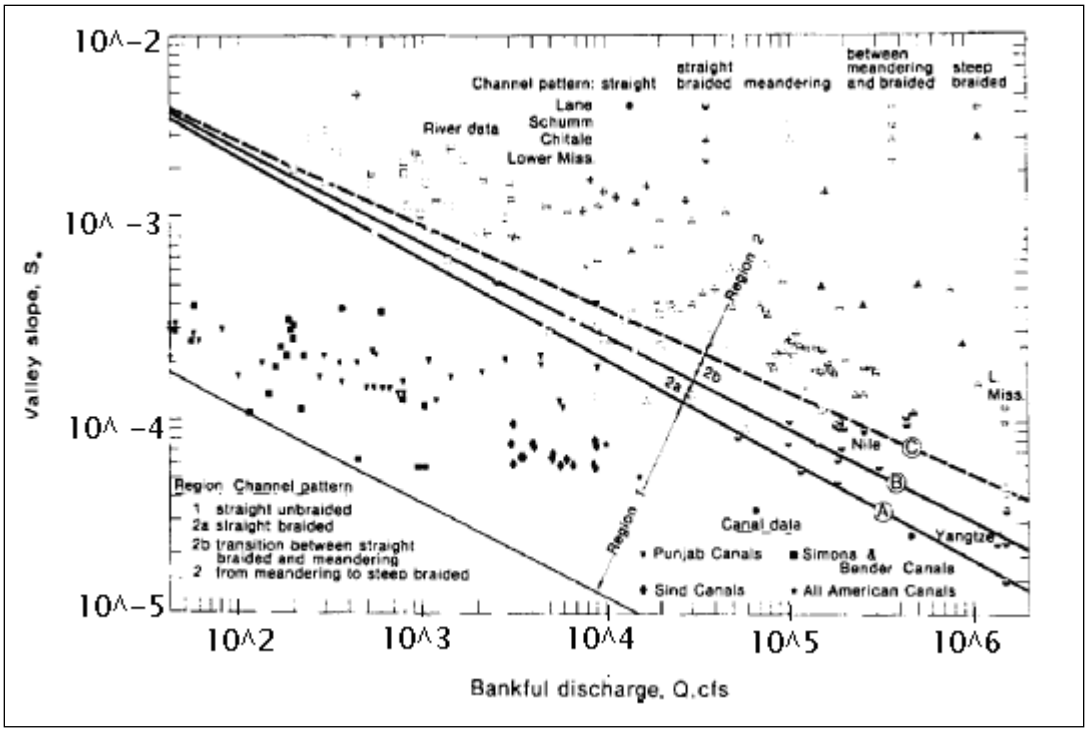


**Figure 3-2: Channel patterns of sand streams (after Chang 1979).**

### Sinuosity

The sinuosity of the study reach and the subreaches were estimated as the ratio of the channel thalweg length to the valley length. Reclamation's GIS and Remote Sensing Group in Denver, CO digitized the channel thalweg and measured valley lengths from aerial photos and topographic maps. The thalweg length was used as the active channel length in the sinuosity computations. Identification of the channel length is subject to the quality of the photos and surveys.

### Valley Slope

Valley slopes were estimated as the ratio of the difference of valley elevations between the upper and lower ends of each subreach to the valley length. Valley elevations were estimated from the agg/deg data. Agg/deg data contain elevation data outside from the main channel. Averaged elevations of those areas were computed and considered as valley elevations. There are not agg/deg data available for 2001, so the valley slope was determined using CO, CR and CA-line cross sectional data from 2001 surveys. Reclamation's GIS and Remote Sensing Group, Denver, CO measured valley lengths from aerial photos and topographic maps. Valley slope

values were used as input to some of the channel classification methods as described in the Channel Classification section.

## Longitudinal Profile

### *Thalweg Elevation*

The thalweg elevation is the lowest elevation in a channel cross section. As mentioned previously, the photogrammetrically surveyed agg/deg lines are available for 1962, 1972, and 1992, but are not available for 2001. Consequently, the only available thalweg elevation data for the Corrales Reach in 2001 are for the CO-lines, CA-lines and CR-lines for the survey dates listed in Table 2-3. Changes in the thalweg elevation with time for each CO-line were plotted to identify temporal trends in the thalweg elevation at these three locations. CA-lines are only located in a short reach upstream and downstream from the confluence of the Rio Grande with the arroyo de las Calabacillas. Changes in thalweg elevation with time at four CA-lines were plotted to identify possible influence of the arroyo in the longitudinal profile of the river.

### *Mean Bed Elevation*

Longitudinal profiles were plotted for the study reach and the subreaches for the years of 1962, 1972, 1992 and 2001. The profiles for the first three sets of years were generated from the agg/deg data. The longitudinal profile for 2001 was generated from the CO, CR and CA-line data and plotted together with the agg/deg line longitudinal profiles. All profiles were generated using the same methodology. Parameters calculated from the U.S. Army Corps of Engineers' Hydrologic Engineering Center-River Analysis System (HEC-RAS®) version 3.1 program (USACE 1998) were utilized in this methodology. The HEC-RAS® runs that were executed using the channel forming discharge (5,000 cfs). To calculate the mean bed elevation (MBE), the following equation was used:

$$MBE = WSE - \frac{A}{Tw} = WSE - h$$

In this equation, WSE represents the water surface elevation (ft), A represents the channel area ($ft^2$), Tw represents the channel top width (ft) and h represents the hydraulic depth (ft) which is seen to be equivalent to the area-to-top width ratio.

*Channel Cross Sections*

Each of the three cross sections from the CO-line surveys was plotted for two different survey dates. These dates were chosen based on the closure of Cochiti Dam (1973). One of the dates represents pre-dam conditions and one of the dates represents post-dam conditions. These survey dates were chosen such to view the impacts of the dam on the channel.

*Friction and Water Surface Slopes*

The energy grade line and water surface slopes were estimated at each cross section and at channel–forming discharge of 5,000 cfs using HEC-RAS®. The slopes were then averaged over the reach and each subreach by using a weighting factor equal to the sum of one half of the distances to each of the adjacent upstream and downstream cross-sections.

**Channel Geometry**

Two methods were used to describe the channel geometry characteristics of the study reach: 1) HEC-RAS® model and 2) digitized aerial photo interpretation. HEC-RAS® was used to model the channel geometry of the study reach with the available agg/deg line data for 1962, 1972 and 1992 and CO, CR and CA-line data for 2001. A total of 109 agg/deg cross sections spaced approximately 500 feet apart were modeled for the 1962, 1972 and 1992 model. The model for 2001 was performed using 3 CO-lines, 14 CR lines and 7 CA-lines spaced from approximately 800 to 4,000 feet apart. A channel forming discharge of 5,000 cfs was routed through the reach. HEC-RAS® was not calibrated. A Manning's n value of 0.02 was used for the channel and 0.1 for the floodplain for all simulations. All HEC-RAS® results for each of the simulated years are summarized in Appendix E. Digitized aerial photos were used for active channel delineation as well as to measure the non-vegetated channel width at each agg/deg line. This was executed through the use of a Geographic Information System (GIS). ArcGIS v. 8.2 was utilized for all digitized aerial photo analysis.

The resulting channel geometry parameters at each cross section were then averaged over each subreach and the entire reach using a weighting factor equal to the sum of one half of the distances to each of the adjacent upstream and downstream cross sections.

The following channel geometry parameters were computed:

Wetted Perimeter = P

Wetted Cross Section Area = A

Mean Flow Velocity = V = Q/A

where, Q = Flow discharge

Top Width = W

Mean Depth = h = A/W

Width-Depth ratio = W/h

Froude Number Fr = $V/\sqrt{gD}$ , where D = A/W

*Overbank Flow/Channel Capacity*

The HEC-RAS® results are divided into main channel flow and overbank flow. The main channel results were used for the analyses of this work, because this is where the majority of the sediment transport occurs.

## Sediment

*Bed Material*

Characterization of the spatial and temporal variability of median bed material size ($D_{50}$) was performed for each subreach. Median grain sizes were computed for 1962, 1972, 1992 and 2001 from USGS gaging stations, CO-line CR-line and CA-line data. Apparent temporal and spatial trends were noted through the generation of bed material gradation curves. Table 3-1 lists the source of the bed material data used in the generation of these gradation curves. In addition, histograms were generated using the $D_{50}$ and $D_{84}$ sizes at each of the three cross sections from the CO-line surveys and from 8 CA-lines. These histograms were generated using the available data for dates as far back as 1970 (see Table 2-5).

**Table 3-1: Source of bed material data used for the bed sediment reach characterization through analysis of gradation curves.**

| Median Bed Material Size Data Source | | |
|---|---|---|
| **Subreach 1** | **Subreach 2** | **Subreach 3** |
| Bernalillo gage | Bernalillo gage | Bernalillo gage |
| CO-33 | CO-34 | CO-35 |
| CO-33 | CA-1,4,6 | CO-35, CA-8,10,12 |
| CO-33, CR-355, 361, 367, 372, 378, 382, 388, 394 | CO-34, CA-1, 2, 6, CR-400, 413 | CO-35, CA-9, 12, 13, CR-443, 448, 458, 462 |

Several samples were collected across each cross section. The average of the median bed material sizes ($D_{50}$) of all the samples collected in the bed of the channel at each station were calculated to characterize the bed material of the reach. These averages were input into the channel classification methods (see Table 3-2). In addition, different statistics such as minimum, maximum and standard deviation of the median bed material sizes were computed for each of the locations and dates in Table 3-1. These statistics were used to further analyze the bed material trends occuring in the subreaches.

## 3.2 Results

### Channel Classification

*Historic and Current Channel Pattern Description*

Historically, the Middle Rio Grande was a relatively straight, braided and aggrading channel (Baird 1996). As a result of the aggradational trend the Middle Rio Grande Conservancy District constructed a floodway along the river during the 1930 to 1936 period (Woodson and Martin 1962) to contain the river in its channel and prevent avulsions from forming in the adjacent areas (Sanchez et. al 1997). The levee system, constructed as a part of the floodway, was laid out to contain the pattern of the river prevailing at that time and no significant attempts were performed to straighten and shorten the channel (Woodson and Martin 1962). By the 1950's, the Rio Grande occupied a wide shallow channel between the levees of the floodway (Woodson and Martin 1962). The channel had no banks and the average level of the bed was above the elevation of the land outside the levees (Woodson and Martin 1962). After the major flood year of 1941, the levees were breached at 25 places and extensive flood damage was experienced (Woodson and Martin 1962). In 1948 the Corps of Engineers and the Bureau of Reclamation recommended the comprehensive plan of improvement for the Rio Grande in New Mexico

(Woodson and Martin 1962). Several jetty fields were placed along the floodway as a part of this plan rehabilitation.

Figure 3-3 was produced from Reclamation's GIS coverages of the Corrales Reach and represents the changes in river planform that occurred in the non-vegetated active channel in 1918, 1935, 1962, 1992 and 2001. It is evident that the study reach planform has not experienced significant changes since 1962. The 1992 and 2001 planforms are comparable and represent a single thread channel with visible islands at low flow. The floodway construction between 1930 and 1936 do not seem to have halted the channel-narrowing trend observed since 1918. Conversely, rehabilitation of the floodway by the 1950's might be responsible for stabilization of the width of the channel, as shown in Figure 3-3.

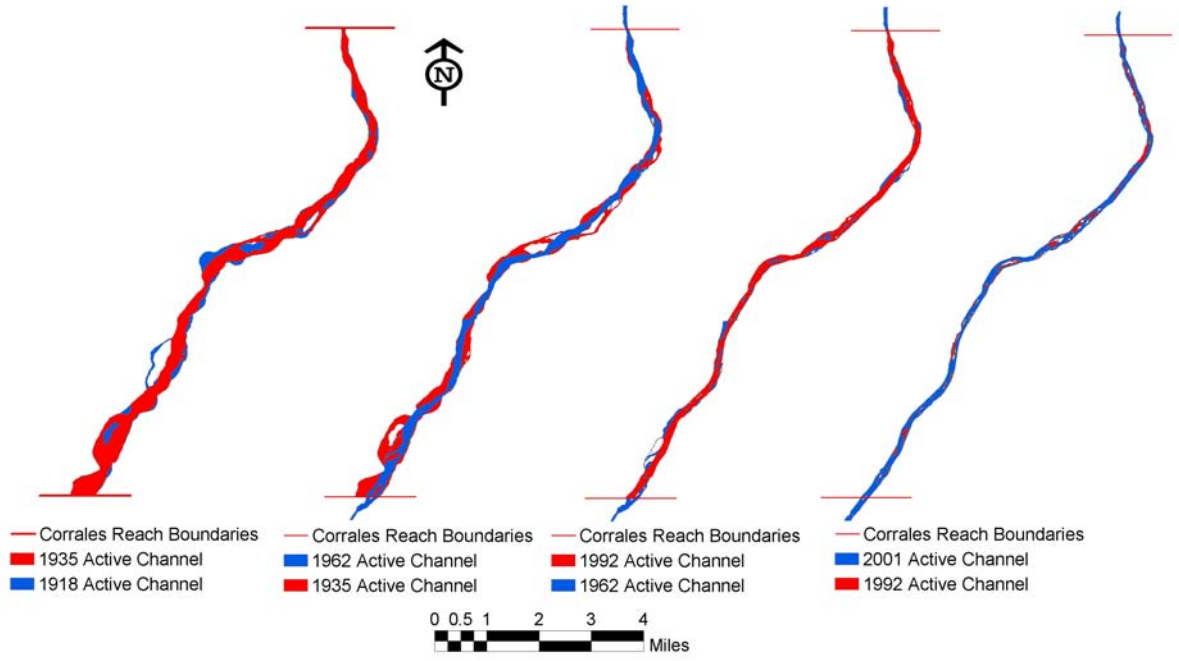


**Figure 3-3: Non-vegetated active channel of the Corrales Reach. 1918 planform from topographic survey. 1935, 1962, 1992 and 2001 planform from aerial photos.**

The current channel pattern description is based on observation of the 2001 set of aerial photos, which were taken during the winter season (Figures 2-4, 2-5 and 2-6). At flows below bankfull (<5,000 cfs), the Corrales Reach exhibits a multi-channel pattern. Formation of sediment bars at low flow is also evident in the aerial photos (Figure 2-4, 2-5 and 2-6) as well as in the cross section plot of CO-35 (Appendix B).

The values of the input parameters for the different channel classification methods applied to the 1962, 1972, 1992 and 2001 surveys of the Corrales Reach are in Table 3-2. These methods produced descriptions of the channel that range from straight to meandering and braided (Tables 3-3 and 3-4). The discrepancy among classification methods is likely due to the fact that this stretch of the Rio Grande is not in a state of equilibrium, and the classification methods were designed under the assumption that the river is in state of equilibrium.

**Table 3-2: Input parameters for channel classification methods.**

| 1962 | Q (cfs) | Channel Slope | Valley Slope | d50 (mm) | d50 (ft) | Width (ft) from Hec-Ras | Depth (ft) | Velocity (ft/s) | Fr | EG Slope | Sinuosity |
|---|---|---|---|---|---|---|---|---|---|---|---|
| **1** | 5,000 | 0.0009 | 0.0011 | 0.21 | 6.40E-05 | 641 | 2.24 | 3.62 | 0.43 | 0.0009 | 1.22 |
| **2** | 5,000 | 0.0010 | 0.0011 | 0.21 | 6.40E-05 | 692 | 2.14 | 3.62 | 0.45 | 0.0011 | 1.21 |
| **3** | 5,000 | 0.0010 | 0.0010 | 0.21 | 6.40E-05 | 627 | 2.35 | 3.97 | 0.47 | 0.0011 | 1.07 |
| **Total** | 5,000 | 0.0009 | 0.0011 | 0.21 | 6.40E-05 | 652 | 2.24 | 3.73 | 0.45 | 0.0010 | 1.17 |
| **1972** | | | | | | | | | | | |
| **1** | 5,000 | 0.0009 | 0.0011 | 0.20 | 6.21E-05 | 665 | 1.52 | 5.28 | 0.77 | 0.0008 | 1.23 |
| **2** | 5,000 | 0.0010 | 0.0011 | 0.18 | 5.49E-05 | 698 | 1.48 | 5.27 | 0.78 | 0.0008 | 1.19 |
| **3** | 5,000 | 0.0010 | 0.0010 | 0.21 | 6.40E-05 | 653 | 1.41 | 5.53 | 0.83 | 0.0009 | 1.14 |
| **Total** | 5,000 | 0.0010 | 0.0011 | 0.20 | 6.03E-05 | 670 | 1.47 | 5.35 | 0.79 | 0.0009 | 1.19 |
| **1992** | | | | | | | | | | | |
| **1** | 5,000 | 0.0010 | 0.0011 | 1.70 | 5.18E-04 | 603 | 2.23 | 3.85 | 0.46 | 0.0010 | 1.21 |
| **2** | 5,000 | 0.0010 | 0.0011 | 0.49 | 1.49E-04 | 640 | 2.21 | 3.75 | 0.45 | 0.0010 | 1.18 |
| **3** | 5,000 | 0.0009 | 0.0010 | 0.51 | 1.55E-04 | 599 | 2.25 | 3.85 | 0.46 | 0.0010 | 1.11 |
| **Total** | 5,000 | 0.0010 | 0.0011 | 0.90 | 2.74E-04 | 612 | 2.22 | 3.84 | 0.46 | 0.0010 | 1.17 |
| **2001** | | | | | | | | | | | |
| **1** | 5,000 | 0.0009 | 0.0011 | 1.73 | 5.27E-04 | 524 | 2.41 | 4.01 | 0.46 | 0.0009 | 1.21 |
| **2** | 5,000 | 0.0010 | 0.0011 | 0.67 | 2.04E-04 | 584 | 2.24 | 3.86 | 0.45 | 0.0009 | 1.18 |
| **3** | 5,000 | 0.0010 | 0.0010 | 0.53 | 1.62E-04 | 598 | 2.22 | 4.03 | 0.49 | 0.0012 | 1.12 |
| **Total** | 5,000 | 0.0009 | 0.0011 | 0.98 | 2.99E-04 | 563 | 2.30 | 3.97 | 0.46 | 0.0010 | 1.17 |

**Table 3-3: Channel pattern classification for 1962 and 1972.**

| Reach # | Slope-discharge | | | | | | Channel Morphology | | Stream Power | |
|---|---|---|---|---|---|---|---|---|---|---|
| | Leopold and Wolman | Lane | Henderson | Ackers & Charlton | | Schumm & Khan | Rosgen | Parker | van den Berg | Chang |
| | | | | Comparing with channel slope | Comparing with valley slope | | | | | |
| **1962** | | | | | | | | | | |
| **1** | Straight | Intermediate | Braided | Meandering | Meandering | Straight | D5c- | Meandering | Low stream power low sinousity single-thread and narrow channel | from meandering to steep braided |
| **2** | Straight | Intermediate | Braided | Meandering | Meandering | Straight | D5 | Meandering | Low stream power low sinousity single-thread and narrow channel | from meandering to steep braided |
| **3** | Straight | Intermediate | Braided | Meandering | Meandering | Straight | D5 | Meandering | Low stream power low sinousity single-thread and | from meandering to steep braided |
| **Total** | Straight | Intermediate | Braided | Meandering | Meandering | Straight | D5c- | Meandering | Low stream power low sinousity single-thread and narrow channel | from meandering to steep braided |
| **1972** | | | | | | | | | | |
| **1** | Straight | Intermediate | Braided | Meandering | Meandering | Straight | D5c- | Meandering | Low stream power low sinousity single-thread and narrow channel | from meandering to steep braided |
| **2** | Straight | Intermediate | Braided | Meandering | Meandering | Straight | D5 | Meandering | Low stream power low sinousity single-thread and narrow channel | from meandering to steep braided |
| **3** | Straight | Intermediate | Braided | Meandering | Meandering | Straight | D5 | Meandering | Low stream power single thread narrow channel | from meandering to steep braided |
| **Total** | Straight | Intermediate | Braided | Meandering | Meandering | Straight | D5 | Meandering | Low stream power low sinousity single-thread and narrow channel | from meandering to steep braided |

**Table 3-4: Channel pattern classification for 1992 and 2001.**

| Reach # | Slope-discharge | | | | | | Channel Morphology | | Stream Power | |
|---|---|---|---|---|---|---|---|---|---|---|
| | Leopold and Wolman | Lane | Henderson | Ackers & Charlton | | Schumm & Khan | Rosgen | Parker | van den Berg | Chang |
| | | | | Comparing with channel slope | Comparing with valley slope | | | | | |
| **1992** | | | | | | | | | | |
| **1** | Straight | Intermediate | Braided | Meandering | Meandering | Straight | D5 | Meandering | Low stream power single thread narrow channel | from meandering to steep braided |
| **2** | Straight | Intermediate | Braided | Meandering | Meandering | Straight | D5 | Meandering | Low stream power single thread narrow channel | from meandering to steep braided |
| **3** | Straight | Intermediate | Braided | Meandering | Meandering | Straight | D5c- | Meandering | Low stream power single thread narrow channel | from meandering to steep braided |
| **Total** | Straight | Intermediate | Braided | Meandering | Meandering | Straight | D5 | Meandering | Low stream power single thread narrow channel | from meandering to steep braided |
| **2001** | | | | | | | | | | |
| **1** | Straight | Intermediate | Braided | Meandering | Meandering | Straight | D5c- | Meandering | Low stream power single thread narrow channel | from meandering to steep braided |
| **2** | Straight | Intermediate | Braided | Meandering | Meandering | Straight | D5c- | Meandering | Low stream power single thread narrow channel | from meandering to steep braided |
| **3** | Straight | Intermediate | Braided | Meandering | Meandering | Straight | D5c- | Meandering | Low stream power single thread narrow channel | from meandering to steep braided |
| **Total** | Straight | Intermediate | Braided | Meandering | Meandering | Straight | D5c- | Meandering | Low stream power single thread narrow channel | from meandering to steep braided |

Channel patterns predicted by each method, yield results with little variation between subreaches for all the three periods. The lack of variation might be due to the constant channel-forming discharge used in the computation (5,000 cfs), little variation in bed material and channel width, etc.

The methods based on slope-discharge relationships (Leopold and Wolman 1957, Lane 1957 - from Richarson et al. 1990, Henderson 1963 - from Henderson 1966, Ackers and Charlton 1970 - from Ackers 1982, Schumm and Khan 1972) produced varying results. These methods do not show any spatial and temporal planform trend, since they predict the same pattern for the entire reach for all years. Leopold and Wolman's (1957) and Schumm and Khan's (1972) methods yield a straight channel planform for all years. Henderson's (1963) method predicts a braided planform for all years. Ackers and Charlton's (1970) classification system produces a meandering pattern and Lane's method an intermediate channel for all years.

Rosgen's (1996) and Parker's (1976) classification systems are based on channel morphology variables. According to Rosgen's method, the Corrales Reach best fits as a D5c- for 1962 and 2001 and D5 for 1972 and 1992. The D5c- is a multiple-channel with very high width-depth ratio (> 40), low sinuosity (<1.2), slope between 0.001 and 0.02 and sand bed. The D5c- has the same configuration as the D5 except for the slope, which is <0.001. Typically D5c- streams are characterized by a braided pattern, a channel slope that approximates the valley slope and high bank erosion rates. Using Parker's (1976) method, the reach is classified as meandering for all years.

van den Berg's (1995) method, which is based on stream power, classifies the Corrales Reach as a low stream power, low sinuosity, single thread and narrow channel in 1962 and 1972 and as low stream power, single thread narrow channel for 1992 and 2001. Chang's (1979) method, which is also based on stream power, yields a meandering to steep braided channel planform for the reach for all years. All the subreaches plot above the C line in Chang's diagram, which corresponds to region 2. According to Chang (1979), region 2 predicts that highly sinuous rivers with low width-depth ratios occur on flat valley slopes and as the valley slope increases, more braided and less sinuous channel patterns are predicted.

Knighton and Nanson (1993) do not quantify thresholds values for flow strength, bank erodibility and sediment supply. However, it is possible to interpret the change in these variables in the Corrales Reach as follows: flow strength (peak water discharge) started to

decrease before regulation of flows began in the middle Rio Grande basin, probably due to climatic changes and intensification of agricultural activities in the upper Rio Grande basin. According to Richard (2001) the magnitude of peak flows at Otowi and Cochiti gaging stations declined with time since 1895. Sediment supply rates (suspended sediment concentration at Albuquerque gage) have decreased since the closure of Cochiti Dam in 1973 (Richard 2001). Bank erodibility has decreased due to the construction of the floodway and other river works that control the lateral movement of the channel (Figure 3-3). The combination of these factors would indicate a likely shift from a braiding to meandering planform.

### Sinuosity

The sinuosity of Corrales Reach remained close to 1.15 from 1918 to 1949. After 1949, the sinuosity increased and remained between 1.15 and 1.20 (Figure 3-4). Subreach 1 maintained its sinuosity close to 1.2 for the entire study period. However, it has been above 1.2 since 1949. Subreach 2 has had a more variable sinuosity than the other reaches. It has fluctuated between 1.15 and 1.23. Subreach 3 increased its sinuosity consistently from 1.05 to around 1.11. This subreach however has the lowest sinuosity. GIS active channel plots (Figure 3-3) show little evidence of channel migration throughout the years. These results indicate that the channel is straight.

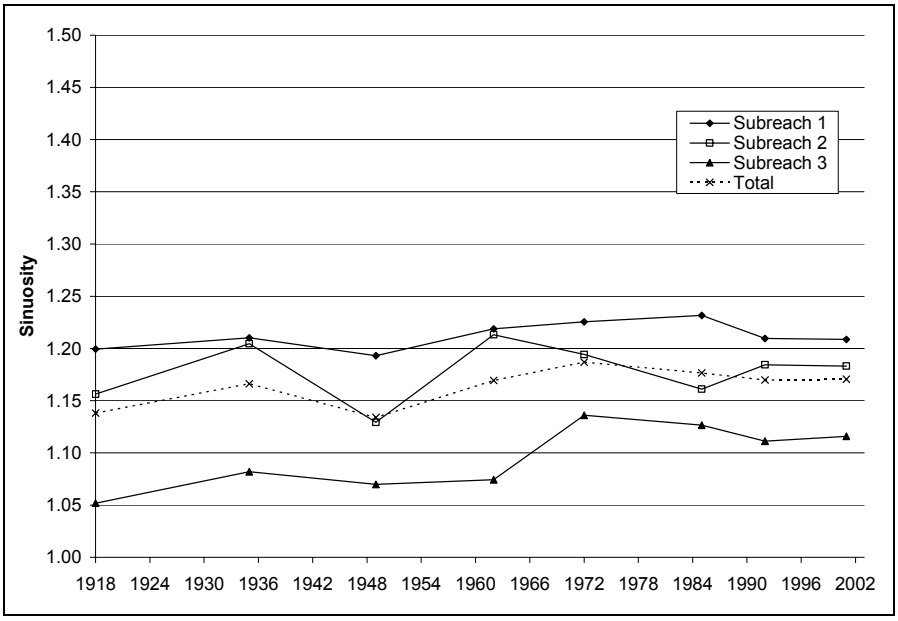


**Figure 3-4: Time series of sinuosity of the Corrales Reach as measured from the digitized aerial photos.**

## Longitudinal Profile

*Thalweg Elevation*

Changes in thalweg elevation with time at each of the three CO-lines are presented in Figure 3-5. These surveys were collected at different times of the year and therefore at different points in the annual flow regime (Table 2-3). Most of the surveys from 1970 to 1986 and 1998 were taken during winter and summer runoffs. 1992 and 1995 surveys were performed during spring runoff. The 2001 surveys were conduced during both spring and summer runoffs. It is expected to observe more degradation in the channel during the spring flows. CO-33, CO-34 and CO-35 do not show much net change between 1970 and 2001. Although changes in thalweg elevation with time do not seem significant at these three stations, cross-section plots (Appendix B) reveal large variability in bed elevation at the CO-lines throughout time and net degradation in the three sections between 1970 and 2001.

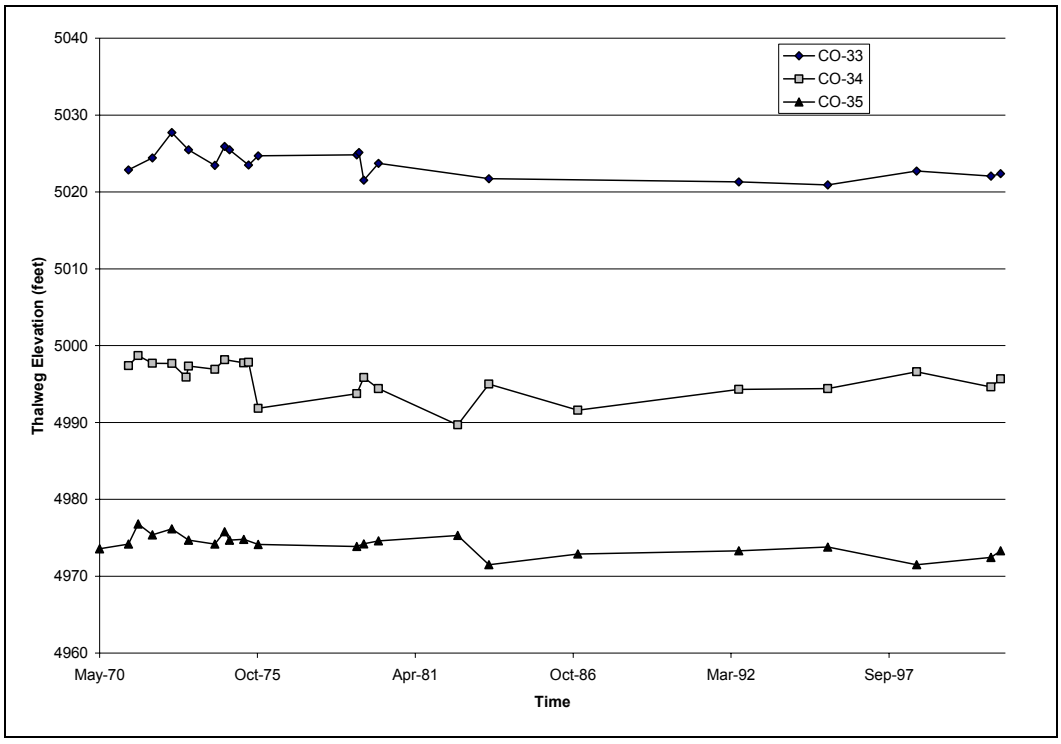


**Figure 3-5: Change in thalweg elevation with time at the CO-lines.**

Changes in thalweg elevation with time at four CA-lines are shown in Figure 3-6; cross section data was not available for CA-lines 7 and 8 for 2001. CA-1, CA-8 and CA-13 show an overall slight degradation between 1988 and 2001. CA-7, CA-8 and CA-13 degraded from 1988 to 1995, aggraded form 1995 to 1996, and then returned to a degradational pattern. CA-1 had an overall degradational trend from 1988 to 1993 and an overall aggradational trend after 1993. It is difficult to determine the local effect of the delta of the arroyo de las Calabacillas (located between CA-7 and CA-8) on the channel bed elevation. Both profiles (CA-7 and CA-8) are in close proximity to one another and display similar patterns.

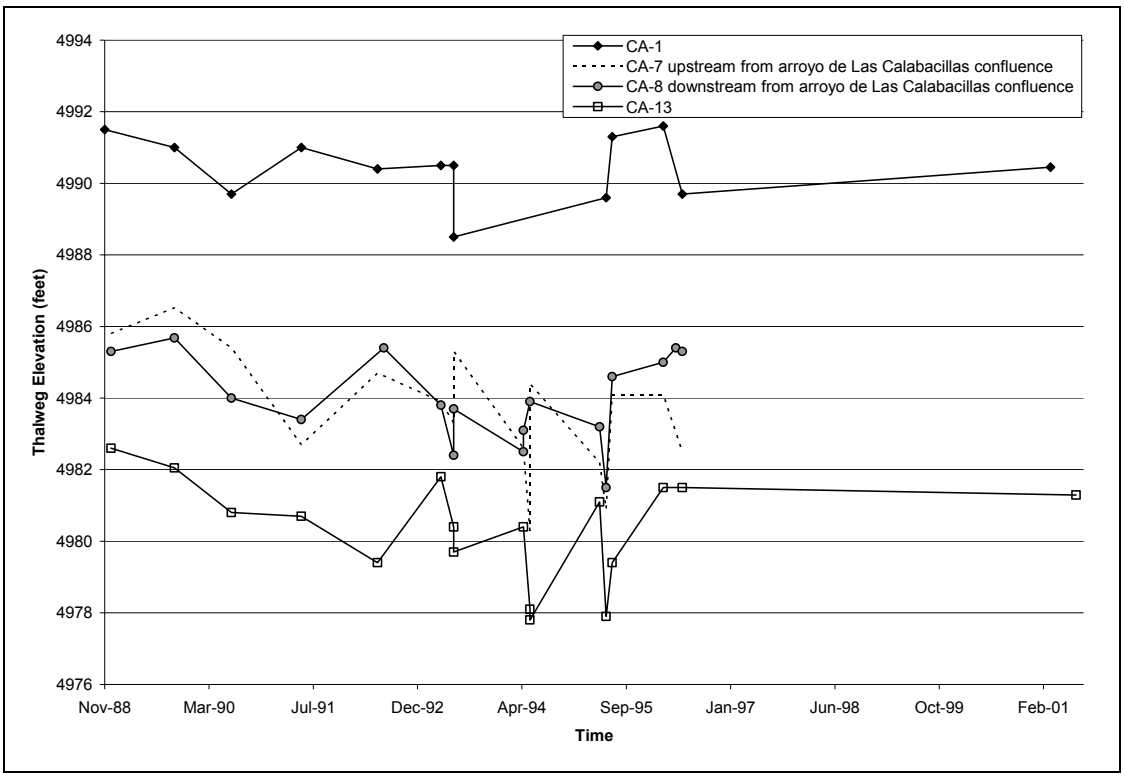


**Figure 3-6: Change in thalweg elevation with time at CA-lines.**

*Mean Bed elevation*

Changes in mean bed elevation with time at the CO-lines are illustrated in Figure 3-7. The general trend is degradation of the bed since 1970. CO-34, located in subreach 2, shows more degradation than the other two subreaches.

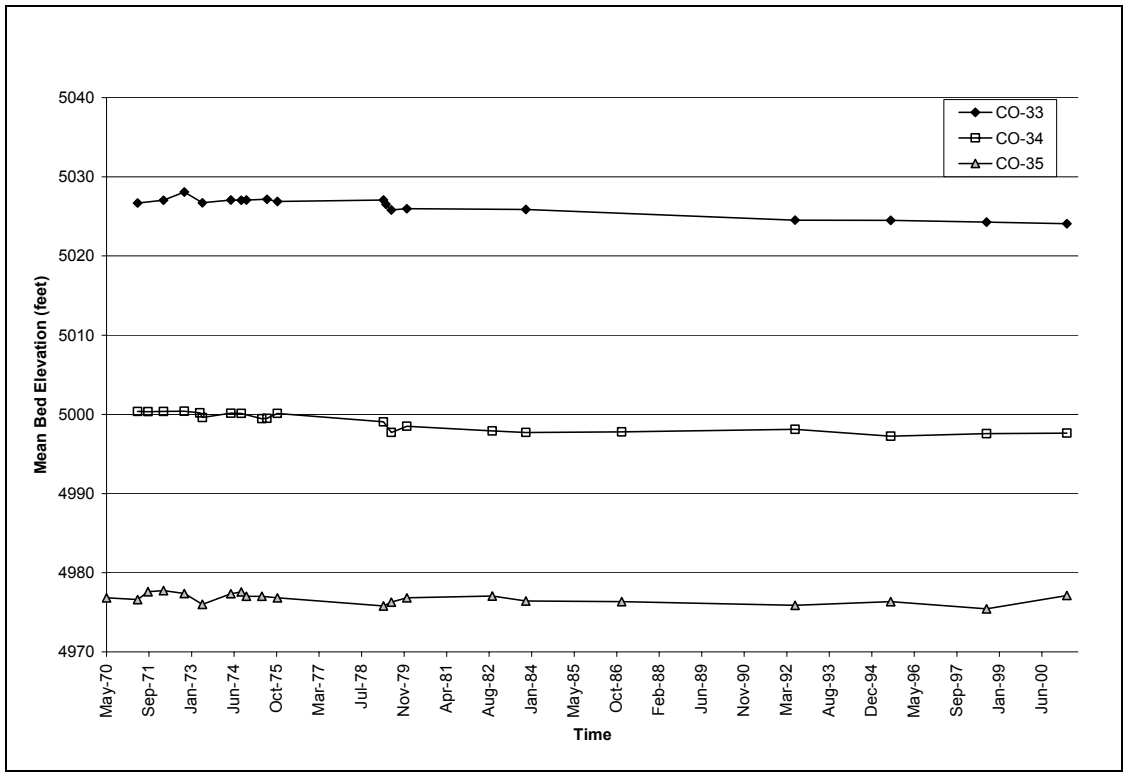


**Figure 3-7: Change in mean bed elevation with time at CO-lines.**

In addition, mean bed elevations were calculated for the years of 1962, 1972, 1992 and 2001 through utilizing HEC-RAS® results. The first three sets of years used available agg/deg line surveys, while the 2001 computations used available CO, CR and CA-line surveys. Table 3-5 summarizes the results from the agg/deg line surveys and the mean bed elevations determined using HEC-RAS®. These results are depicted in Figure 3-8. It can be seen that the average mean bed elevation from 1962 to 1972 from subreaches 2 and 3 remained essentially constant while subreach 1 showed slight aggradation (Figure 3-8). A degradational trend was seen in all three subreaches from 1972 to 1992, with subreach 1 degrading the most (Table 3-5). The degradational trend continued in all the subreaches from 1992 to 2001 according to the HEC-RAS® analysis (Figure 3-8). These trends are not observed in the mean bed elevation profile plots (Figures 3-9 and 3-10).

**Table 3-5: Reach-averaged change in mean bed elevation in feet from agg/deg surveys.**

| Reach # | 1962-72 Agg/Deg (ft) | 1972-92 Agg/Deg (ft) | 1962-92 Agg/Deg (ft) |
|---|---|---|---|
| **1** | 0.37 | -2.47 | -2.10 |
| **2** | -0.09 | -2.38 | -2.48 |
| **3** | -0.09 | -2.43 | -2.54 |
| ***Total*** | 0.09 | -2.45 | -2.36 |

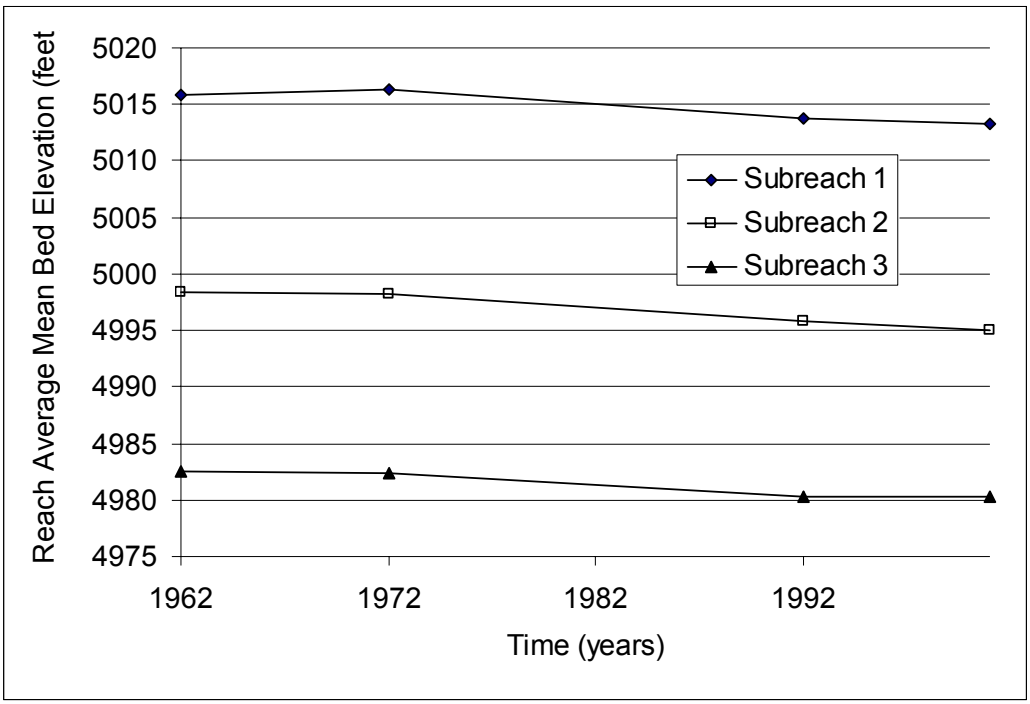


**Figure 3-8: Time series of reach-averaged mean bed elevation, computed from the 1962, 1972 and 1992 agg/deg surveys and 2001 CO, CR and CA-line surveys.**

The reach-averaged aggradation from 1962 to 1972 is approximately 0.1 feet and the reach-average degradation from 1972 to 1992 is approximately 2.5 feet (Table 3-4). The net change in mean bed elevation between 1962 and 1992 is approximately 2.4 feet of degradation. From 1992 to 2001 the bed aggraded as much as 3 feet. Subreach 1 degraded slightly (less than one foot on average), subreach 2 aggraded slightly (less than one foot on average) and subreach 3 aggraded significantly (upwards of 3 feet). This can be seen in Figure 3-9. CO-line cross section plots reveal these trends as well (Appendix B).

Some sections of the channel degraded between 1962 and 1972. Most of these sections are located in subreaches 2 and 3. Maximum aggradation (3 feet) occurred in subreach 3 between 1992 and 2001. Maximum degradation (3.5 feet) occurred in subreach 2 between 1962 and 1992. The reach-averaged change in mean bed elevation (degradation) from 1972 to 1992 was much larger than the reach-averaged change (aggradation) between 1962 and 1972. As a result, the net trend in mean bed elevation is degradational between 1962 and 1992 (Table 3-5 and Figure 3-9).

Longitudinal profiles of the mean bed elevation for the entire reach and subreaches are presented in Figures 3-9 and 3-10. The majority of the reach aggraded between 1962 and 1972. The entire reach degraded from 1972 to 1992. The 1992 elevations are lower than 1962 elevations.

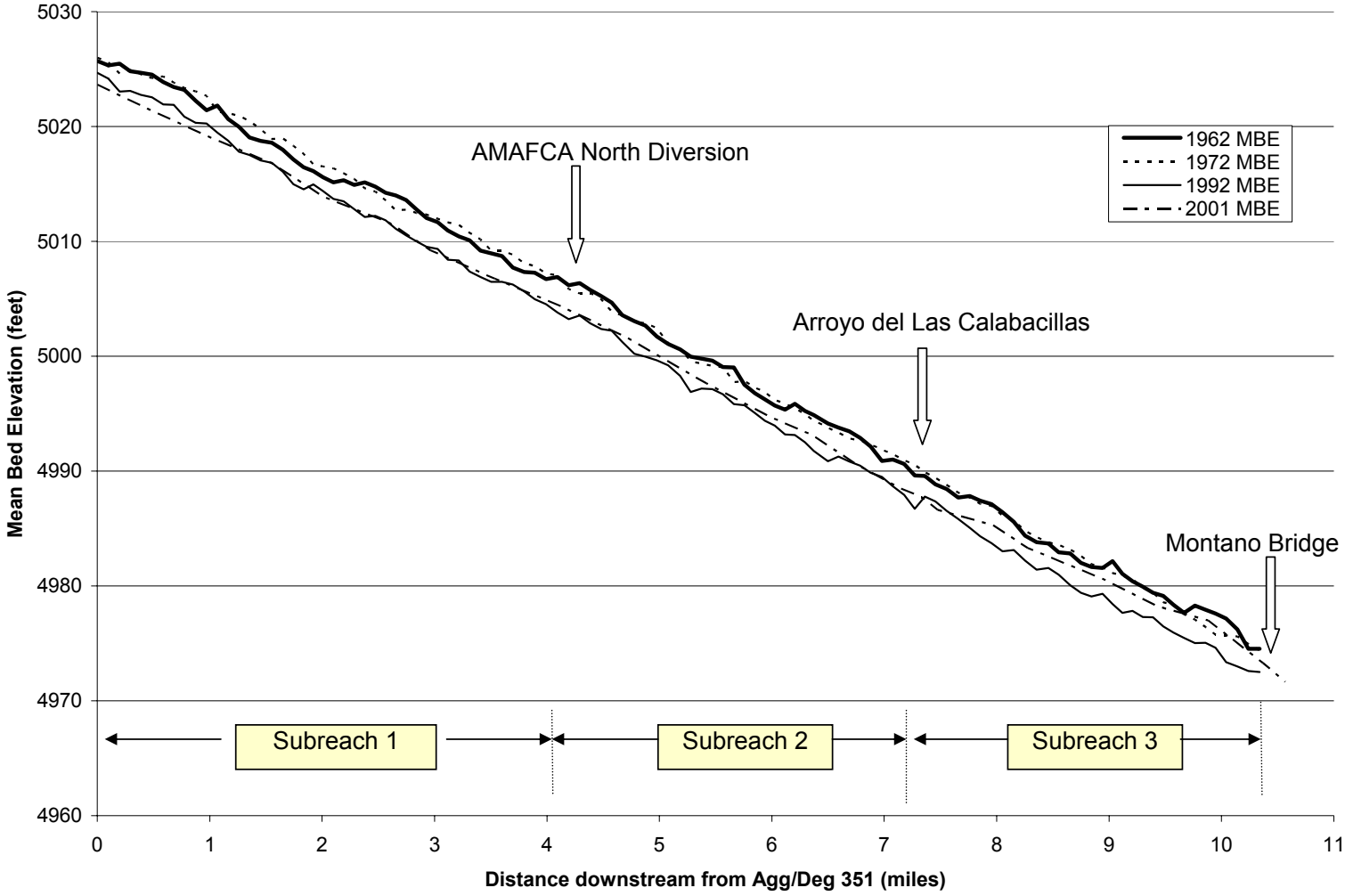


**Figure 3-9: Mean bed elevation profile of entire Corrales Reach. Distance downstream is measured from agg/deg 351.**

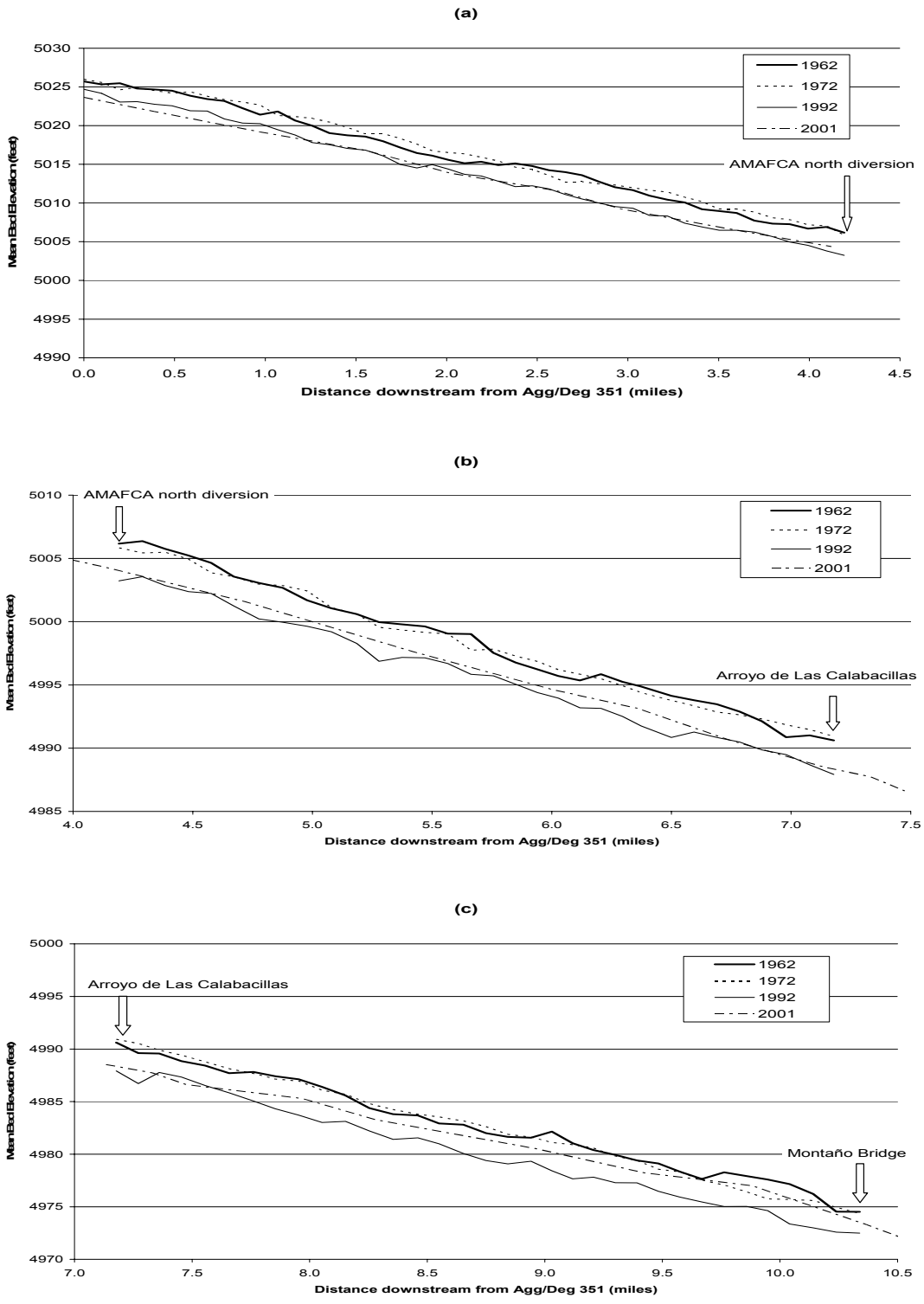


**Figure 3-10: Mean bed elevation profiles of the subreaches from the agg/deg surveys. (a) Subreach 1, (b) Subreach 2, (c) Subreach 3.**

*Channel Cross Sections*

The cross section for CO-33 representing the channel conditions in 1971 and 1998 is graphically displayed in Figure 3-11. The 1971 cross-section represents the pre-dam conditions, while the 1998 cross-section represents post-dam conditions. It can be seen that as much as five feet of degradation has occurred since the closure of Cochiti Dam. These results are consistent with the trend of the longitudinal profiles (Figure 3-9). Similar results can be seen in the other two cross sections. All CO-line cross-sections are attached in Appendix B. These results are displayed both graphically.

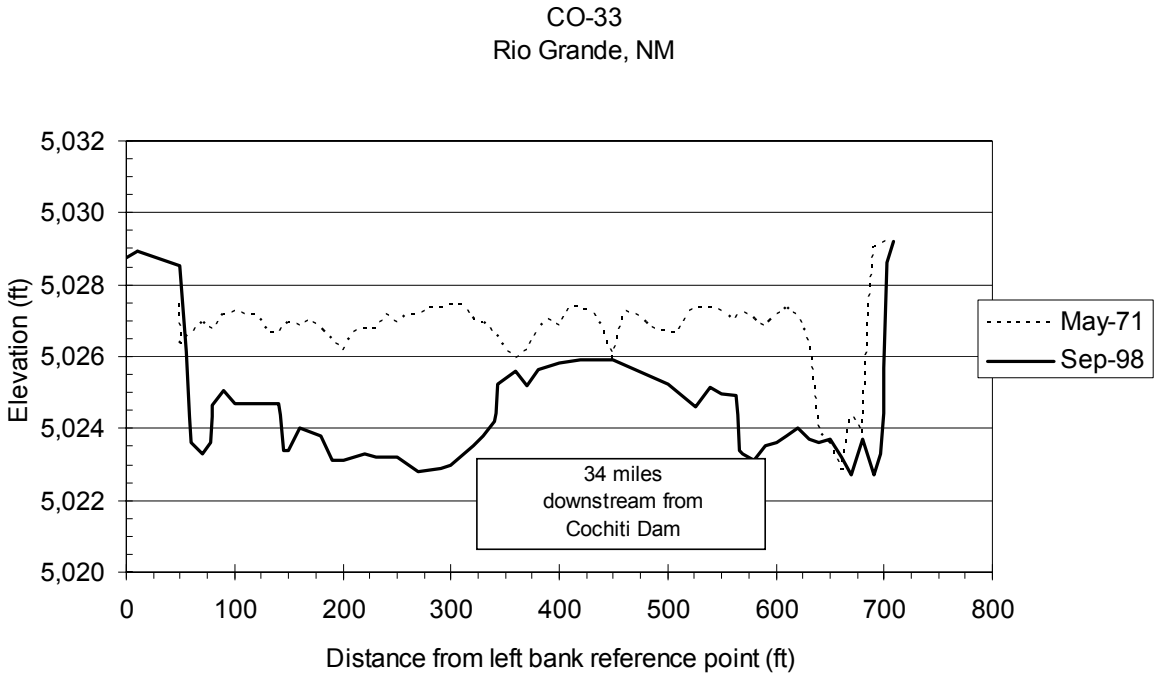


**Figure 3-11: Cross section CO-33 representing pre and post-dam conditions.**

*Friction Slope*

A time series of the energy grade is shown in Figure 3-12. The energy grade line slopes in the entire reach as well as in the subreaches decreased from 1962 to 1972 and increased from 1972 to 1992. From 1992 to 2001, subreaches 1 and 2 decreases while subreach 3 continued to increase. These results are not in agreement with the aggradational and degradational trends observed during these periods (Figures 3-9 and 3-10).

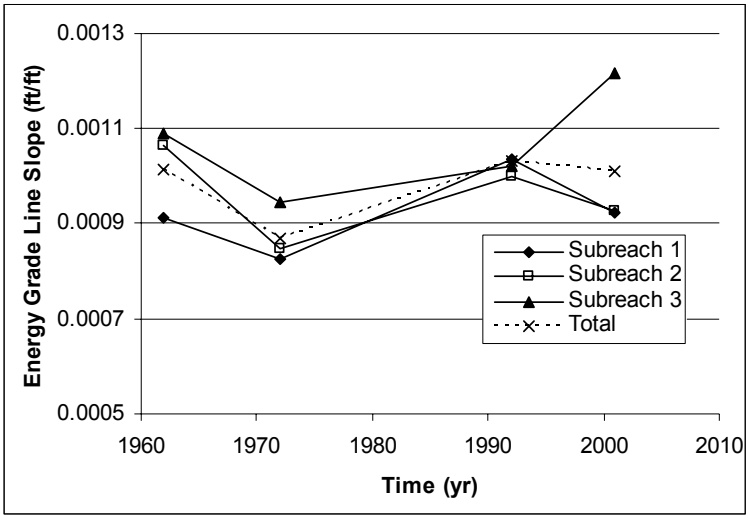


**Figure 3-12: Time series of energy grade line slope of the subreaches and the entire reach from HEC-RAS® modeling results.**

*Water Surface Slope*

Figure 3-13 shows a time series of the water surface slope. Water surface slope of the entire reach remains nearly constant from 1962 to 1992. The slope of subreach 3 increased from 1962 to 2001. Subreaches 1 and 2 follow similar patterns for the time periods of 1962 to 1972 and 1992 to 2001 where each of their slopes decreased. From 1972 to 2001 the water surface slope of Subreach 1 increased while the slope of subreach 2 decreased. The averaged water surface slope decreased from 1962 to 2001.

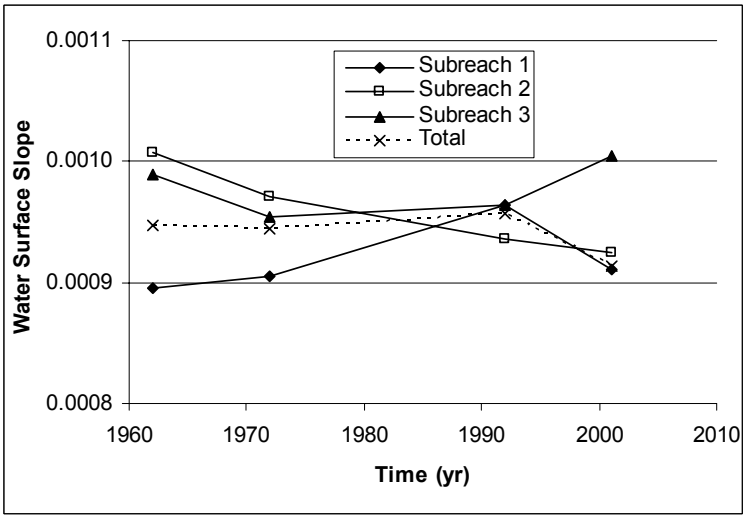


**Figure 3-13: Time series of water surface slope of the subreaches and the entire reach from HEC-RAS® modeling results.**

### Channel Geometry

The temporal changes in reach-averaged channel geometry are summarized in Figure 3-14. The changes in channel geometry generally show similar trends for all subreaches from 1962 to 1992, which are increases in mean velocity, width-to-depth ratio and wetted perimeter and decreases in cross section area and average depth from 1962 to 1972. From 1972 to 1992 the opposite trends are observed, that being an increase in cross section area and average depth and decrease in velocity, width-to-depth ratio and wetted perimeter. Subreaches 1 and 2 continue to follow similar trends from 1992 to 2001, which is an increase in velocity and depth, and a decrease in flow area, width-depth ratio and wetted perimeter. Subreach 3 experiences an increase in velocity, average depth, width-to-depth ratio and wetted perimeter and a decrease in flow area from 1992 to 2001.

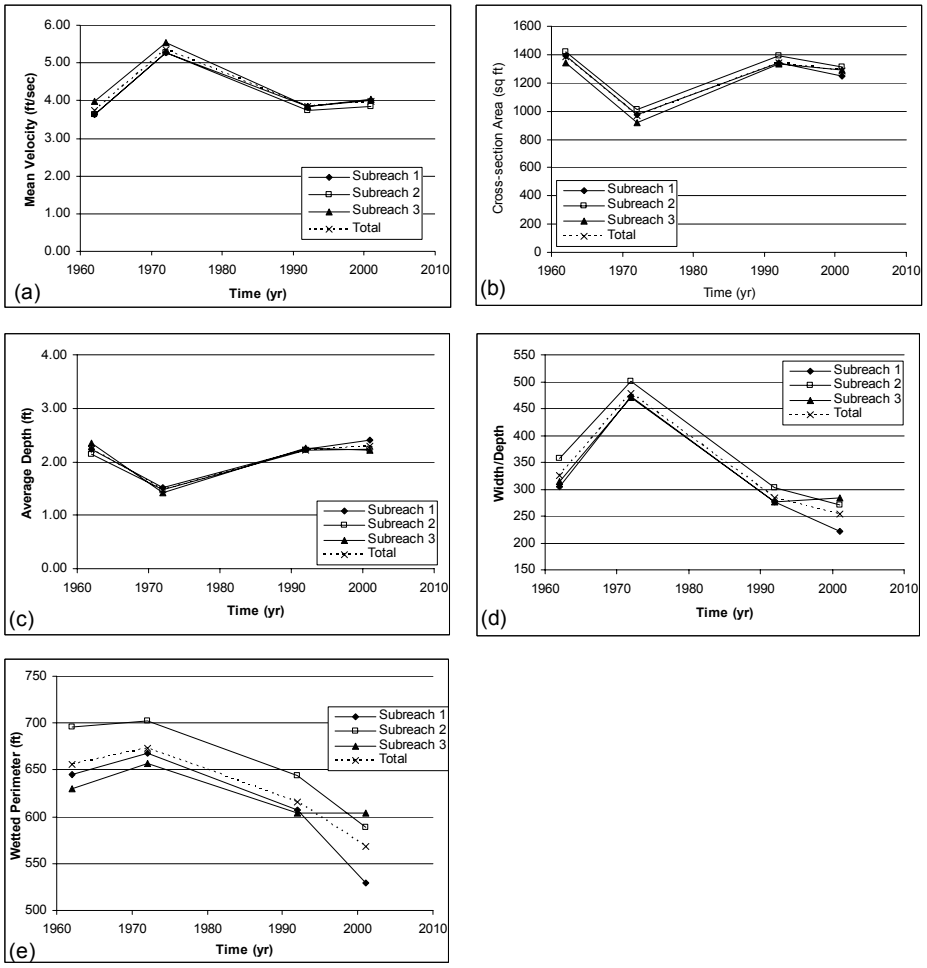


**Figure 3-14: Reach-averaged main channel geometry from HEC-RAS® results for Q = 5,000 cfs. (a) mean velocity, (b) cross-section area, (c) average depth, (d) width-to-depth ratio, (e) wetted perimeter.**

*Width*

Active channel width time series from the digitized vegetation boundaries are presented in Figure 3-15. All of the reaches exhibit declining width with time. Maximum changes in channel width occurred from 1918 to 1962. All the subreaches achieved nearly the same width after 1962. From 1962 to 1972, the channel width increased slightly. After 1972, channel width began to decline again at a slower rate than prior to 1962. The main-channel widths predicted by the HEC-RAS® model at 5,000 cfs (Figure 3-16) exhibit similar trends observed in Figure 3-15 for the 1962 to 2001 time period.

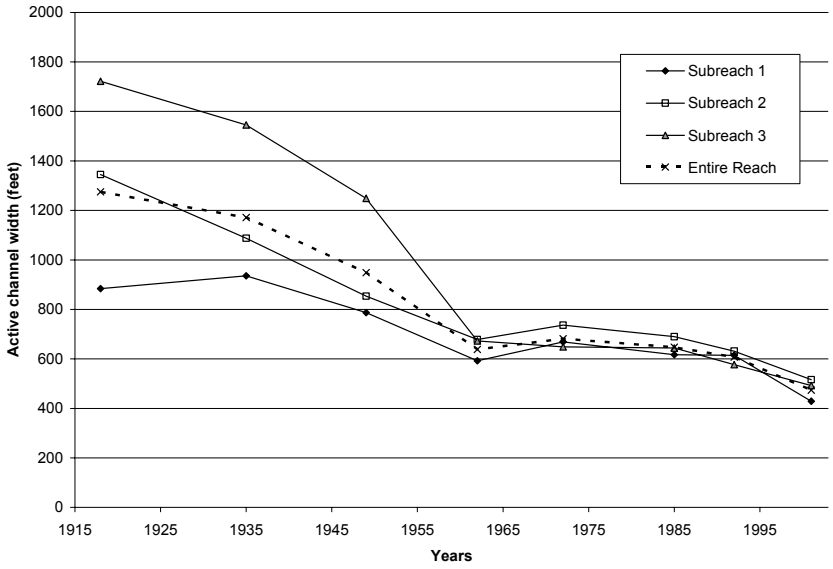


**Figure 3-15: Reach averaged active channel width from digitized aerial photos (GIS).**

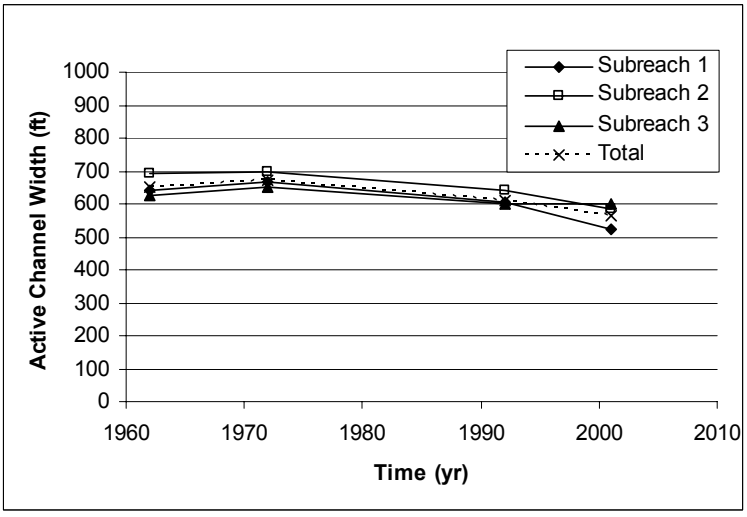


**Figure 3-16: Reach averaged main channel width from HEC-RAS® at Q =5,000 cfs.**

*Overbank Flow/Channel Capacity*

Most of the flow occurs in the main channel and not in the overbank region in 1962, 1972, 1992 and 2001 according to the HEC-RAS® results at 5,000 cfs. However, more overbank flow is seen in 1972 which demonstrates the evident aggradational trend during the 1962 to 1972 time period, which is seen in the mean bed elevation profiles (Figure 3-9).

## Sediment

*Bed Material*

The median grain sizes from the bed material samples at the Bernalillo gage and CO lines are comprised of fine sand for all the subreaches for 1962 and 1972. In 1992, the median size material is medium sand to coarse gravel in subreach 1, fine sand to coarse gravel in subreach 2 and medium sand to coarse gravel in subreach 3. The median grain size in 2001 consisted of medium sand to medium gravel in subreach 1, medium sand to very coarse sand in subreach 2 and medium sand to coarse sand in subreach 3. Table 3-6 summarizes these results.

**Table 3-6: Range of median grain sizes in Subreaches 1, 2 and 3 for 1962, 1972, 1992, and 2001.**

| | Median Bed Material Size | | |
|---|---|---|---|
| | **Subreach 1** | **Subreach 2** | **Subreach 3** |
| **1962** | fine sand | fine sand | fine sand |
| **1972** | fine sand | fine sand | fine sand |
| **1992** | medium sand to coarse gravel | fine sand to coarse gravel | medium sand to coarse gravel |
| **2001** | medium sand to medium gravel | medium sand to very coarse sand | medium sand to coarse sand |

In general, the grain size coarsens with time from 1962 to 1992. This trend likely due to sediment detention by Cochiti Dam and tributary sediment detention structures, which leads to clear water scour. However, this does not account for the finer material observed in 2001. This finer material is likely due the time of year in which the sediment was collected. The 2001 data were collected in early April and late August when low flows are common, which wouldn't likely transport the sand off the bed. Conversely, the 1992 data were collected in July when high flows are more likely to be observed (Figure 2-1). These high flows would likely transport the smaller sand particles downstream, leaving behind the coarser gravels.

A histogram showing how the $D_{50}$ and $D_{84}$ sizes change with time for CO-33 is shown in

Figure 3-17. It can be seen that both the $D_{50}$ and $D_{84}$ values coarsen after 1974, which roughly corresponds to the closure of Cochiti Dam. Histograms for the remaining two CO-lines and for eight CA-lines (CA-1, 2, 4, 6, 8, 10, 12, and 13) are attached in Appendix D.

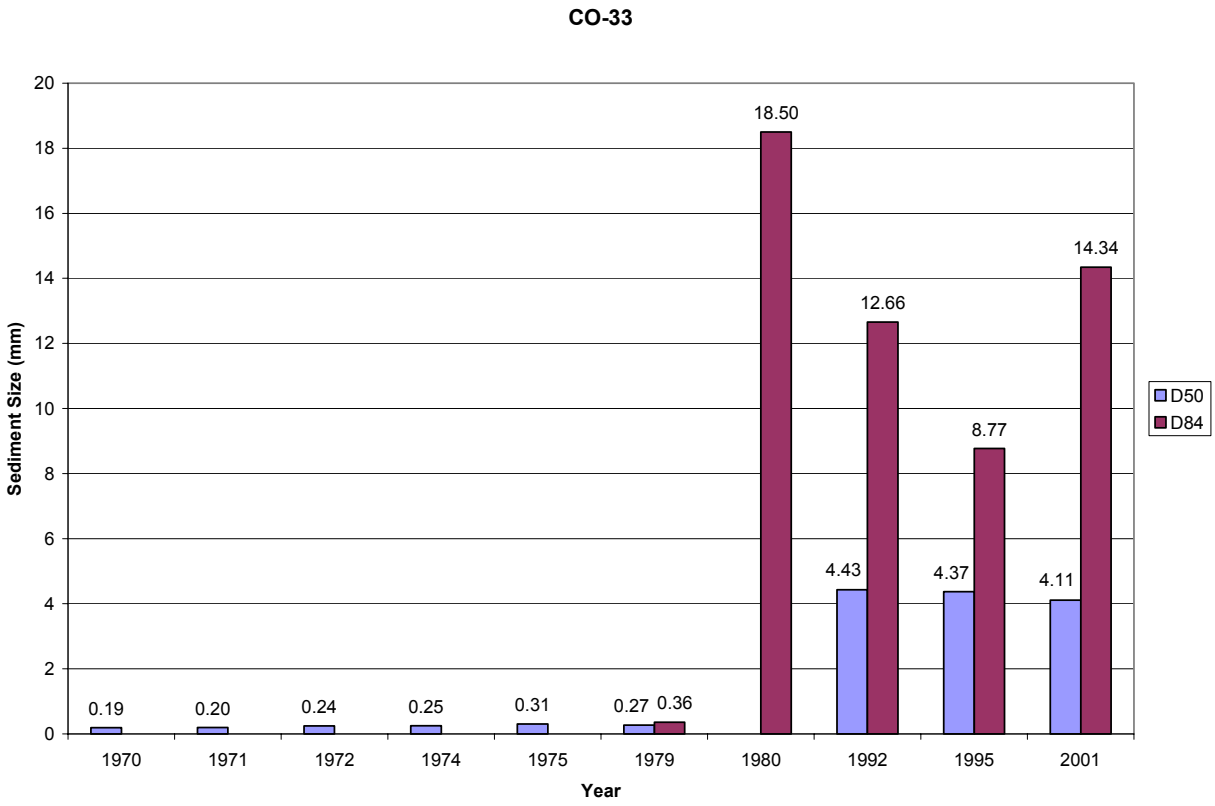


**Figure 3-17: Histogram depicting the $D_{50}$ and $D_{84}$ change with time for CO-33.**

The average, maximum, minimum and standard deviation of the median bed material sizes at each station were computed for all the years. Table 3-7 presents these results. The 1992 bimodal character of the bed material size distributions of the Corrales Reach can be best described through these statistics.

**Table 3-7: Median grain size statistics from the bed material samples at Bernalillo gage, CO-lines, CA-lines and CR-lines.**

| | | | | | $d_{50}$ | | | | | |
|---|---|---|---|---|---|---|---|---|---|---|
| Reach | Year | Station | Number of Observations | Range of flow discharges (cfs) | Minimum value (mm) | Maximum value (mm) | Mean value (mm) | Standard deviation (mm) | # of d50 in the sand range | # of d50 in the gravel range |
| Entire reach | 1961 | Bernalillo Gage | 3 | 2140-3850 | 0.20 | 0.22 | 0.21 | 0.01 | 3 | 0 |
| Subreach 1 | 1972 | CO-33 | 2 | 996-1010 | 0.21 | 0.27 | 0.24 | 0.05 | 2 | 0 |
| Subreach 2 | 1972 | CO-34 | 2 | 607-1010 | 0.179 | 0.181 | 0.180 | 0.001 | 2 | 0 |
| Subreach 3 | 1972 | CO-35 | 2 | 685-1250 | 0.179 | 0.249 | 0.21 | 0.050 | 2 | 0 |
| Subreach 1 | 1992 | CO-33 | 5 | 517 | 0.70 | 16.05 | 5.73 | 6.29 | 2 | 3 |
| Subreach 2 | 1992 | CA-1 | 8 | 3260 | 0.40 | 0.76 | 0.53 | 0.15 | 8 | 0 |
| Subreach 2 | 1992 | CA-4 | 5 | 3260 | 0.31 | 22.45 | 8.9 | 11.7 | 3 | 2 |
| Subreach 2 | 1992 | CA-6 | 5 | 3030 | 0.16 | 4.49 | 1.30 | 1.80 | 4 | 1 |
| Average Subreach 2 | 1992 | CA-1,CA-4, CA-6 | 18 | 3030-3260 | 0.16 | 22.45 | 3.07 | 6.85 | 15 | 3 |
| Subreach 3 | 1992 | CO-35 | 5 | 575 | 0.340 | 0.460 | 0.45 | 0.05 | 5 | |
| Subreach 3 | 1992 | CA-8 | 6 | 3030 | 0.4 | 44.93 | 14.44 | 21.41 | 4 | 2 |
| Subreach 3 | 1992 | CA-10 | 6 | 3030 | 0.33 | 8.4 | 1.85 | 3.21 | 5 | 1 |
| Subreach 3 | 1992 | CA-12 | 6 | 2610 | 0.36 | 0.75 | 0.51 | 0.15 | 6 | 0 |
| Average Subreach 3 | 1992 | CO-35, CA-8, CA-10, CA-12 | 23 | 575-3030 | 0.33 | 44.93 | 4.48 | 11.98 | 20 | 3 |
| Subreach 1 | 2001 | CO-33 | 4 | 422-892 | 0.78 | 12.44 | 4.11 | 5.59 | 2 | 2 |
| Subreach 1 | 2001 | CR-355 | 1 | 2130 | 0.56 | 0.56 | 0.56 | 0 | 1 | 0 |
| Subreach 1 | 2001 | CR-361 | 1 | 2410 | 0.5 | 0.5 | 0.5 | 0 | 1 | 0 |
| Subreach 1 | 2001 | CR-367 | 1 | 2410 | 0.54 | 0.54 | 0.54 | 0 | 1 | 0 |
| Subreach 1 | 2001 | CR-372 | 1 | 2410 | 0.72 | 0.72 | 0.72 | 0 | 1 | 0 |
| Subreach 1 | 2001 | CR-378 | 1 | 2410 | 0.57 | 0.57 | 0.57 | 0 | 1 | 0 |
| Subreach 1 | 2001 | CR-382 | 1 | 2410 | 0.48 | 0.48 | 0.48 | 0 | 1 | 0 |
| Subreach 1 | 2001 | CR-388 | 1 | 2460 | 0.45 | 0.45 | 0.45 | 0 | 1 | 0 |
| Subreach 1 | 2001 | CR-394 | 1 | 2460 | 0.53 | 0.53 | 0.53 | 0 | 1 | 0 |
| Average Subreach 1 | 2001 | CO-33, CR-355, 361, 367, 372, 378, 382, 388, 394 | 12 | 422-2460 | 0.45 | 12.44 | 1.73 | 3.41 | 10 | 2 |
| Subreach 2 | 2001 | CO-34 | 3 | 422-952 | 0.5 | 0.84 | 0.63 | 0.18 | 3 | 0 |
| Subreach 2 | 2001 | CA-1 | 2 | 824-892 | 0.59 | 1.32 | 0.92 | 0.52 | 2 | 0 |
| Subreach 2 | 2001 | CA-2 | 1 | 892 | 0.51 | 0.51 | 0.51 | 0 | 1 | 0 |
| Subreach 2 | 2001 | CA-6 | 2 | 438 | 0.59 | 0.59 | 0.59 | 0 | 2 | 0 |
| Subreach 2 | 2001 | CR-400 | 1 | 2600 | 0.49 | 0.49 | 0.49 | 0 | 1 | 0 |
| Subreach 2 | 2001 | CR-413 | 1 | 2600 | 0.69 | 0.69 | 0.69 | 0 | 1 | 0 |
| Average Subreach 2 | 2001 | CO-34, CA-1, 2, 6, CR-400, 413 | 10 | 422-2600 | 0.49 | 1.32 | 0.67 | 0.25 | 10 | 0 |
| Subreach 3 | 2001 | CO-35 | 4 | 438-952 | 0.49 | 0.59 | 0.52 | 0.050 | 4 | 0 |
| Subreach 3 | 2001 | CA-9 | 1 | 824 | 0.57 | 0.57 | 0.57 | 0 | 1 | 0 |
| Subreach 3 | 2001 | CA-12 | 3 | 438-952 | 0.63 | 0.81 | 0.7 | 0.1 | 3 | 0 |
| Subreach 3 | 2001 | CA-13 | 1 | 1050 | 0.47 | 0.47 | 0.47 | 0 | 1 | 0 |
| Subreach 3 | 2001 | CR-443 | 1 | 1050 | 0.36 | 0.36 | 0.36 | 0 | 1 | 0 |
| Subreach 3 | 2001 | CR-448 | 1 | 1050 | 0.48 | 0.48 | 0.48 | 0 | 1 | 0 |
| Subreach 3 | 2001 | CR-458 | 1 | 1050 | 0.46 | 0.46 | 0.46 | 0 | 1 | 0 |
| Subreach 3 | 2001 | CR-462 | 1 | 1050 | 0.38 | 0.38 | 0.38 | 0 | 1 | 0 |
| Average Subreach 3 | 2001 | CO-35, CA-9, 12, 13, CR-443, 448, 458, 462 | 13 | 438-1050 | 0.36 | 0.81 | 0.53 | 0.12 | 13 | 0 |

All of the median grain sizes ($D_{50}$) are in the sand range for 1961 and 1972. Some of the samples contain median grain sizes in the gravel range in 1992. Gravel sediment particles were surveyed at both high (3,260 cfs) and low (517 cfs) flows. A slight shift from coarser to finer material can be observed in the material distribution curves for all three subreaches from 1992 to 2001 (Figures 3-18 to 3-20).

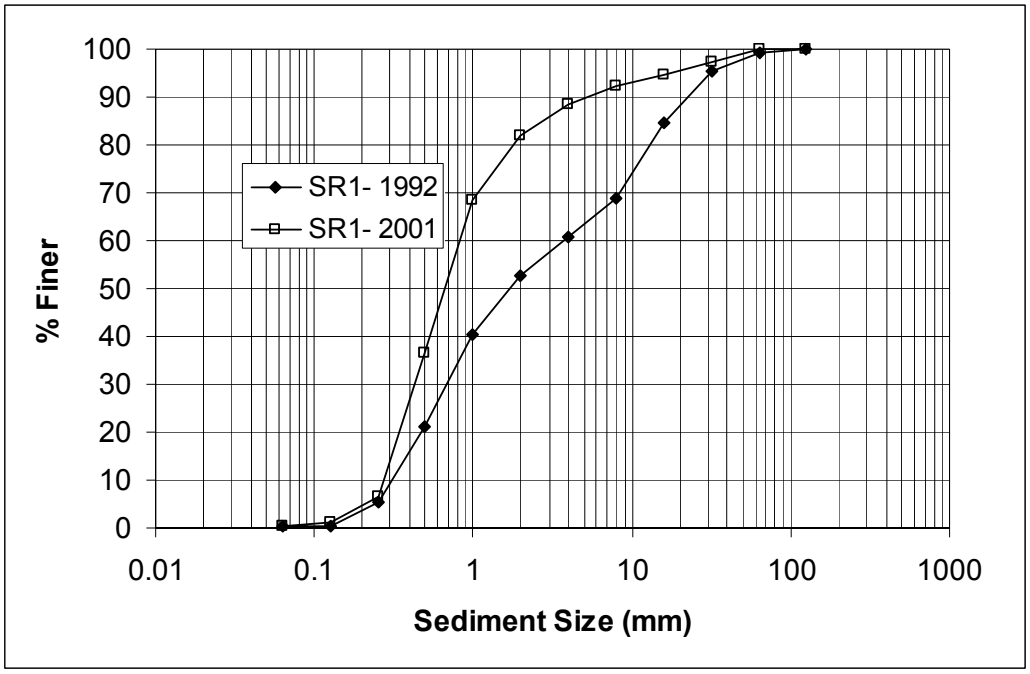


**Figure 3-18: Comparison of 1992 and 2001 bed material gradation curves for subreach 1.**

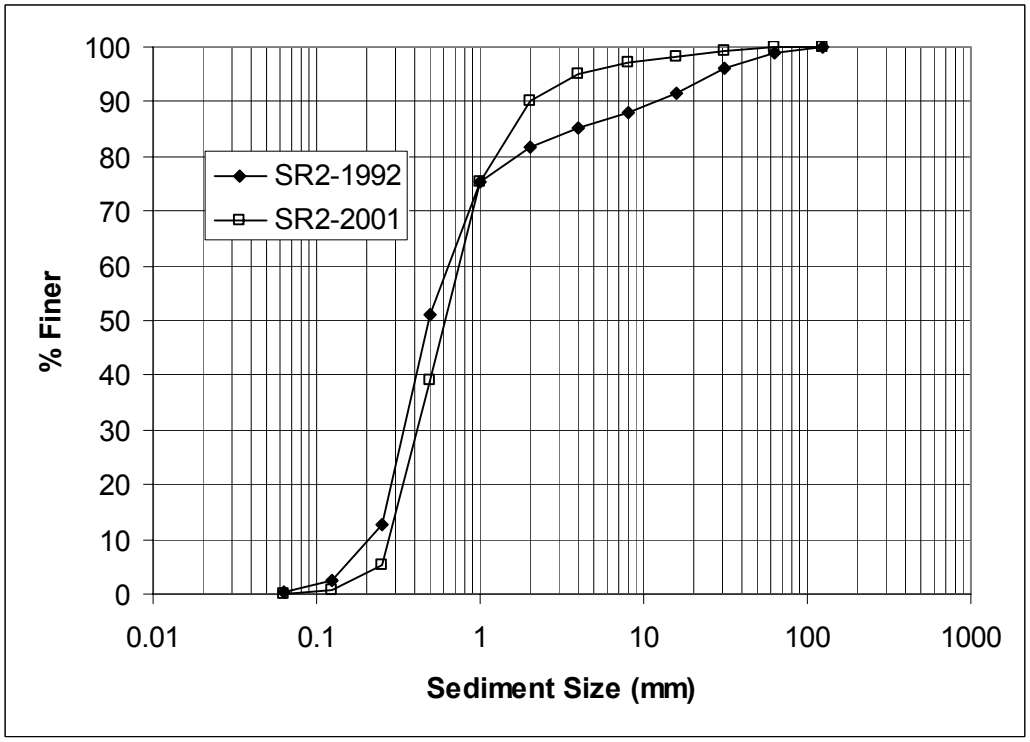


**Figure 3-19: Comparison of 1992 and 2001 bed material gradation curves for subreach 2.**

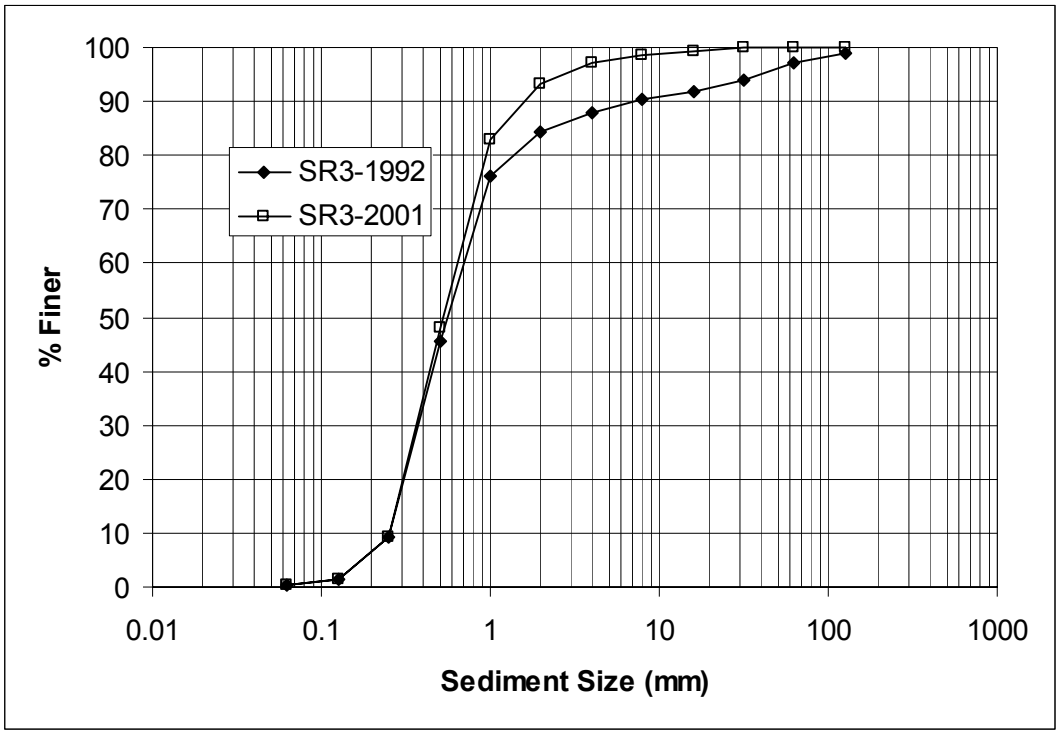


**Figure 3-20: Comparison of 1992 and 2001 bed material gradation curves for subreach 3.**

Figure 3-21 shows the averaged bed material size distribution curves for each subreach and the entire reach for 2001. These curves were used as input for the 2001 sediment transport and equilibrium analyses. The 1992 gradation curves in Figures 3-18 to 3-20 were also used in the sediment transport analysis for that year.

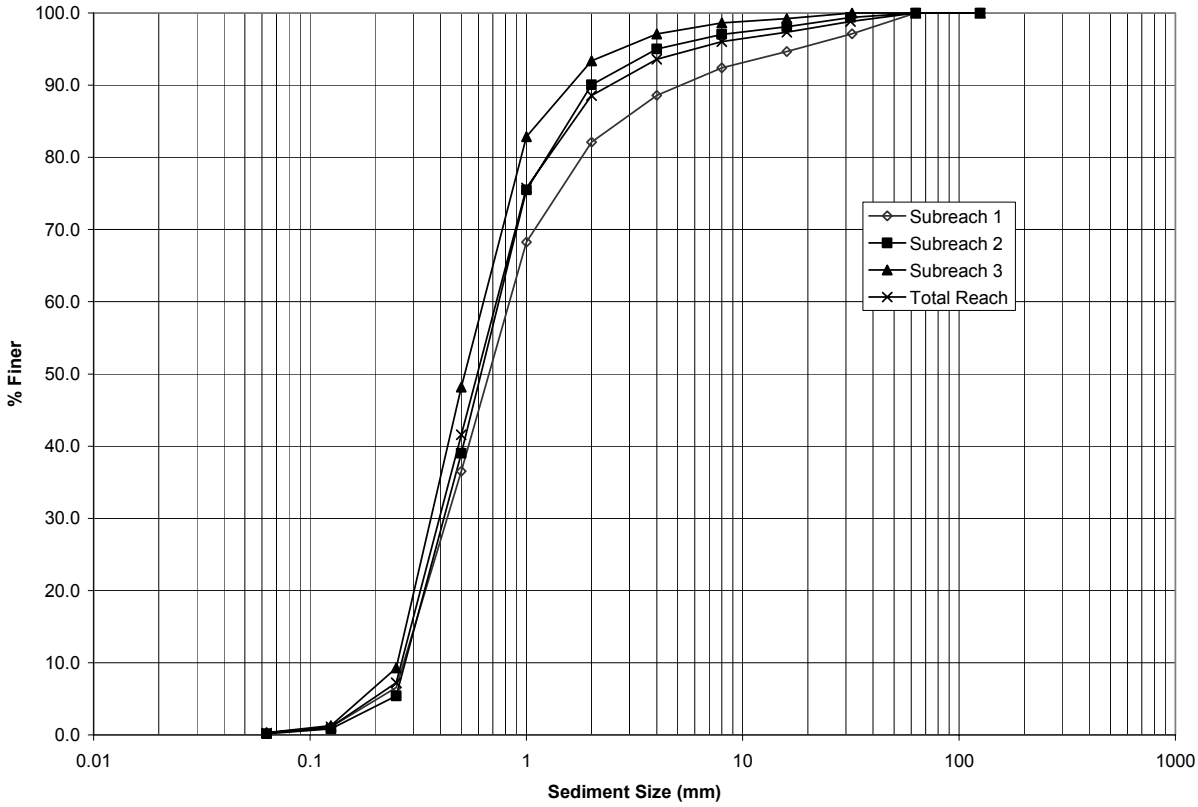


**Figure 3-21: 2001 Bed-material samples used in the sediment transport and equilibrium analyses.**

# 4 SUSPENDED SEDIMENT AND WATER HISTORY

## 4.1 METHODS

Water and sediment flow trends in the Corrales Reach were analyzed through the development of single-mass curves and double-mass curves. Not enough suspended sediment data were available to generate difference-mass curves and perform a sediment continuity analysis of the reach.

The following curves were developed for the Bernalillo and Albuquerque gages, for the entire period of record:

- Mass curve of water discharge (acre-feet/year) from 1942 to 2000.
- Mass curve of sediment discharge (tons/year) from 1956 to 1999.
- Double mass curve with water and sediment discharge for trends in sediment concentration (mg/l) from 1956 to 1999.

The slopes of each curve and the time periods of breaks in the curves were also estimated.

## 4.2 RESULTS

### Single Mass Curves

*Discharge Mass Curve*

The discharge mass curve for Bernalillo and Albuquerque gages (Figure 4-1) have similar trends, indicating that there is not significant water input from the ephemeral tributaries between the two gages. There are three breaks in slope in the discharge mass curve (1942-1978, 1978 - 1987 and 1987 – 2000 periods), with an increase in annual discharge rate from 1978 to 1987 and a slight decrease from 1987 to 2000 (Figure 4-1 and Table 4-1). The drier water discharge period (1942-1978) at Bernalillo and Albuquerque Gages coincides with the drier water period at Cochiti Gage, as identified by Richard (2001). These slope breaks in the mass curve represent changes in water regime in the river. These changes may be due to changes in climate and/or flood management or regulation in the Rio Grande Basin.

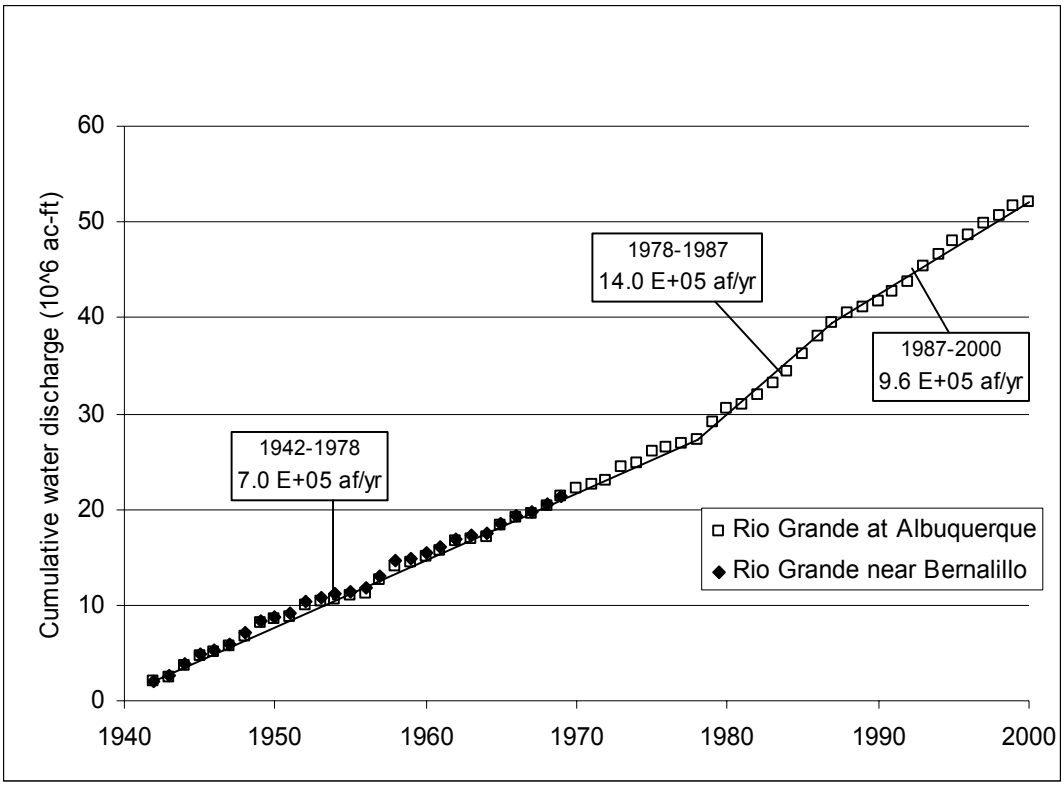


**Figure 4-1: Discharge mass curve at Bernalillo and Albuquerque Gages (1942-2000).**

**Table 4-1: Summary of the discharge mass curve slope breaks at Bernalillo and Albuquerque Gages (1942-2000).**

| Time Period | Slopes of the water discharge mass curve (10^6 ac-ft/yr) |
|---|---|
| 1942-1978 | 7.0 E+05 |
| 1978-1987 | 14.0 E+05 |
| 1987-2000 | 9.6 E+05 |

*Suspended Sediment Mass Curve*

The suspended sediment mass curve for Bernalillo and Albuquerque shows nine slope breaks (Figure 4-2). In general, the slopes are steeper from 1956 to 1973 than after 1973. The slope values range from 2.3 to 10.8 tons per year between 1956 and 1973. After 1973, the slope values are between 0.25 to 2.79 tons per year. This change in sediment rate in 1973

coincides with the closure of Cochiti Dam. There was an increase of suspended sediment discharge from 1993 to 1995 (2.79 E+06 tons/yr) with respect to the 1978-1993 discharges (1.11 E+06 tons/yr and 0.25 E+06 tons/yr). However, the 1995-1999 suspended sediment discharge has decreased to 0.8 E+06 tons/yr and is comparable to the 1978-1985 sediment discharge (1.11 E+06 tons/yr).

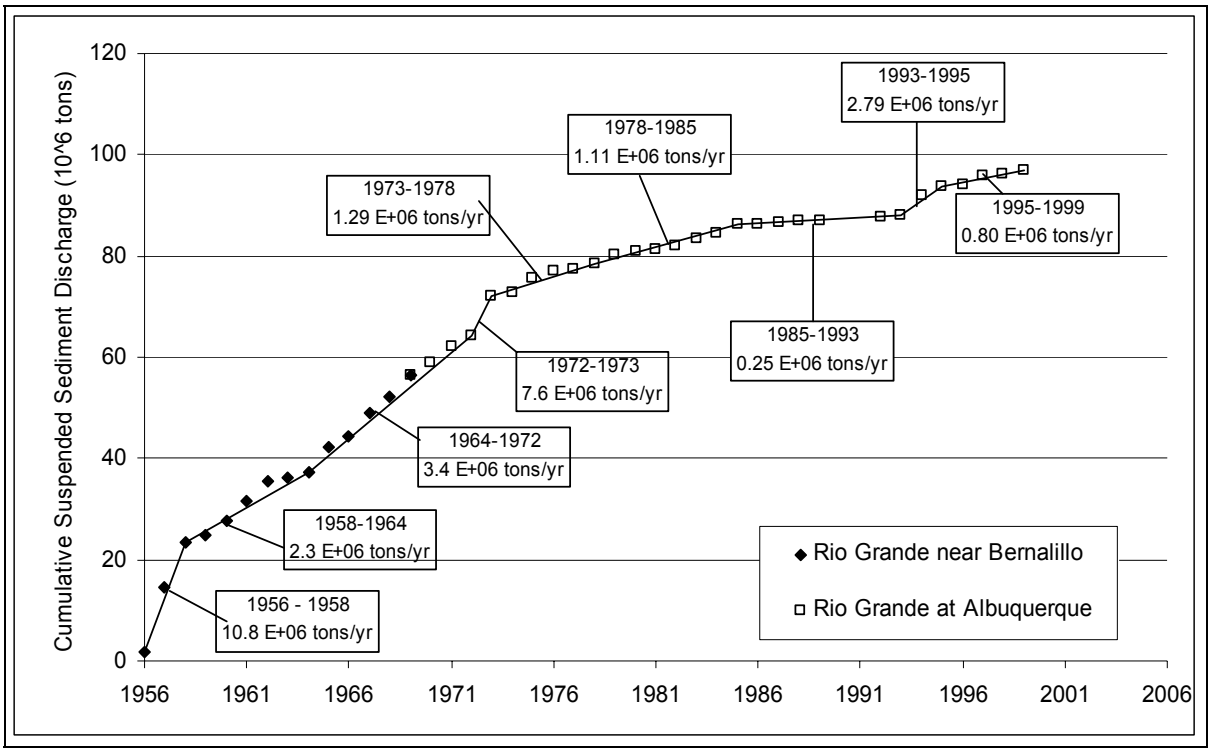


**Figure 4-2: Suspended sediment mass curve at Bernalillo and Albuquerque Gages (1956-1999).**

**Table 4-2: Summary of the suspended sediment discharge mass curve slope breaks at Bernalillo and Albuquerque Gages (1956-1999).**

| Time Period | Slopes of the suspended sediment discharge mass curve (10^6 ac-ft/yr) |
|---|---|
| 1956-1958 | 1.08E+07 |
| 1958-1964 | 2.30E+06 |
| 1964-1972 | 3.40E+06 |
| 1972-1973 | 7.55E+06 |
| 1973-1976 | 1.29E+06 |
| 1976-1985 | 1.11E+06 |
| 1985-1993 | 2.48E+05 |
| 1993-1995 | 2.79E+06 |
| 1995-1999 | 8.01E+05 |

### Double Mass Curve

The double mass curve of cumulative water discharge versus cumulative sediment discharge shows the changes of suspended sediment concentration with time. Figure 4-3 shows higher concentrations of suspended sediment from 1956 to 1973 with average concentration varying from 3,741 mg/l to 6,670 mg/l. After 1973, the concentration does not exceed 1,602 mg/l. In general, the double mass curve shows a similar trend as the suspended sediment single mass curve. An average concentration of 664 mg/l has persisted from 1995 to 1999 and is close to the 1978-1984 average concentration (650 mg/l). Table 4-3 summarizes the suspended sediment concentrations at Bernalillo and Albuquerque Gages between 1956 and 1999.

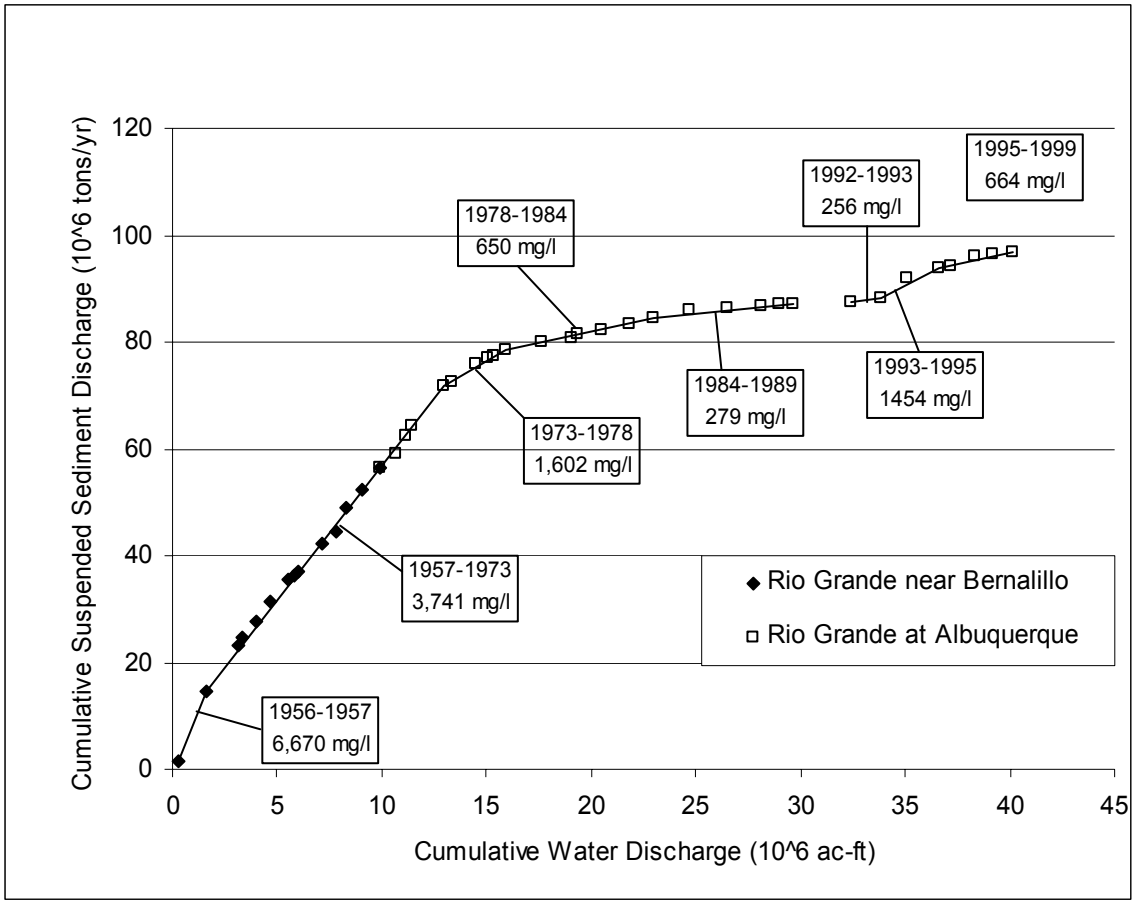


**Figure 4-3: Cumulative discharge vs. cumulative suspended sediment load at Rio Grande at Bernalillo and Rio Grande at Albuquerque (1956 - 1999).**

**Table 4-3: Summary of suspended sediment concentrations at Bernalillo and Albuquerque Gages (1956-1999).**

| Time Period | Concentration (mg/l) |
|---|---|
| 1956-1957 | 6670 |
| 1957-1973 | 3741 |
| 1973-1978 | 1602 |
| 1978-1984 | 650 |
| 1984-1989 | 279 |
| 1992-1993 | 256 |
| 1993-1995 | 1465 |
| 1995-1999 | 664 |

# 5 EQUILIBRIUM STATE PREDICTORS

## 5.1 METHODS

### Sediment Transport Analysis

The purpose of this section is to compare the subreach transport capacity with: 1) the incoming sand load (0.0625 mm < $d_s$ < 2 mm); and 2) the incoming bed material load (0.30 mm < $d_s$ < 2 mm).

Field observations performed by the USBR indicate that sand size particles are mobile at all flows greater than 300 cfs as bedload material and become suspended at flows greater than 3,000 cfs (Massong pers. communication 2001). According to these field observations, it is believed that the bed material load is comparable to the sand load (0.0625 mm and 2 mm) (Massong pers. communication 2001).

However, very fine and fine sand size particles (0.0625 mm to 0.25 mm) are not found in large quantities in the bed ($D_{10}$ of bed material = 0.27 mm (Figure 3-21)) at flows close to 5,000 cfs, which suggest that they behave as washload (Appendix H, Table 5-1). In addition, the amount of sand particles in suspension finer than 0.27 mm ($D_{10}$ of the bed material) is approximately 65% or more at flows close to 5,000 cfs (Table 5-1, Appendix H). As a result, the bed material load comprises only the sediment particles coarser than 0.27 mm at flows close to 5,000 cfs.

**Table 5-1: Percents of total load that behave as washload and bed material load at flows close to 5,000 cfs.**

| Date | Inst. Discharge (cfs) | % washload | % bed material load |
|---|---|---|---|
| 5/22/1978 | 4260 | 53 | 47 |
| 4/23/1979 | 4980 | 82 | 18 |
| 7/9/1979 | 6040 | 78 | 22 |
| 4/28/1980 | 4730 | 53 | 47 |
| 5/24/1982 | 4280 | 81 | 19 |
| 6/7/1982 | 4570 | 79 | 21 |
| 4/24/1984 | 4270 | 86 | 14 |
| 5/8/1984 | 4440 | 77 | 23 |
| 6/13/1994 | 5030 | 97 | 3 |
| 6/27/1994 | 4860 | 66 | 34 |
| 5/5/1995 | 3980 | 64 | 36 |
| 6/6/1995 | 4960 | 44 | 56 |
| 7/3/1995 | 5620 | 30 | 70 |
| 6/3/1997 | 5040 | 29 | 71 |
| 5/24/1999 | 4080 | 65 | 35 |
| **Average =** | **4743** | **66** | **34** |

Total sediment input to the reach was estimated using the Modified Einstein Procedure (MEP) (Colby and Hembree 1955, USBR 1955). Cross-section geometry measurements, suspended sediment and bed material samples at the Albuquerque Gage from 1978 to 1999 were used for the purpose of estimating the incoming total sediment load and sand-load to the reach using the MEP. The Albuquerque Gage is located downstream from the study reach. As a result, the total load might be slightly over estimated since sediment is probably mined from the bed and banks between the study reach and the gage. The data were subdivided by separating snowmelt and summer flows. The snowmelt period was defined as April to July based on interpretation of the mean-daily discharge record for the Albuquerque gaging station from 1978 to 1999. Non-linear regression functions were fit to the MEP results to develop sand load rating curves.

The bed material transport capacity of the subreaches was estimated for 1992 and 2001 using the following sediment transport equations: Laursen, Engelund and Hansen, Ackers and White ($d_{50}$ and $d_{35}$), Yang – Sand ($d_{50}$ and size fraction), Einstein and Toffaleti (Stevens et al. 1989, Julien 1995). The bed material gradation analysis indicate that the median grain sizes of all the subreaches are fine to medium sand and therefore most of the bed material transport relationships are appropriate to use (Table 5-2). The input data to the sediment transport

equations are the reach-averaged channel geometry values resulting from HEC-RAS® run at 5,000 cfs (Table 5-3).

The transport capacity equations are functions of the slope of the channel. Therefore, the channel slope was adjusted to produce a transport capacity that approximated the incoming bed material load. An adjusted slope was obtained from each sediment transport equation.

**Table 5-2: Appropriateness of bedload and bed-material load transport equations (Stevens et al. 1989).**

| *Author of Formula* | *Date* | *Bedload (BL) or Bed-material Load (BML)* | *Type of Formula (D/P)* | *Sediment Type (S/M/O)* | *Sediment Size (S/G)* |
|---|---|---|---|---|---|
| ***Ackers & White*** | 1973 | BML | D | S | S,G |
| ***Einstein (BL)*** | 1950 | BL | P | M | S,G |
| ***Einstein (BML)*** | 1950 | BML | P | M | S |
| ***Engelund & Hansen*** | 1967 | BML | D | S | S |
| ***Laursen*** | 1958 | BML | D | M | S |
| ***Meyer-Peter and Muller*** | 1948 | BL | D | S | S,G |
| ***Schoklitsch*** | 1934 | BL | D | M | S,G |
| ***Toffaleti*** | 1968 | BML | D | M | S |
| ***Yang (sand)*** | 1973 | BML | D | O | S |
| ***Yang (gravel)*** | 1984 | BML | D | O | G |

*D/P - Deterministic/Probabilistic*
*S/M/O - Single Size Fraction/Mixture/Optional*
*S/G - Sand/Gravel*

**Table 5-3: Hydraulic input data at all subreaches for sediment transport capacity computations from 1992 and 2001 HEC-RAS® run at 5,000 cfs.**

| 1992 Data | | | | |
|---|---|---|---|---|
| **Subreach #** | **Width (ft)** | **Depth (ft)** | **Velocity (ft/s)** | **Channel slope** |
| | | | | |
| 1 | 603 | 2.23 | 3.85 | 0.001 |
| 2 | 640 | 2.21 | 3.75 | 0.001 |
| 3 | 599 | 2.25 | 3.85 | 0.0009 |

| 2001 Data | | | | |
|---|---|---|---|---|
| **Subreach #** | **Width (ft)** | **Depth (ft)** | **Velocity (ft/s)** | **Channel slope** |
| | | | | |
| 1 | 524 | 2.41 | 4.01 | 0.0009 |
| 2 | 584 | 2.24 | 3.86 | 0.0010 |
| 3 | 598 | 2.22 | 4.03 | 0.0010 |

### Hydraulic Geometry

Hydraulic geometry equations have been developed to estimate geometric characteristics of stable channels based on a channel forming discharge. Some methods use bed material size, channel slope and/or sediment concentration. Most hydraulic geometry methods have been developed from man-made canals or single-thread natural channels.

The equilibrium width of the Corrales Reach for 1962, 1972, 1992 and 2001 were estimated by the following hydraulic geometry equations:

- Leopold & Maddock (1953) developed a set of empirical equations that relate the hydraulic geometry variables (width, depth and velocity) to discharge in the form of power functions:

$$W = aQ^{b}$$
$$D = cQ^{e}$$
$$V = kQ^{m}$$

  Where, ack = 1 and b+e+m = 1 by continuity of water (Q = V.D.W) and the exponent of the equations b,f and m are on average equal to 0.5, 0.4 and 0.1 regardless the flow regime, sediment characteristics and physiographic location of the rivers (ASCE Task Committee on Hydraulics 1998).

- Julien and Wargadalam's (1995) regime geometry equations are "semi-theoretical" equations based on four fundamental hydraulic relationships – continuity, resistance, sediment transport and secondary flow. Depth, width, velocity and Shield's parameter are expressed as functions of discharge, bed material size and slope as follows:

$$D = 0.200Q^{\frac{2}{6m+5}} d_s^{\frac{6m}{6m+5}} S^{-\frac{1}{6m+5}}$$

$$W = 1.330Q^{\frac{4m+2}{6m+5}} d_s^{-\frac{4m}{6m+5}} S^{-\frac{2m+1}{6m+5}}$$

$$V = 3.758Q^{\frac{2m+1}{6m+5}} d_s^{-\frac{2m}{6m+5}} S^{\frac{2m+1}{6m+5}}$$

$$\tau_* = 0.121Q^{\frac{2}{6m+5}} d_s^{-\frac{5}{6m+5}} S^{\frac{6m+4}{6m+5}}$$

$$m = \frac{1}{(\ln \frac{12.2D}{d_{50}})}$$

- Simons & Albertson (1963), developed equations from analysis of Indian and American canals. Five data sets were used in the development of the equations. Simons and Bender's data were collected from irrigation canals in Wyoming, Colorado and Nebraska during the summers of 1953 and 1954 and consisted of cohesive and non-cohesive bank material. The USBR data were collected from canals in the San Luis Valley of Colorado. This data consisted of coarse non-cohesive material. Indian canal data were collected from the Punjab and Sind canals. The average diameter of the bed material is approximately 0.43 mm for the Punjab canals and between 0.0346 mm to 0.1642 mm for the Sind canals. The Imperial Valley canal data were collected in the Imperial Valley canal systems. Bed and bank conditions of these canals are similar to the Punjab, Sind and Simons and Bender canals (Simons et. al 1963).

  The relationship between wetted perimeter (P) and water discharge (Q) is represented in Figure 5-1. Once the wetted perimeter is obtained from Figure 5-1, the averaged channel width is estimated using Figure 5-2.

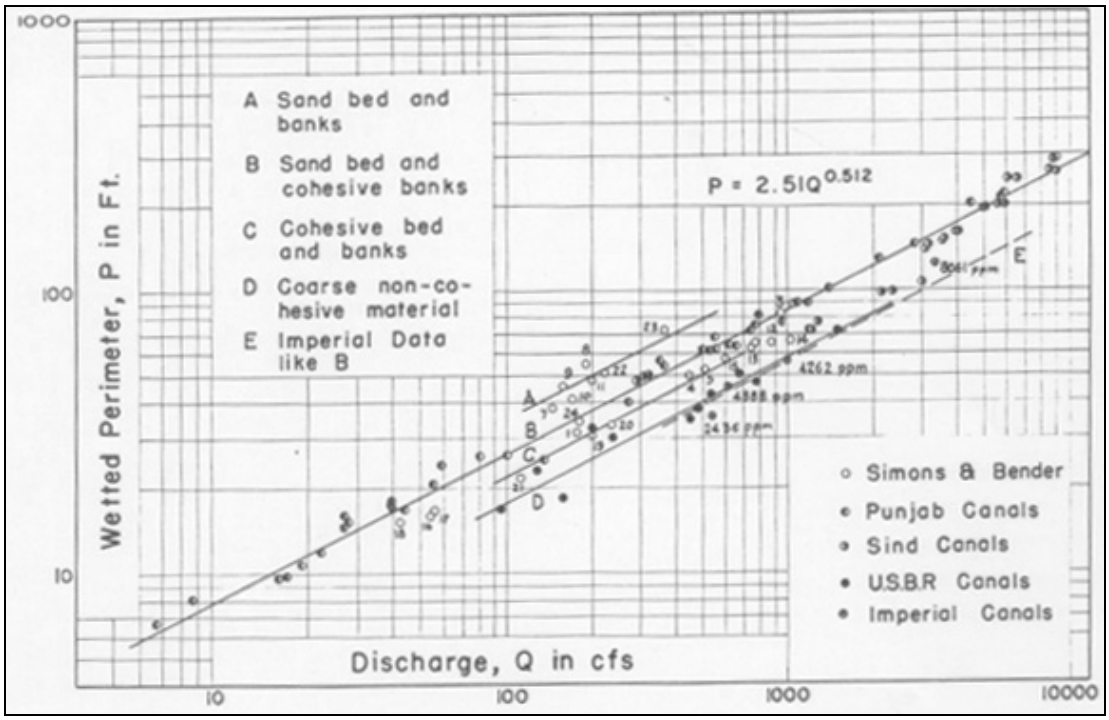


**Figure 5-1: Variation of wetted perimeter (P) with discharge (Q) and type of channel (after Simons and Albertson 1963).**

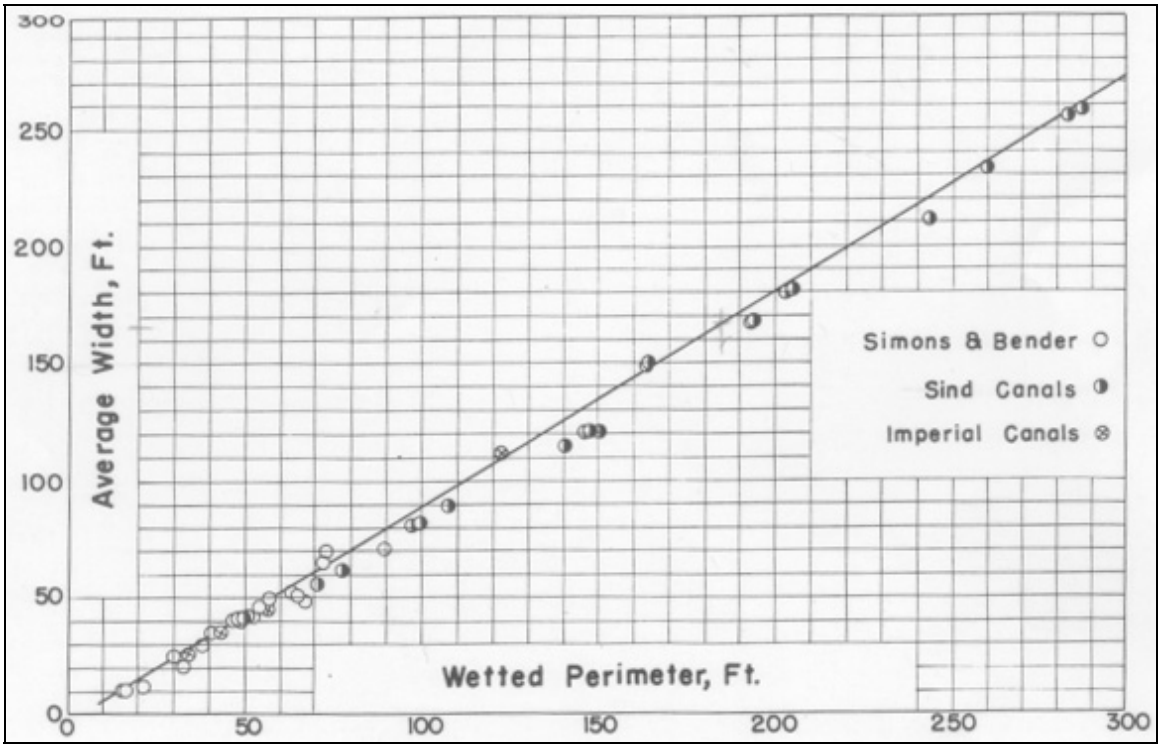


**Figure 5-2: Variation of average width (W) with wetted perimeter (P) (after Simons and Albertson 1963).**

- Blench (1957) developed regime equations from flume data. The equations account for the differences in bed and bank material by means of a bed and a side factor ($F_s$) (Thorne et al. 1997). The range of application of Blench's equation is (Thorne et al. 1997):

  Discharge (Q): 0.03-2800 $m^3/s$

  Sediment concentration (c): 30-100 ppm

  Bed material size (d): 0.1-0.6 mm

  Bank material type: cohesive

  Bedforms: ripples – dunes

  Planform: straight

  Profile: uniform

  The size factor is defined by $F_s = V^3/b$, where b is defined as the breadth, that multiplied by the mean depth d, gives the area of a mean trapezoidal section, and V is the mean flow velocity (Blench 1957).

  The regime equation for channel width (W) is [from Wargadalam (1993)]:

$$W = \left( \frac{9.6(1 + 0.012c)}{F_s} \right)^{\frac{1}{2}} d^{\frac{1}{4}} Q^{\frac{1}{2}} \text{ , (ft)}$$

  Where:

  c = sediment load concentration (ppm),

  d = $d_{50}$ (mm), and

  $F_s$ = 0.1 for slight cohesiveness of banks

- Lacey [(1930-1958), from Wargadalam (1993)]

$$P = 2.667Q^{0.5} \text{ (ft)}$$

  Where:

  P = wetted perimeter (feet)

  Q = water discharge ($ft^3/s$)

- Klaassen-Vermeer (1988) developed a width relationship for braided rivers based on work on the Jamuna River in Bangladesh:

$$W = 16.1Q^{0.53} \text{ (m)}$$

Where:

Q = water discharge ($m^3/s$)

- Nouh (1988) developed regime equations from ephemeral channels located in the South and Southwest regions of Saudi Arabia. The equations provide information of channel dimensions under varying flash flood and sediment flow conditions in an extremely arid zone. The following regression equation was obtained for the channel width:

$$W = 28.3\left(\frac{Q_{50}}{Q}\right)^{0.83} + 0.018(1+d)^{0.93} c^{1.25}, \text{ (m)}$$

Where:

$Q_{50}$ = peak discharge for 50 yr. return period ($m^3/s$)

Q = annual mean discharge ($m^3/s$)

d = $d_{50}$ (mm)

c = mean suspended sediment concentration ($Kg/m^3$).

Additionally, an empirical width-discharge relationship specific to the Corrales Reach was developed from the digitized active channel widths from GIS coverage's and the peak flows from the 5-years prior to the survey date. Peak flows were obtained from the Rio Grande at Otowi Gage for 1918 and Rio Grande near Bernalillo and Rio Grande at Albuquerque USGS gages for the remaining years. The resulting equation takes the following form:

$$W = a\,Q^b$$

Where:

W = Active channel width (feet)

Q = Peak discharge (cfs)

Table 5-4 contains the input data for the empirical width-discharge equations. Peak flow data are included in Appendix F.

**Table 5-4: Input data for the empirical width-discharge relationship.**

| | 1918 | 1935 | 1949 | 1962 | 1972 | 1985 | 1992 | 2001 |
|---|---|---|---|---|---|---|---|---|
| **Averaged 5-yr peak flows (cfs)** | 11630 | 6608 | 8010 | 5768 | 3490 | 6256 | 4142 | 4146 |
| **Subreach 1 Width (ft)** | 884 | 935 | 787 | 592 | 668 | 617 | 615 | 429 |
| **Subreach 2 Width (ft)** | 1345 | 1088 | 854 | 679 | 736 | 690 | 631 | 516 |
| **Subreach 3 Width (ft)** | 1722 | 1546 | 1249 | 672 | 648 | 644 | 577 | 492 |
| **Total Width (ft)** | 1275 | 1171 | 948 | 638 | 682 | 647 | 607 | 474 |

Table 5-5 contains the input data for the hydraulic geometry calculations. The peak discharges for 50 year-return period are from Bullard and Lane (1993) report. The averaged suspended sediment concentration values are estimated from the double mass curve (Figure 4-3), which was developed from the Rio Grande near Bernalillo and Rio Grande at Albuquerque USGS gaging stations.

**Table 5-5: Input data for the hydraulic geometry calculations.**

| 1962 | Q (cfs) | $Q_{50}$ (cfs) | $d_{50}$ (mm) | Channel Slope (ft/ft) | Avg C (ppm) |
|---|---|---|---|---|---|
| **Reach 1** | 5,000 | 23,500 | 0.21 | 0.0009 | 3732 |
| **Reach 2** | 5,000 | 23,500 | 0.21 | 0.0010 | 3732 |
| **Reach 3** | 5,000 | 23,500 | 0.21 | 0.0010 | 3732 |
| **Total Reach** | 5,000 | 23,500 | 0.21 | 0.0009 | 3732 |
| **1972** | | | | | |
| **Reach 1** | 5,000 | 10,000 | 0.20 | 0.0009 | 3732 |
| **Reach 2** | 5,000 | 10,000 | 0.18 | 0.0010 | 3732 |
| **Reach 3** | 5,000 | 10,000 | 0.21 | 0.0010 | 3732 |
| **Total Reach** | 5,000 | 10,000 | 0.20 | 0.0010 | 3732 |
| **1992** | | | | | |
| **Reach 1** | 5,000 | 10,000 | 1.70 | 0.0010 | 255 |
| **Reach 2** | 5,000 | 10,000 | 0.49 | 0.0010 | 255 |
| **Reach 3** | 5,000 | 10,000 | 0.51 | 0.0009 | 255 |
| **Total Reach** | 5,000 | 10,000 | 0.89 | 0.0010 | 255 |
| **2001** | | | | | |
| **Reach 1** | 5,000 | 10,000 | 1.73 | 0.0011 | 663 |
| **Reach 2** | 5,000 | 10,000 | 0.67 | 0.0011 | 663 |
| **Reach 3** | 5,000 | 10,000 | 0.53 | 0.0010 | 663 |
| **Total Reach** | 5,000 | 10,000 | 0.98 | 0.0011 | 663 |

### Equilibrium Channel Width Analysis

- Williams and Wolman (1984) Hyperbolic Model

Williams and Wolman (1984) studied the downstream effects of dams on alluvial rivers. The changes in channel width with time were described by hyperbolic equations of the form

$(1/Y) = C_1 + C_2 (1/t)$, where Y is the relative change in channel width, $C_1$ and $C_2$ are empirical coefficients and t is time in years after the onset of the particular channel change. The relative change in channel width is equal to the ratio of the width at time t ($W_t$) to the initial width ($W_i$). Coefficients $C_1$ and $C_2$ might be a function, at least, of flow discharges and boundary materials.

Hyperbolic equations were fitted to the entire Corrales Reach and to each subreach data set. The time t = 0 was taken as the year when narrowing of the channel began. Channel narrowing started in 1935 in subreach 1 and 1918 in subreaches 2 and 3. To adjust the data to an origin of 0, 1.0 was subtracted from each $W_t/W_1$ before performing the regression. The data to which the hyperbolic regressions were applied is in Table 5-6.

**Table 5-6: Input data for Williams and Wolman hyperbolic model.**

| Subreach 1 | | | | | |
|---|---|---|---|---|---|
| Year | t (year) | 1/t | Wi (ft) | Wt (ft) | 1/((Wt/Wi)-1) |
| 1918 | 0 | | 884 | 884 | |
| 1935 | 17 | 0.05882 | | 935 | 17.1733 |
| 1949 | 31 | 0.03226 | | 787 | -9.1231 |
| 1962 | 44 | 0.02273 | | 592 | -3.0337 |
| 1972 | 54 | 0.01852 | | 668 | -4.1008 |
| 1985 | 67 | 0.01493 | | 617 | -3.3165 |
| 1992 | 74 | 0.01351 | | 615 | -3.2850 |
| 2001 | 83 | 0.01205 | | 429 | -1.9436 |

| Subreach 2 | | | | | |
|---|---|---|---|---|---|
| Year | t (year) | 1/t | Wi (ft) | Wt (ft) | 1/((Wt/Wi)-1) |
| 1918 | 0 | | 1345 | 1345 | |
| 1935 | 17 | 0.0588 | | 1088 | -5.2322 |
| 1949 | 31 | 0.0323 | | 854 | -2.7372 |
| 1962 | 44 | 0.0227 | | 679 | -2.0184 |
| 1972 | 54 | 0.0185 | | 736 | -2.2100 |
| 1985 | 67 | 0.0149 | | 690 | -2.0532 |
| 1992 | 74 | 0.0135 | | 631 | -1.8846 |
| 2001 | 83 | 0.0120 | | 516 | -1.6224 |

| Subreach 3 | | | | | |
|---|---|---|---|---|---|
| Year | t (year) | 1/t | Wi (ft) | Wt (ft) | 1/((Wt/Wi) -1) |
| 1918 | 0 | | 1722 | 1722 | |
| 1935 | 17 | 0.0588 | | 1546 | -9.7632 |
| 1949 | 31 | 0.0323 | | 1249 | -3.6418 |
| 1962 | 44 | 0.0227 | | 672 | -1.6400 |
| 1972 | 54 | 0.0185 | | 648 | -1.6041 |
| 1985 | 67 | 0.0149 | | 644 | -1.5971 |
| 1992 | 74 | 0.0135 | | 577 | -1.5034 |
| 2001 | 83 | 0.0120 | | 492 | -1.4005 |

| Corrales Reach | | | | | |
|---|---|---|---|---|---|
| Year | t (year) | 1/t | Wi (ft) | Wt (ft) | 1/((Wt/Wi) -1) |
| 1918 | 0 | | 1275 | 1275 | |
| 1935 | 17 | 0.0588 | | 1171 | -12.2946 |
| 1949 | 31 | 0.0323 | | 948 | -3.9040 |
| 1962 | 44 | 0.0227 | | 638 | -2.0019 |
| 1972 | 54 | 0.0185 | | 682 | -2.1488 |
| 1985 | 67 | 0.0149 | | 647 | -2.0294 |
| 1992 | 74 | 0.0135 | | 607 | -1.9093 |
| 2001 | 83 | 0.0120 | | 474 | -1.5909 |

- Richard (2001) Exponential Model

Richard (2001) developed an exponential model to describe the change in channel width with time of the Cochiti reach of the Rio Grande. The hypothesis of the model is that the magnitude of the slope of the width vs. time curve increases with deviation from the equilibrium width, $W_e$. The exponential function is:

$$W = W_e + (W_o - W_e).e^{-k_1 t}$$

Where:

$K_1$ = rate constant

$W_e$ = Equilibrium width at time $t_o$

$W_o$ = Channel width at time $t_o$, and

W = Channel width at time t

Richard (2001) used three methods to estimate $k_1$ and $W_e$. The first method consists of empirically estimating the value of $k_1$ and $W_e$ by plotting the width change rate vs. the width and generating a regression line. The rate constant, $k_1$, is the slope of the regression line and the intercept is $k_1W_e$. The second method consists of using the empirically determined k-values from the first method and varying the equilibrium width values to produce a "best-fit" equation that minimizes the sum-square error (SSE) between the predicted and observed widths. This method was developed in an effort to better estimate the equilibrium width. The value for the intercept ($K_1W_e$) was assigned a value of zero to yield consistent and reasonable results in each subreach. The third method consists of estimating the equilibrium width, $W_e$, using a hydraulic geometry equation. The $k_1$ value was determined by varying it until the SSE between the predicted and observed width was minimized. The input data used in this analysis is included in Appendix G.

### Stable Channel Analysis (SAM®)

HEC-RAS® hydraulic stable channel design functions, based on the SAM® Hydraulic Design Package for Flood Control Channels (v. 3.07, 10 August 1994), developed by the US Army Corps of Engineers, were applied to estimate the equilibrium channel width and slope given specified water and sediment discharges and bed material composition. SAM® uses Brownlie's flow resistance and sediment transport equations to produce multiple solutions for the width and slope given the input values. The minimum point in the resulting width versus slope curve represents the point of minimum stream power for the given input conditions. The method assumes a trapezoidal cross-section and steady uniform flow conditions.

The resulting stable channel dimensions analysis was applied to the 2001 conditions of the Corrales reach. A series of curves with varying incoming bed-material sediment concentrations were plotted. The input data to SAM® are water discharge in cfs, sediment concentration in mg/l, average valley slope = 0.0011, bank roughness of n = 0.02 , a median channel width

from HEC-RAS® = 563 feet and bank slopes of 3.1H/1V for the right bank and 2.4H/1V for the left back. The bank slopes are the average bank slopes computed from the CO-line cross section plots (CO-33, CO-34 and CO-35). These bank slopes are summarized in Table 5-7.

**Table 5-7: Estimated bank slopes at CO-lines.**

| | 2001 Bank Slopes | | | |
|---|---|---|---|---|
| | Left bank | | Right bank | |
| | V | H | V | H |
| CO-33 | 1 | 2.3 | 1 | 1.2 |
| CO-34 | 1 | 1.8 | 1 | 3.5 |
| CO-35 | 1 | 3.2 | 1 | 4.4 |
| Average | 1 | 2.4 | 1 | 3.1 |

The model was run for a channel forming discharge of 5,000 cfs and concentrations of 284, 449, 1,125 and 1,304 mg/l. These concentrations correspond to incoming discharges of 500, 1,000, 4,000 and 5,000 cfs, respectivley. The incoming sand load to the reach was estimated for each discharge using the sand load rating curve (Figure 5-3). Each sand load value was then divided by their corresponding discharge to compute the incoming concentrations to the reach in mg/l after the necessary conversions.

In addition, the bed material particle size distribution for the Corrales Reach was also input into the SAM® model. The bed material curve for the entire reach was obtained by averaging the bed material size distribution curves of the three subreaches (Figure 3-21).

## 5.2 RESULTS

### Sediment Transport Analysis

Figure 5-3 presents the spring and summer sand load rating curves at the Albuquerque Gage. Using a channel forming discharge of 5,000 cfs, the estimated MEP sand load at the Albuquerque gaging station is 17,593 tons/day. It is evident that the variability of the data points around the regression line is about one order of magnitude (Figure 5-3). As a result, the real sand load could considerably vary from the estimated value.

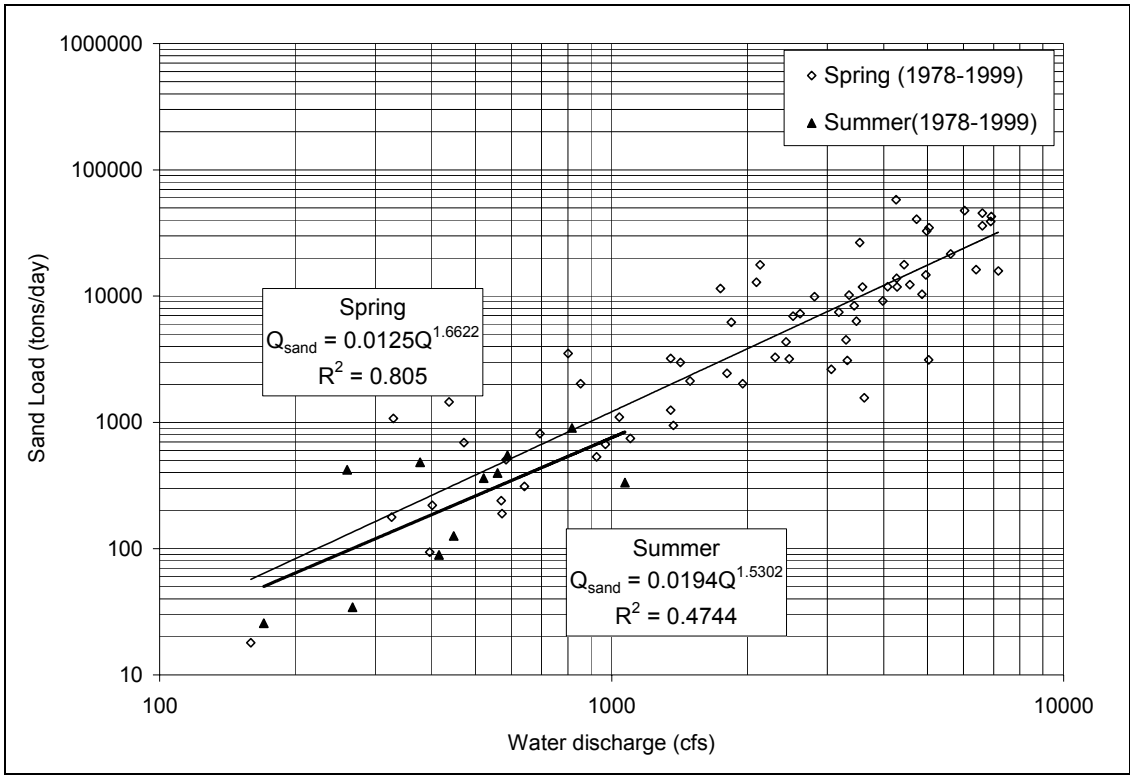


**Figure 5-3: Albuquerque Gage sand load rating curve for spring and summer.**

Table 5-8 lists the bed material transport capacity estimates for the 1992 and 2001 subreach slopes. The different equation results varied widely for each subreach. In general, subreaches 1 and 3 exhibit similar trends from 1992 to 2001. For these two subreaches, all of the transport equations, with the exception of Laursen and Toffaleti, predict a larger capacity in 2001. This corresponds with the finer material observed in 2001. Subreach 2 generally exhibits the opposite trend whereby having higher sediment transport capacities in 1992 with the same slope. To account for this phenomenon, the grain size distribution curve for this subreach (Figure 3-19) is referred to. It can be seen that half of the subreach bed material got coarser while the other half got finer from 1992 to 2001. Since there is no identifiable consistent trend throughout the subreach, unusual results can be expected. No sediment transport capacity exceeds 16,000 tons/day. The sediment transport equations are comparable for some years and slopes, but for the most part significantly different capacities are calculated by each (Table 5-8).

The average bed material load transport capacity in 1992 is lower than the average transport capacity in 2001 for subreaches 1 and 3. The average bed material load transport

capacity in 1992 is higher than the average transport capacity in 2001 for subreach 2. Again, this trend is seen to be different from subreaches 1 and 3, likely due to the subreach being in a transitional state. All transport capacities are lower than the incoming sand load (17,593 tons/day). This would indicate aggradation in all subreaches, which is not in agreement with the observed degradation of subreach 1, but is in agreement with the observed aggradation of subreaches 2 and 3 that occurred between 1992 and 2001 (Figure 3-9).

In general, the washload is comprised of the fine particles not sound in large quantities in the bed ($D_s < D_{10}$) (Julien 1995). The $D_{10}$ of the bed material is on average 0.27 mm (Figure 3-21). The percent of material in suspension finer than 0.27 mm is roughly 66 percent at flows close to 5,000 cfs (Table 5-1), which suggests that very fine and fine sand particles behave as washload. As a result, the incoming bed material load is approximately 5,982 tons/day, which represents 34 percent of the sand load (Appendix H). This methodology for the bed material load estimation is carried out under the assumption that the silt load is small enough to be neglected.

**Table 5-8: Bed material transport capacity for the 1992 and 2001 slopes.**

| Bed-material Transport Equations | Existing Slopes | | | | | |
|---|---|---|---|---|---|---|
| | s = 0.0010 Subreach 1 1992 | s = 0.0009 Subreach 1 2001 | s=0.0010 Subreach 2 1992 | s = 0.0010 Subreach 2 2001 | s=0.0009 Subreach 3 1992 | s = 0.0010 Subreach 3 2001 |
| **Laursen** | 7,904 | 5,455 | 12,125 | 5,444 | 8,757 | 7,472 |
| **Engelund & Hansen** | 3,913 | 8,978 | 13,486 | 10,687 | 11,211 | 13,806 |
| **Ackers and White (d50)** | 3,901 | 8,448 | 11,132 | 9,147 | 10,559 | 12,188 |
| **Ackers and White (d35)** | 7,850 | 10,941 | 14,100 | 11,704 | 12,998 | 15,309 |
| **Yang Sand (d50)** | 7,828 | 8,106 | 9,604 | 8,919 | 8,400 | 10,594 |
| **Yang Sand (size fraction)** | 14,030 | 10,672 | 14,216 | 11,023 | 11,024 | 13,258 |
| **Einstein** | 1,001 | 5,248 | 6,476 | 6,993 | 6,589 | 9,093 |
| **Toffaleti** | 8,354 | 8,334 | 17,813 | 7,657 | 13,430 | 12,322 |
| **Average =** | **6,848** | **8,273** | **12,369** | **8,947** | **10,371** | **11,755** |

The slopes of each subreach were adjusted to match the capacity with the incoming bed material load (5,982 tons/day). The resulting slope predictions for each method and subreach are summarized in Table 5-9. Ackers and White ($D_{50}$) and Ackers and White ($D_{35}$) produced very small slopes for all subreaches. Laursen's method produced slopes closest to the 2001 slopes for all subreaches. All other equations predicted slopes that were flatter than the 2001 slopes with the exception of Einstein's equation for subreach 1.

**Table 5-9: Resulting slope predictions from sediment transport capacity equations for 2001.**

| Bed-material Transport Equations | Subreach 1 Q = 5000 cfs | | Subreach 2 Q = 5000 cfs | | Subreach 3 Q = 5000 cfs | |
|---|---|---|---|---|---|---|
| | Capacity | Slope | Capacity | Slope | Capacity | Slope |
| **Laursen** | 5,956 | 0.001 | 5,875 | 0.0011 | 6,207 | 0.0008 |
| **Engelund & Hansen** | 6,158 | 0.0007 | 6,259 | 0.0007 | 6,417 | 0.0006 |
| **Ackers & White (d50)** | 5,968 | 0.0003 | 5,982 | 0.0003 | 6,264 | 0.0002 |
| **Ackers & White (d35)** | 5,589 | 0.0002 | 5,380 | 0.0002 | 6,520 | 0.0002 |
| **Yang Sand (d50)** | 5,982 | 0.0007 | 5,763 | 0.0007 | 5,584 | 0.0006 |
| **Yang Sand (size fraction)** | 5,286 | 0.0005 | 5,898 | 0.0006 | 5,500 | 0.0005 |
| **Einstein** | 6,081 | 0.0012 | 5,882 | 0.0007 | 5,977 | 0.0004 |
| **Toffaleti** | 6,660 | 0.0005 | 6,248 | 0.0005 | 9,244 | 0.0005 |

### Hydraulic Geometry

The equilibrium width predicted by the hydraulic geometry equations for 5,000 cfs are summarized in Table 5-10. Simons and Albertson's, Julien-Wargadalam's and Lacey's equations under estimate the width for all subreaches for all the years. Blench's equation over estimates the width for all the subreaches for 1962, 1972, 1992 (subreach 1) and 2001 while under estimating the width for 1992 for subreaches 1 and 3. Nouh's equation over estimates the width for all the subreaches in 1962 and 1972 and subreach 1 in 2001 while it underestimates for all subreaches in 1992 as well as subreaches 2 and 3 in 2001. Klassen and Vermeer's equation over estimates the width for all subreaches for all years analyzed. Overall, Klassen and Vermeer's equation yields the closest results to the active channel widths for all the years but it does not show any temporal variation. Blench's equation predicts larger widths for 1962, 1972, and 2001. However, Blench's equation produces equilibrium widths close to the 1992 width for all the subreaches.

**Table 5-10: Predicted equilibrium widths from hydraulic geometry equations for Q = 5,000 cfs.**

| Q = 5,000 cfs | | Reach-Averaged HEC-RAS Main Channel Width (feet) | Klassen & Vermeer | Nouh | Blench | Simons and Albertson | Julien-<br>Wargadalam | Lacey |
|---|---|---|---|---|---|---|---|---|
| **1962** | **1** | 641 | 729 | 2064 | 1417 | 167 | 268 | 189 |
| | **2** | 692 | 729 | 2064 | 1417 | 167 | 265 | 189 |
| | **3** | 627 | 729 | 2064 | 1417 | 167 | 265 | 189 |
| | **Total** | 652 | 729 | 2064 | 1417 | 167 | 267 | 189 |
| **1972** | **1** | 665 | 729 | 2050 | 1406 | 167 | 269 | 189 |
| | **2** | 698 | 729 | 2012 | 1363 | 167 | 264 | 189 |
| | **3** | 653 | 729 | 2060 | 1417 | 167 | 263 | 189 |
| | **Total** | 670 | 729 | 2041 | 1396 | 167 | 265 | 189 |
| **1992** | **1** | 603 | 729 | 155 | 712 | 167 | 262 | 189 |
| | **2** | 640 | 729 | 91 | 521 | 167 | 263 | 189 |
| | **3** | 599 | 729 | 92 | 527 | 167 | 268 | 189 |
| | **Total** | 612 | 729 | 113 | 606 | 167 | 264 | 189 |
| **2001** | **1** | 524 | 729 | 909 | 1318 | 167 | 262 | 189 |
| | **2** | 584 | 729 | 318 | 828 | 167 | 275 | 189 |
| | **3** | 598 | 729 | 302 | 796 | 167 | 271 | 189 |
| | **Total** | 563 | 729 | 431 | 984 | 167 | 267 | 189 |

Figure 5-4 is a plot of the reach-averaged active channel width versus the predicted width from the hydraulic geometry equations. Klassen and Vermeer produce width values close to the non-vegetated active channel width obtained from the HEC-RAS® analysis but none of the other methods do. The predicted widths are nearly constant for all the subreaches from 1962 to 2001. This trend is in agreement with the historical trends of channel width during the 1962 to 2001 time period (Figure 3-15 and 3-16). In summary, most of the equations do not predict the historical widths very well. However, they do predict the nearly constant width trend observed in the river between 1962 and 2001 (Figure 3-15 and 3-16).

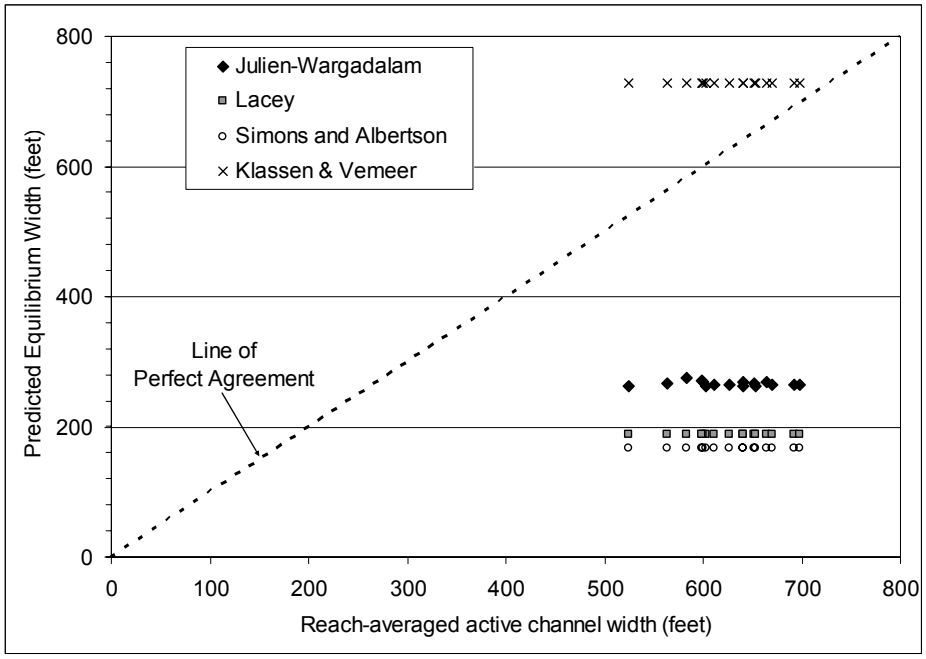


**Figure 5-4: Hydraulic geometry equation results – Predicted equilibrium width vs. reach-averaged active channel width.**

Empirical width-discharge relationships ($w=aQ^b$) were developed for the subreaches and the entire study reach based on the active channel width measured from the GIS coverages of the non-vegetated active channel (Figure 3-15, Table 5-4). The results of this analysis are shown in Figure 5-5. The width was over predicted using the empirical relationships (Table 5-11).

**Table 5-11: Predicated widths from empirical width-discharge relationships.**

| | 2001 GIS width (ft) | Predicted width from Empirical eq. (ft) |
|---|---|---|
| Subreach 1 | 429 | 630 |
| Subreach 2 | 516 | 711 |
| Subreach 3 | 492 | 724 |
| Entire reach | 474 | 685 |

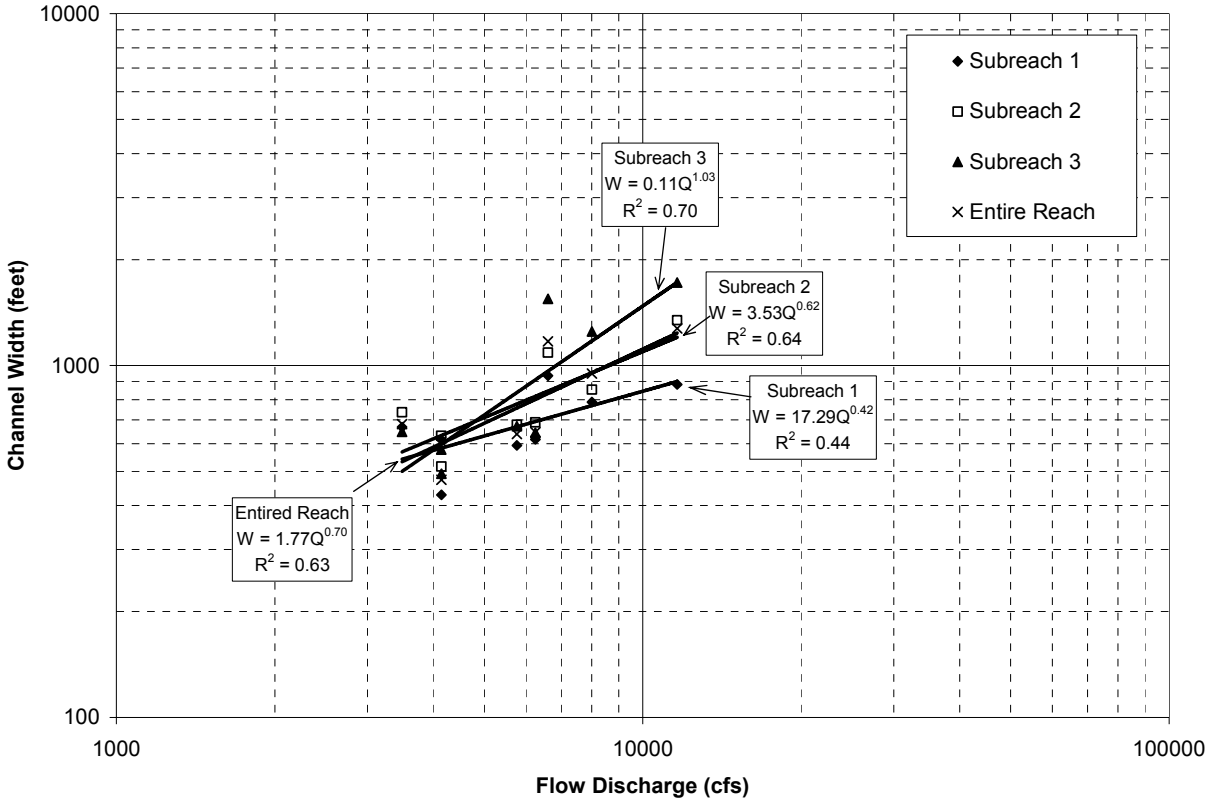


**Figure 5-5: Empirical width-discharge relationships for the Corrales Reach and subreaches.**

### Equilibrium Channel Width Analysis

- Williams and Wolman (1984) Hyperbolic Model

Four hyperbolic equations were fitted to the subreaches and entire study reach data to describe the changes in channel width with time. Subreaches 1 and 2 were the only subreaches in which the regression equations produced satisfactory results. Model results for the entire reach and subreach 3 predicted increasing rates of change in width with time (concave downward curves). Table 5-12 lists the fitted equations and the regression coefficients for all the reaches. Figures 5-6 (a,b,c,d) illustrate the results.

**Table 5-12: Change in width with time hyperbolic equations and regression coefficients.**

| Subreach | Fitted Equation | r² |
|---|---|---|
| 1 | $\frac{W_t}{W_i} = \frac{t}{-1.28454t - 66.61653} + 1$ | 0.8458 |
| 2 | $\frac{W_t}{W_i} = \frac{t}{-0.73337t - 75.05186} + 1$ | 0.9563 |
| 3 | $\frac{W_t}{W_i} = \frac{t}{1.44714t - 181.00301} + 1$ | 0.9499 |
| Entire reach | $\frac{W_t}{W_i} = \frac{t}{1.8699t - 225.49520} + 1$ | 0.9327 |

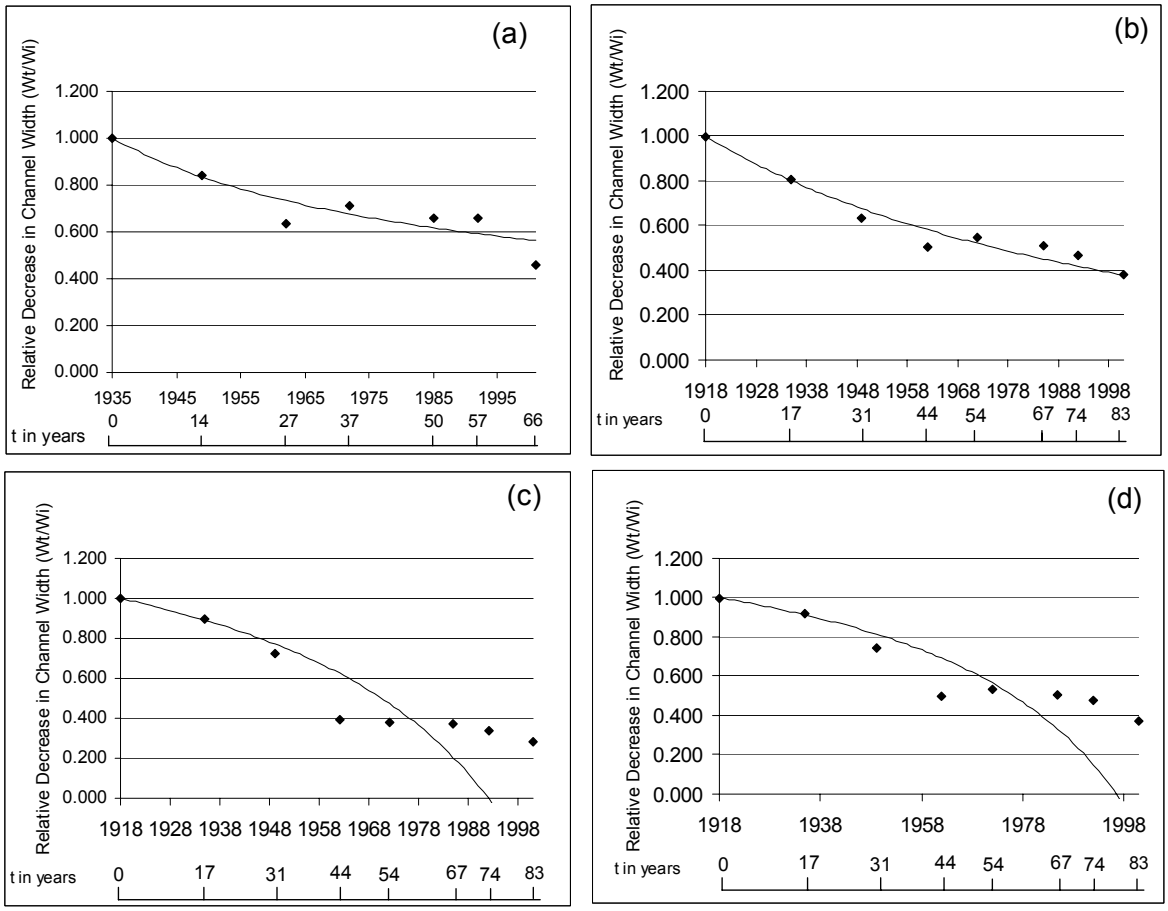


**Figure 5-6: Relative decrease in channel width in (a) Subreach 1, (b) Subreach 2, (c) Subreach 3 and (d) Corrales Reach.**

- Richard (2001) Exponential Model

The exponential model was fitted to the data of the three subreaches and to the entire study reach. The $K_1$ and $W_e$ values were estimated using methods 1 and 2; recall that the intercept ($K_1W_e$) was set to zero. See section 5.1 for a description of the three methods. Method 3 was not used because none of the hydraulic geometry equations yielded good results. Figure 5-7 (a,b,c,d) contain the regression lines between the width change rate vs. the non-vegetated active channel width for the subreaches and the entire reach from 1918 to 2001. The resulting empirically determined $K_1$ and $W_e$ values are listed in Table 5-13. Figures 5-8a, 5-8b, 5-8c and 5-8d show the plots of the resulting exponential models developed from both methods.

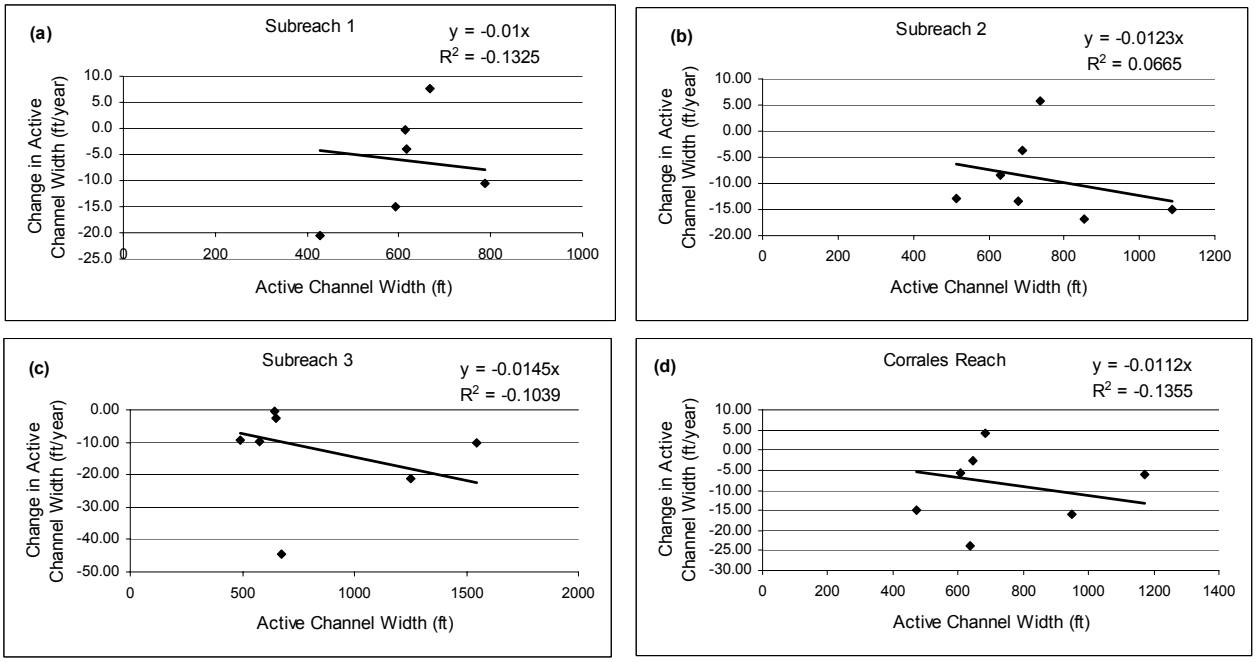


**Figure 5-7: Linear regression results of subreach and entire reach data – observed width change (ft/year) with observed channel width (feet). (a) Subreach 1, (b) Subreach 2, (c) Subreach 3, (d) Corrales Reach.**

**Table 5-13: Empirical estimation of $k_1$ and $W_e$ from linear regressions of width vs. change data (Method 1).**

| | $K_1$ | $K_1We$ | We | r-sq |
|---|---|---|---|---|
| Subreach 1 | 0.01 | 0 | 0 | -0.1325 |
| Subreach 2 | 0.0123 | 0 | 0 | 0.067 |
| Subreach 3 | 0.0145 | 0 | 0 | -0.1039 |
| Entire Reach | 0.0112 | 0 | 0 | -0.1355 |

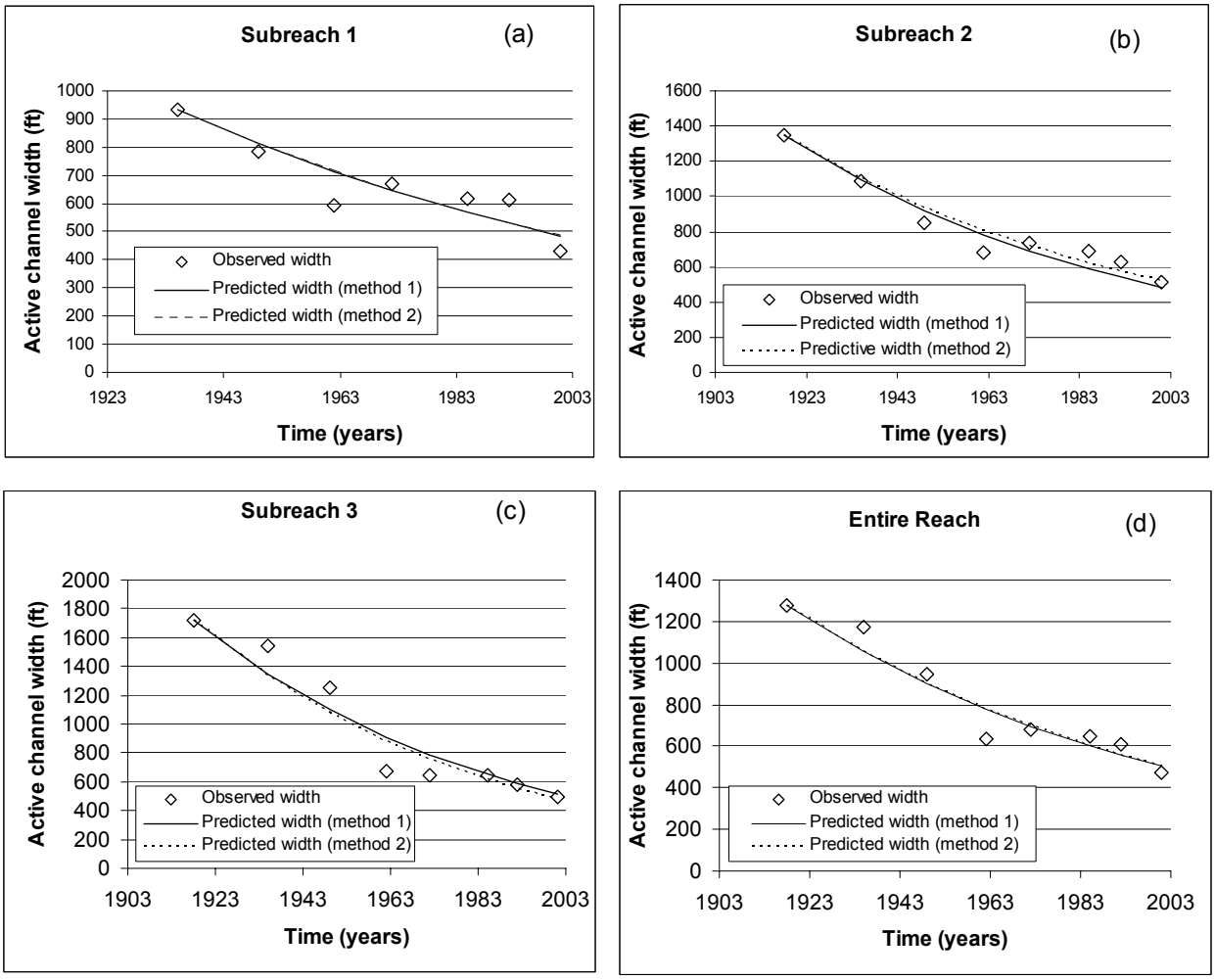


**Figure 5-8: Exponential model of width change applied to (a) Subreach 1, (b) Subreach 2, (c) Subreach 3 and (d) Corrales Reach.**

Both models fit the data well and could be used to describe past trends of channel width. These models indicate that the channel width did not change significantly between 1962 and 2001. These models also show an expected continual slight decrease in width with time. Tables 5-14 and 5-15 show the results obtained from the exponetial model and the resulting exponential equations, respectively.

**Table 5-14: Exponential model results using methods 1 and 2.**

| Subreach 1 | | Method 1 | Method 2 | | |
|---|---|---|---|---|---|
| Year | Wt (ft) | Predicted width (ft) with empirical $k_1$ and $W_e$ | Predicted width (ft) with empirical $k_1$ and varying $W_e$ | guessed $W_e$ | SSE |
| 1935 | 0 | 935 | 935 | 7 | 0 |
| 1949 | 14 | 813 | 814 | | 735 |
| 1962 | 27 | 714 | 716 | | 15184 |
| 1972 | 37 | 646 | 648 | | 400 |
| 1985 | 50 | 567 | 570 | | 2224 |
| 1992 | 57 | 529 | 532 | | 6832 |
| 2001 | 66 | 483 | 487 | | 3348 |
| | | | | SSE = | 28723 |
| **Subreach 2** | | | | | |
| Year | Wt (ft) | | | | |
| 1918 | 0 | 1345 | 1345 | 53 | 0 |
| 1935 | 17 | 1091 | 1101 | | 178 |
| 1949 | 31 | 918 | 935 | | 6698 |
| 1962 | 44 | 783 | 805 | | 15996 |
| 1972 | 54 | 692 | 718 | | 335 |
| 1985 | 67 | 590 | 620 | | 4911 |
| 1992 | 74 | 541 | 573 | | 3387 |
| 2001 | 83 | 484 | 519 | | 7 |
| | | | | SSE = | 31512 |
| **Subreach 3** | | | | | |
| Year | Wt (ft) | | | | |
| 1918 | 0 | 1722 | 1722 | -60 | 0 |
| 1935 | 17 | 1346 | 1333 | | 45300 |
| 1949 | 31 | 1099 | 1077 | | 29642 |
| 1962 | 44 | 910 | 882 | | 43996 |
| 1972 | 54 | 787 | 755 | | 11281 |
| 1985 | 67 | 652 | 615 | | 839 |
| 1992 | 74 | 589 | 550 | | 722 |
| 2001 | 83 | 517 | 475 | | 298 |
| | | | | SSE = | 132077 |
| **Corrales Reach** | | | | | |
| Year | Wt (ft) | | | | |
| 1918 | 0 | 1275 | 1275 | 5 | 0 |
| 1935 | 17 | 1054 | 1055 | | 13572 |
| 1949 | 31 | 901 | 902 | | 2116 |
| 1962 | 44 | 779 | 781 | | 20358 |
| 1972 | 54 | 696 | 699 | | 286 |
| 1985 | 67 | 602 | 605 | | 1779 |
| 1992 | 74 | 557 | 559 | | 2293 |
| 2001 | 83 | 503 | 506 | | 1063 |
| | | | | SSE = | 41468 |

**Table 5-15: Exponential equations of change in width with time using methods 1 and 2.**

| Subreach | Method 1 | Method 2 |
|---|---|---|
| 1 | $W_1 = 935 * e^{0.01*t}$ | $W_1 = 7 + 928 * e^{0.01*t}$ |
| 2 | $W_2 = 1345 * e^{0.0123*t}$ | $W_2 = 53 + 1292 * e^{0.0123*t}$ |
| 3 | $W_3 = 1722 * e^{0.0145*t}$ | $W_3 = -60 + 1782 * e^{0.0145*t}$ |
| Corrales Reach | $W_t = 1275 * e^{0.0112*t}$ | $W_t = 5 + 1270 * e^{0.0112*t}$ |

### Stable Channel Analysis (SAM®)

Figure 5-9 represents the width-slope curves resulting from the application of SAM® in HEC-RAS®. The minimum slope on each curve corresponds to the equilibrium channel or minimum stream power width. SAM® uses Brownlie's bedload transport equation. Therefore, the sediment concentration used in this analysis corresponds to the incoming sand-size bed material sediment concentration to the reach. The sand-size bed material sediment concentration was estimated by dividing the incoming bed material load to the reach (5,982 tons/day) by the channel forming discharge of 5,000 cfs. The resulting sand-size bed material sediment concentration is 1,304 mg/l. The resulting slope of the channel for the estimated sand-size bed material sediment concentration of 1,304 mg/l and the non-vegetated channel width from the 2001 GIS coverage (474 ft) is 0.0018. Steeper slopes than the 2001 slope are also predicted when using the subreach width data. The minimum slope of the 1,304 mg/l curve is 0.0011 and corresponds to a 56 foot channel width. For all of the bed material sediment concentrations modeled, the minimum stream power width is narrower than the 2001 reach averaged width of the Corrales Reach. The 2001 non-vegetated channel widths and channel slopes for all the subreaches and the entire reach are plotted in Figure 5-9. The 2001 width-slope conditions fall between the 449 mg/l and the 1,000 mg/l curves, indicating that the 2001 channel is transport limited.

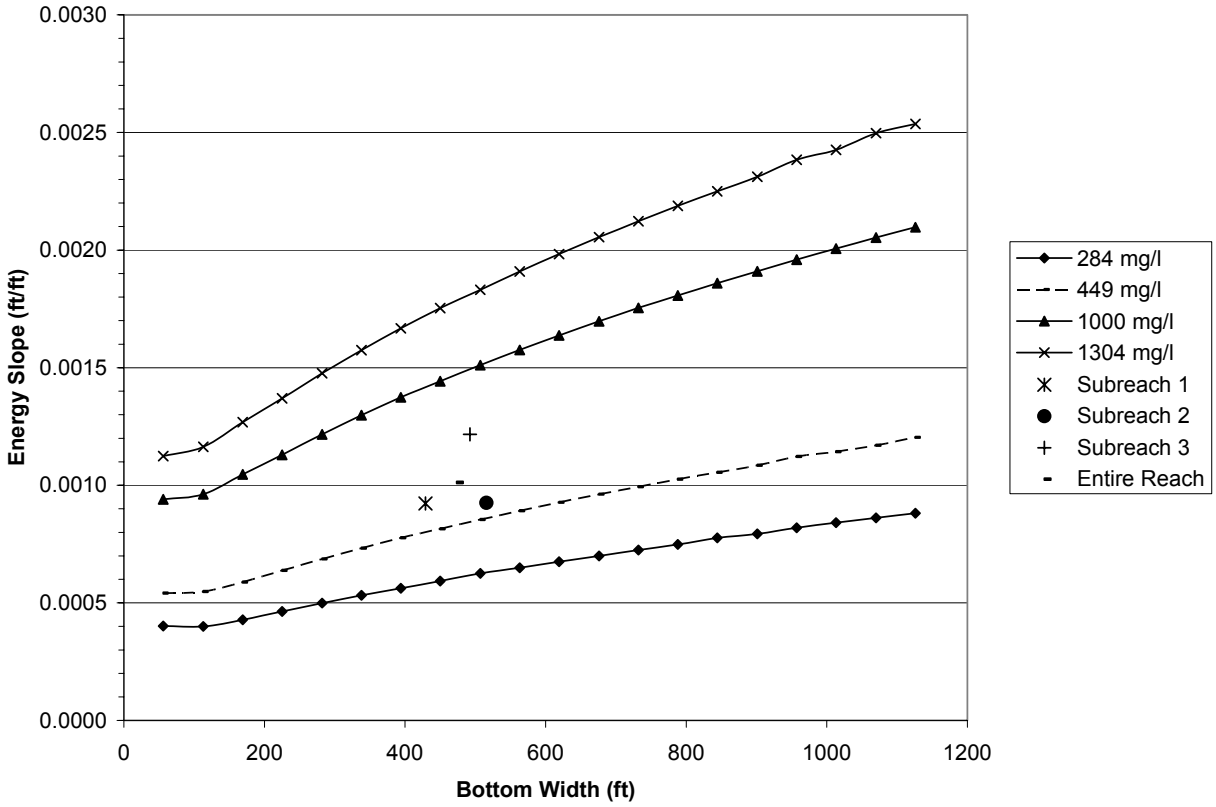


**Figure 5-9: Results from stable channel analysis (SAM®) for 2001 conditions at 5,000 cfs.**

# 6 DISCUSSION

## 6.1 HISTORIC TREND ANALYSIS AND CURRENT CONDITIONS

### Corrales Reach

Discharge – Total annual water discharge at the Albuquerque Gage increased from 1978 to 1987 by a factor of two (Figure 4-1). After 1987, the total annual water discharge declined to a value slightly higher than the total annual water discharge prior to 1978. Factors such as management of Cochiti Dam, climatic changes, irrigation and other water diversions could be responsible for this change.

Suspended Sediment – The total annual suspended sediment discharge at the Albuquerque Gage has decreased since 1973 (Figure 4-2). This decrease coincides to the closure of Cochiti Dam.

Bed Material – The median bed material size in the Corrales Reach is comprised of fine sand in 1962 and 1972, very fine sand to coarse gravel in 1992, and medium sand to coarse gravel in 2001. The channel bed was composed of sand at all water discharges during the 1952 to 1969 time period at the Bernalillo Gage (Nordin and Beverage 1964, León C. 1998). However, recent field observations indicate that the bed material is characterized by a bimodal distribution (Masson pers. comm. 2000). This observation suggests that the time of the survey might be an important factor in describing the current bed material of the channel. Most of the 1992 surveys were performed during the summer season, when gravel sized material could have been exposed by the higher flows, while most of the surveys performed in 2001 were conducted at times of low flow. In summary, the bed material in the study reach has changed from sand to sand–gravel sized material with a bimodal behavior.

Channel Width – Qualitative observation of the GIS coverages of the non-vegetated active channel show that the greatest change in channel width occurred from 1918 to 1962, before the rehabilitation of the floodway. Channel width decreased consistently during the 1918 to 1962 period and achieved almost a constant width after 1962. From 1962 to 1972, the channel width slightly increased likely due to aggradation of the river bed. After 1972, the channel width started to decline at a much smaller rate than the narrowing rate prior to 1962, suggesting that the channel was approaching a new stable state. The narrowing trend after 1972 coincides with the river bed degradational trend.

Channel Pattern – 1962 and 1972 aerial photos show the reach as a low sinuosity, straight channel. 2001 aerial photos reveal several islands at discharges below bankfull, indicative of a braided planform. HEC-RAS® results at 5,000 cfs suggest that the mid-channel bars are not inundated by bankfull or higher discharges, giving the channel the appearance of a braided channel as well.

Based on the results of the channel classification methods, the 1962 to 1972 observed spatial and temporal trends in the channel pattern at bankfull discharge are represented best by Lane and Leopold's, Wolman's and Schumm and Khan's methods. These methods illustrated the low sinuosity (<1.5) of the channel during the 1962 to 1972 time period. The 1992 to 2001 braided planform is best described by Henderson's method.

Vertical Movement – Analysis of the mean bed elevation indicates that the channel aggraded from 1962 to 1972, degraded from 1972 to 1992 then aggraded again from 1992 to 2001. The reach-averaged aggradation from 1962 to 1972 is approximately 0.1 feet and the reach-averaged degradation from 1972 to 1992 is approximately 2.5 feet (Table 3-5). The net change in channel elevation between 1962 and 1992 is approximately 2.4 feet (degradation). From 1992 to 2001 the bed aggraded as much as 2.0 feet, but the average elevation of the entire reach remained essentially constant (Figure 3-9). CO-line cross section plots reveal these trends as well (Appendix B).

Channel Geometry – General trends in channel geometry based on HEC-RAS® results at 5,000 cfs from 1962 to 2001 were decreasing width, width-depth ratio, area, water surface slope, energy-grade line slope and wetted perimeter and increases in mean velocity and depth. The changes in active channel width measured from the GIS coverages also show an overall decreasing width since 1918 (Figure 3-15).

Overbank Flow/Channel Capacity – Based on the results from HEC-RAS® runs at 5,000 cfs the 1972 channel had the largest cross sections in which the channel forming discharges flowed out of the main channel into the overbank area. This illustrates the aggradational trend between 1962 and 1972, which is evident in the mean bed elevation profiles (Figure 3-9).

### Subreach Trends

Channel Width and Pattern – In general, the channel has maintained virtually the same width since 1962. The greatest change in width occurred between 1918 and 1962. Subreach 1

is the narrowest of the three subreaches and subreach 3 is the widest in 2001. The three subreaches are fairly straight as indicated by their low sinuosity (Figure 3-4) and reflect a braided configuration at flows below bankfull (< 5,000 cfs) in 2001.

Vertical Movement – All three subreaches exhibit different trends from 1962 to 2001. Subreach 1 aggraded from 1962 to 1972 then degraded from 1972 to 2001, while subreach 2 shows a degrading trend for all years and subreach 3 degraded from 1962 to 1992 and aggraded from 1992 to 2001 (Figure 3-8). Maximum aggradational changes in mean bed elevation occurred in subreach 3 (approximately 2.0 feet) from 1992 to 2001, maximum degradational changes occurred in subreach 2 (approximately 3.3 feet) from 1972 to 2001. Minimum changes in mean bed elevations (less than 2.0 feet) from 1962 to 2001 occurred in the transition from subreaches 2 and 3 and at the middle of subreach 1 (Figure 3-9).

Channel Geometry – In general, cross-section area, width depth ratio, wetted perimeter and width decreased in the three subreaches between 1962 and 2001. Conversely, mean flow velocity decreased in the three subreaches from 1962 to 2001. The mean depth increased in subreaches 1 and 2 and decreased in subreach 3. In summary, the 2001 channel is narrower, deeper and with smaller flow area than the 1962 channel. In addition, the 1992 mean flow velocities are lower than 1962 velocities. Table 6-1 summarizes the net channel changes between 1962 and 2001 for all the subreaches and the entire reach. A plus (+) indicates an increase in the magnitude of the parameter, a minus (-) a decrease and the equal sign (=) indicates no change.

**Table 6-1: Summary of channel changes between 1962 and 2001 based on reach-averaged main channel parameters from HEC-RAS® modeling runs at Q = 5,000 cfs.**

| 1962-2001 Period | | | | | | | | |
|---|---|---|---|---|---|---|---|---|
| **Reach** | **W** | **EG-Slope** | **Velocity** | **Area** | **D** | **F =W/D** | **WP** | **WS slope** |
| **1** | - | = | + | - | + | - | - | = |
| **2** | - | - | + | - | + | - | - | - |
| **3** | - | + | + | - | - | - | - | = |
| **Total** | - | = | + | - | + | - | - | = |

W = width, EG-Slope = energy grade line slope, D = depth, F = width/depth ratio, WP = wetted perimeter, WS slope = water surface slope

Table 6-2 summarizes the channel changes during 1962-1972, 1972-1992 and 1992-2001 time periods. The active channel width, flow velocity, width-depth ratio and wetted perimeter increased in all subreaches in the 1962 to 1972 period. Channel area, flow depth and energy

grade line slope decreased while water surface slope did not change. The opposite trends are observed in all subreaches from 1972 to 1992. The opposite trends are again seen from 1992 to 2001 except for subreach 3, where the active channel width-to-depth ratio and energy grade line both increased. Channel aggradation was accompanied by channel widening in the 1962 to 1972 time period. Bed degradation and channel narrowing characterized the channel changes between 1972 and 1992.

**Table 6-2: Summary of channel changes during 1962-1972, 1972-1992 and 1992-2001 periods based on reach-averaged main channel parameters from HEC-RAS® modeling runs at Q = 5,000 cfs.**

| 1962-1972 Period | | | | | | | | |
|---|---|---|---|---|---|---|---|---|
| Reach | W | EG-Slope | Velocity | Area | D | F =W/D | WP | WS slope |
| 1 | + | - | + | - | - | + | + | = |
| 2 | + | - | + | - | - | + | + | = |
| 3 | + | - | + | - | - | + | + | = |
| Total | + | - | + | - | - | + | + | = |

| 1972-1992 Period | | | | | | | | |
|---|---|---|---|---|---|---|---|---|
| Reach | W | EG-Slope | Velocity | Area | D | F =W/D | WP | WS slope |
| 1 | - | + | - | + | + | - | - | + |
| 2 | - | + | - | + | + | - | - | - |
| 3 | - | + | - | + | + | - | - | = |
| Total | - | + | - | + | + | - | - | + |

| 1992-2001 Period | | | | | | | | |
|---|---|---|---|---|---|---|---|---|
| Reach | W | EG-Slope | Velocity | Area | D | F =W/D | WP | WS slope |
| 1 | - | - | + | - | + | - | - | - |
| 2 | - | - | + | - | + | - | - | = |
| 3 | - | + | + | - | + | + | = | = |
| Total | - | = | + | - | + | - | - | - |

W = width, EG-Slope = energy grade line slope, D = depth, F = width/depth ratio, WP = wetted perimeter, WS slope = water surface slope

## 6.2 SCHUMM'S (1969) RIVER METAMORPHOSIS MODEL

Schumm's (1969) qualitative model of channel metamorphosis is based on the concept that the dimensions, shape, gradient and pattern of stable alluvial rivers are controlled by the quantity of water and sediment as well as the type of sediment moved through their channels. The application of this model is appropriate for rivers in semi-arid regions because they are usually more adjustable than rivers in humid regions due to their less cohesive and less developed bank vegetation. The following equations summarize Schumm's results. A plus sign

(+) exponent indicates an increase in the magnitude of a parameter while a minus sign (-) indicates a decrease:

- Decrease in bed material load:

$$Q_s^- \sim \frac{W^- L^- S^-}{D^+ P^+}$$

- Increase in bed material load:

$$Q_s^+ \sim \frac{W^+ L^+ S^+}{D^- P^-}$$

- Increase in water discharge:

$$Q^+ \sim \frac{W^+ D^+ L^+}{S^-}$$

- Decrease in water discharge:

$$Q^- \sim \frac{W^- D^- L^-}{S^+}$$

- Increase in water discharge and bed material load:

$$Q^+ Q_t^+ \sim \frac{W^+ F^+ L^+ S^{\pm} D^{\pm}}{P^-}$$

- Decrease in water discharge and decrease in bed material load:

$$Q^- Q_t^- \sim \frac{W^- F^- L^- S^{\pm} D^{\pm}}{P^+}$$

Where,

Q = water discharge,

$Q_s$ = bed material load,

$Q_t$ = percentage of total sediment load that is bed-load or ratio of bedload (sand size or larger) to total sediment load x 100 at mean annual discharge,

W = channel width,

D = flow depth,

F = width/depth ratio,

L = meander wavelength,

P = sinuosity, and

S = channel slope.

These equations are summarized in Table 6-3. Table 6-4 summarizes the trends in channel changes in the Corrales Reach for the 1962 to 1972, 1972 to 1992 and 1992 to 2001 time periods in a similar manner as Table 6-3 for purposes of comparison.

**Table 6-3: Summary of Schumm's (1969) channel metamorphosis model.**

| | W | D | S | F=W/D | P | L |
|---|---|---|---|---|---|---|
| $Qs^-$ | - | + | - | | + | - |
| $Q^+$ | + | + | - | | | + |
| $Qs^+$ | + | - | + | | - | + |
| $Q^-$ | - | - | + | | | - |
| $Q^-Qs^-$ | - | + - | + - | - | + | - |
| $Q^+Qs^+$ | + | + - | + - | + | - | + |

**Table 6-4: Summary of channel changes during 1962-1972, 1972-1992 and 1992-2001 time periods.**

| 1962-1972 Period | | | | | |
|---|---|---|---|---|---|
| Reach | W | D | EG-Slope | F =W/D | P |
| 1 | + | - | - | + | + |
| 2 | + | - | - | + | - |
| 3 | + | - | - | + | + |
| Total | + | - | - | + | + |

| 1972-1992 Period | | | | | |
|---|---|---|---|---|---|
| Reach | W | D | EG-Slope | F =W/D | P |
| 1 | - | + | + | - | + |
| 2 | - | + | + | - | - |
| 3 | - | + | + | - | - |
| Total | - | + | + | - | - |

| 1992-2001 Period | | | | | |
|---|---|---|---|---|---|
| Reach | W | D | EG-Slope | F =W/D | P |
| 1 | - | + | = | - | = |
| 2 | - | + | + | - | = |
| 3 | + | + | + | - | + |
| Total | - | + | = | - | = |

According to Schumm's (1969) metamorphosis model, changes in channel geometry, slope and planform in the Corrales Reach from 1962 to 1972 were the response to increasing mean annual flood ($Q^+$) and increasing bed material load ($Q_s^+$). The large suspended sediment concentration (Figures 4-2 and 4-3) observed at the Bernalillo and Albuquerque Gages are in agreement with the modeled results, assuming that the bed material load was also large during the 1962 to 1972 time period. Conversely, annual peak flows appear to be lower between 1962 and 1972 than during previous years (Figure 2-9).

The 1972-1992 changes in channel geometry, slope and planform in the study reach are best explained by decrease in discharge ($Q^-$) and bed material load ($Q_s^-$). The model results are supported by the decrease in suspended sediment concentration since 1973 (Figure 4-2 and 4-3). Annual peak flows at Albuquerque decreased after 1958 with the same pattern being maintained since (Figure 2-9). Therefore, changes in annual peak flows support Schumm's (1969) model.

Decreased discharge ($Q^-$) and bed material load ($Q_s^-$) best explain the channel geometry, slope and planform for subreaches 1 and 2 from 1992 to 2001, while an increase in discharge ($Q^+$) and bed material load ($Q_s^+$) describe subreach 3 for the same time period. Annual peak flows from 1992 to 2001 tend to be lower than that of previous years which support the model for subreaches 1 and 2. However the bed material load increased since 1992 thus supporting the model for subreach 3. Schumm's model is not supported in any of the reaches for the time period of 1992 to 2001.

Schumm's (1969) model uses mean-annual flood instead of annual peak flows. It is possible that peak discharges are not indicative of the channel forming discharge regime. Additionally, changes in water regime could have been less significant than changes in sediment load and therefore, the channel could have been responding primarily to the changes in the sediment regime.

## 6.3 POTENTIAL FUTURE EQUILIBRIUM CONDITIONS

### Equilibrium Slope

Laursen's bed material transport equation predicts the transport capacity of the three subreaches closest to the calculated incoming bed material load (5,982 tons/day). The different equation results varied widely for each subreach. In general subreaches 1 and 3 exhibit similar

trends from 1992 to 2001, all of the transport equations, except Laursen, predict a larger capacity in 2001. Subreach 2 tends to have higher sediment transport capacities in 2001 with the same slope as 1992.

When matching the incoming bed material load to the channel capacity, most of the predicted slopes were lower than the 2001 slopes (Table 5-9). Laursen's equation produced the best results for all the subreaches; the equation suggests a slight increase in slope to attain equilibrium for subreaches 1 and 2. All other equations predicted slopes that were flatter than the 2001 slopes with the exception of Einstein's equations for subreach 1.

Laursen yields the closest slopes to the 2001 slopes of the three subreaches. According to Laursen's equation, the equilibrium slopes should be 0.0010, 0.0011 and 0.0008 for subreaches 1, 2, and 3 respectively, which are close to the 2001 slopes of 0.0009, 0.0010 and 0.0010. In summary, most of the sediment transport equations do not yield similar results to the 2001 incoming bed material load to the reach (Table 5-8) for all subreaches. As a result, the subreaches do not appear to be in a stable state. A decrease in slope might be necessary to attain equilibrium in the entire reach (Table 5-9).

### Equilibrium Channel Width Analysis

- Williams and Wolman (1984) Hyperbolic Model

Hyperbolic equations fit the historical data well for subreaches 1 and 2. As a result, these equations could be used to describe the past trends in channel width and predict future changes at these subreaches. Table 6-5 contains the 1991-1992 rate of decrease in channel width in feet per year, the 2001 active channel widths in feet from GIS and the 2001 channel widths in feet predicted with the hyperbolic functions. The 1991-1992 rates of decrease in channel width were computed as the slope of the hyperbolic function between 1991 and 1992. These rates are low, suggesting that the channel widths are still decreasing at a low rate. This model indicates that the channel width did not change significantly between 1962 and 1992.

**Table 6-5: 1991-1992 rate of decrease in channel width according to the hyperbolic model and 2001 predicted and measured widths.**

| Reach | 1991-1992 rate of decrease in channel width (ft/yr) | 2001 active channel width from GIS (ft) | 2001 width from regression (ft) |
|---|---|---|---|
| 1 | -3.0 | 429 | 528 |
| 2 | -6.1 | 516 | 511 |

- Richard (2001) Exponential Model

Exponential equations fit the historical data well and therefore could be used to describe the past or future trends in channel width. Table 6-6 summarizes the 1992-2001 rate of change of width in feet per year, the predicted 2001 widths in feet from the exponential equations and the 2001 active channel widths in feet from the digitized aerial photos. The exponential model produces slightly higher rates of decreasing channel width with time than the hyperbolic model. The predicted 2001 width using method one is higher than the GIS measurements for subreaches 1 and 3, and lower for subreach 2. The predicted 2001 width using method two is higher than the GIS measurements for subreaches 1 and 2, and lower for subreach 3. This model indicates that the channel width did not change significantly between 1962 and 2001.

**Table 6-6: 1992-2001 rate of decrease in channel width according to the exponential model and 2001 predicted and measured widths.**

| Reach | 1992-2001 rate of decrease in channel width (ft/yr) | | Predicted 2001 active channel width from exponential equations (ft) | | 2001 active channel width from GIS (ft) |
|---|---|---|---|---|---|
| | Method 1 | Method 2 | Method 1 | Method 2 | |
| 1 | -5.1 | -5.0 | 483 | 487 | 429 |
| 2 | -6.3 | -6.1 | 484 | 519 | 516 |
| 3 | -8.0 | -8.3 | 517 | 475 | 492 |
| Total | -5.9 | -5.9 | 503 | 506 | 474 |

### Hydraulic Geometry

Channel width started to level off after the rehabilitation of the floodway in the 1950's. From all the hydraulic geometry equations, Klassen and Vermeer's method best resembles the channel width for all the years, but does not show any spatial or temporal variation, it predicts the same width for every subreach and every year. The rest of the equations do not the fit the data well. The predicted widths are nearly constant for all the subreaches from 1962 to 2001. This trend is in agreement with the historical trends of channel width during the 1962 to 2001 time period (Figure 3-15 and 3-16). These results suggest that the study reach has been historically close to an equilibrium state.

### Stable Channel Analysis (SAM®)

The results from the SAM® stable channel analysis were used to predict the stable slope based on the equilibrium width of each subreach and the bed material sand-sized sediment

concentration of 1,304 mg/L (corresponding to Q = 5,000 cfs and $Q_s$ = 5,982 tons/day). 2001 non-vegetated GIS widths were used to estimate the slopes. The SAM® curve provides a combination of slope and width that can transport the given bed-material concentration. The active channel width measured from the GIS coverages from the 2001 aerial photos, the enrgy grade line slope determined through the 2001 HEC-RAS® analysis and the energy grade line slopes from the 1,304 mg/l curve are listed in Table 6-6.

**Table 6-7: Equilibrium channel slope predicted from SAM® stable channel analysis for 1,304 mg/l sand-size sediment concentration.**

| Subreach | GIS Width (ft) | 2001 EG Slope | EG Slope from SAM |
|---|---|---|---|
| | | | |
| **1** | 429 | 0.0009 | 0.0017 |
| **2** | 516 | 0.0009 | 0.0018 |
| **3** | 492 | 0.0012 | 0.0018 |
| **Total** | 474 | 0.0010 | 0.0018 |

The SAM® analysis over predicts the 2001 channel slopes, which suggest that the channel is not able to transport the sediment supply to the reach. The SAM® results are not in agreement with the historic degradation trend observed from 1972 to 2001. In addition, the incoming bed material concentration should be between 449 mg/l and 1,000 mg/l to obtain the 2001 slope-width combinations for all subreaches (Figure 5-9). In summary, the SAM® analysis indicates that the slope should be increased to attain equilibrium in the channel.

# 7 SUMMARY

This work pertains to the hydraulic modeling analysis of the Corrales Reach of the Middle Rio Grande, which spans 10.3 miles from the Corrales Flood Channel (agg/deg 351) to the Montano Bridge (agg/deg 462). This report characterizes the historic conditions of the study reach and evaluates potential future equilibrium conditions. The general trend of the study reach includes a decrease in width, width-to-depth ratio, area, water surface slope, energy-grade line slope and wetted perimeter and an increase in mean velocity and depth during the 1962 to 2001 time period.

Most of the reach aggraded approximately 0.1 feet from 1962 to 1972 and degraded about 2.5 feet between 1972 and 1992. Degradation during the 1972 to 1992 time period exceeded the aggradation that occurred between 1962 and 1972. Therefore, the net change has been degradation between 1962 and 1992. From 1992 to 2001 the bed degraded slightly in subreach 1 and aggraded in subreaches 2 and 3. Maximum aggradation for this time period was about 2.0 feet, which occurred in subreach 3.

The main conclusions for this hydraulic modeling analysis on the Corrales Reach are as follows:

1. The median bed material size in the Corrales Reach comprises of fine sand in 1962 and 1972, fine sand to coarse gravel in 1992, and medium sand to coarse gravel in 2001. Recent field observations indicate that the bed material is characterized by a bimodal distribution (Masson pers. comm. 2000).

2. The active channel width of the study reach decreased from 1275 feet in 1918 to 474 feet in 2001. The largest change in width occurred from 1918 to 1962. A slight increase in channel width occurred during the 1962 to 1972 time period as a result of the aggradational trend of the river bed. Bed degradation after 1972 induced a small narrowing trend of the channel. The channel width was essentially stable from 1972 to 1992 with a width of approximately 650 feet. From 1992 to 2001 the channel narrowed significantly from 607 feet to 474 feet.

    - Williams and Wolman Hyperbolic Model produces equations that fit the data well from 1918 to 2001 for subreaches 1 and 2. Exponential

equations fit the historical data well and therefore could be used to describe the past or future trends in channel width.

- Three of the hydraulic geometry equations shown in figure 5-4 (Julien-Wargadalam, Lacey, Simons and Albertson) under predict the historical channel widths. Klassen and Vermeer over predict the historical channel widths but predict widths closest to the actual widths.

3. Planform geometry of the entire reach is a straight, single-thread channel for 1962 and 1972 and straight, braided channel for 1992 and 2001 at a bankfull discharge of 5,000 cfs. The channel sinuosity ranges increased slightly from 1.14 to 1.17 throughout the entire period analyzed. These values are indicative of a nearly straight channel.

4. According to the modeling results from HEC-RAS®, the 1962, 1992, and 2001 channels have greater capacity to convey the modeled discharge (5,000 cfs) without overbank flow than the channel in 1972.

5. Channel geometry changes are similar in all three subreaches, which suggest that the sediment and water input from the tributaries and the diversion channel do not affect the morphology of the reach.

6. At flows close to 5,000 cfs, very fine and fine sand particles (0.0625 mm < $d_s$ < 0.25 mm) behave as washload. The bed material load is approximately 34% of the sand load (17,593 tons/day). Therefore, the incoming bed material load is approximately 5,982 tons/day.

7. The bed material transport capacity of the subreaches was estimated for 1992 and 2001 using the following sediment transport equations: Laursen, Engelund and Hansen, Ackers and White ($d_{50}$ and $d_{35}$), Yang – Sand ($d_{50}$ and size fraction), Einstein and Toffaleti (Stevens et al. 1989, Julien 1995). Laursen's equation most closely resembles the 2001 conditions, for both slope and transport capacity of the three subreaches, suggesting a slight increase of slope in subreach 1 and 2 and a slight decrease in subreach 3 is necessary to reach a state of equilibrium. The transport capacity results for each subreach are summarized in Table 7-1; more details can be seen in Tables 5-8 and 5-9.

**Table 7-1: Summarized sediment transport results for 1992 and 2001.**

| Year | Subreach | BML average (tons/day) | Minimum BML (tons/day) | Maximum BML (tons/day) |
|---|---|---|---|---|
| 1992 | 1 | 6,848 | 1,001 | 14,030 |
| | 2 | 12,369 | 6,476 | 17,813 |
| | 3 | 10,371 | 6,589 | 13,430 |
| | | | | |
| 2001 | 1 | 8,273 | 5,248 | 10,941 |
| | 2 | 8,947 | 5,444 | 11,704 |
| | 3 | 11,755 | 7,472 | 15,309 |

8. SAM® analysis indicates that the channel slope should be increased to attain equilibrium. This result is not in agreement with the historic trend of degradation observed from 1972 to 2001.

## 8 REFERENCES


Ackers, P. 1982. Meandering Channels and the Influence of Bed Material. *Gravel Bed Rivers. Fluvial Processes, Engineering and Management*. Edited by R. D. Hey, J.C. Bathurst and C.R. Thorne. John Wiley & Sons Ltd. pp 389-414.

Arritt, S. 1996. Rio Grande Silvery Minnow: Symbol of an Embattled River. New Mexico Wildlife. 41. pp 8-10

ASCE Task Committee on Hydraulics, Bank Mechanics and Modeling of River Width Adjustment. 1998. River Width Adjustment. I: Processes and Mechanisms. Journal of Hydraulic Engineering, ASCE. 124 (9): 881-902.

Baird, D. C. 1996. River Mechanics Experience on the Middle Rio Grande. 6th Federal Interagency Sediment Conference. March 11-14. 8 pp.

Bestgen, K.R. and Platania, S.P.1991. Status and Conservation of the Rio Grande Silvery Minnow, Hybognathus Amarus. The Southwestern Naturalist. 36(2): 225-232.

Blench, T. 1957. *Regime Behaviour of Canals and Rivers*. Butterworths Scientific Publications, London.138 pp.

Brownlie, W.R. 1981. Prediction of Flow Depth and Sediment discharge in Open Channels. W. M. Keck Laboratory of Hydraulics and Water Resources. Division of Engineering and Applied Science. California Institute of Technology. Pasadena, California. Report No. KH-R-43A. 228 pp.

Bullard, K. L. and Lane, W. L. 1993. Middle Rio Grande Peak Flow Frequency Study. U.S. Department of Interior, Bureau of Reclamation, Albuquerque, NM. 36+p.

Burton, G.L. 1997. America's National Wildlife Refuges. Where Wildlife Comes Naturally! Rio Grande Silvery Minnow [Web Page]. Available at: http:// refuges.fws.gov/NWRSFiles/Wildli...nts/Fish/Rio_Grande_Silvery_Minnow.html.

Chang, H.H. 1979. Minimum stream power and river channel patterns. *Journal of Hydrology*, 41, 303-327.

Colby, B.R. and Hembree, C.H. 1955. Computations of Total Sediment Discharge Niobrara River near Cody, Nebraska. Geological Survey Water-Supply Paper 1357. pp.187

Henderson, F.M. 1966. *Open channel flow.* Macmilllan Publishing Co., Inc. New York, NY, 522 pp.

Julien, P. Y. 1995. *Erosion and Sedimentation*, Cambridge University Press, Ny, Ny, 280 pp.

Julien, P. Y. and Wargadalam, J. 1995. Alluvial Channel Geometry: Theory and Applications. *Journal of Hydraulic Engineering*, 121(4), 312-25.

Klaassen, G. J. and Vermeer, K. 1988. Channel Characteristics of the Braiding Jamuna River, Bangladesh. In *International Conference on River Regime, 18-20 May, 1988*, W.R. White (ed.), Hydraulics Research Limited, Wallingford, UK, 173-89.

Knighton, A.D. and Nanson, G.C. 1993. Anastomosis and the continuum of channel pattern. *Earth Surface Processes and Landforms*, 18, 613-625.

Lagasse, P.F. 1981. Geomorphic Response of the Rio Grande to Dam Construction. New Mexico Geological Society, Special Publication. No. 10. pp. 27-46.

León C. 1998. Morphology of the Middle Rio Grande from Cochiti Dam to Bernalillo Bridge, New Mexico. Master Thesis, Colorado State University, 210 pp.

Leopold, L. B. and Maddock, T. Jr. 1953. The Hydraulic Geometry of Stream Channels and Some Physiographic Implications: USGS Professional Paper 252, 57 pp.

Leopold, L.B. and Wolman, M.G. 1957. River Channel Patterns: Braided, Meandering and Straight, USGS Professional Paper 282-B, 85 pp.

Massong, T. 2000. Personal Communication. U.S. Bureau of Reclamation, Albuquerque, NM.

Molnár, P. 2001. Precipitation and Erosion Dynamics in the Rio Puerco Basin. Ph.D. Dissertation. Department of Civil Engineering. Colorado State University, Fort Collins, Colorado. pp. 258.

Mosley, H. and S. Boelman. 1998. Santa Ana Geomorphic Report. Draft. U.S. Bureau of Reclamation, Albuquerque, NM. pp.29.

Nordin, C. and Beverage J. 1965. *Sediment Transport in the Rio Grande, New Mexico*. Geological Survey Professional Paper 462-F, 35 pp.

Nordin, C. and J.K. Culbertson. 1961. Particle-size distribution of stream bed material in the Middle Rio Grande Basin. New Mexico. *Short Papers in the Geologic and Hydrologic Sciences*, Article 147-292, C-323-C-326.

Nouh, M. 1988. Regime channels of an extremely arid zone. *International Conference on River Regime, 18-20 May, 1988*, W.R. White (ed.), Hydraulics Research Limited, Wallingford, UK, 55-66.

Parker, G. 1976. On the cause and characteristic scales of meandering and braiding in rivers. *Journal of Fluid Mechanics*, vl.76, part 3, pp. 457-480.

Pemberton, E.L. 1964. Sediment Investigations-Middle Rio Grande. Journal of the Hydraulic Division. Proceedings of the American Society of Civil Engineers. Vol.90, No. HY2. pp. 163-185.

Platania, S.P. 1991. Fishes of the Rio Chama and Upper Rio Grande, New Mexico, with Preliminary Comments on their Longitudinal Distribution. The Southwestern Naturalist. Vol 36, No. 2. pp.186-193.

Richard G. 2001. Quantification and Prediction of Lateral Channel Adjustments Downstream from Cochiti Dam, Rio Grande, NM. Ph.D. Dissertation. Department of Civil engineering. Colorado State University, Fort Collins, Colorado. pp. 276.

Richardson, E.V, D.B. Simons and P.Y. Julien 1990. Highways in the River Environment. U.S. Department of Transportation. Federal Highway Administrartion, 610 pp.

Robinson, S. 1995. The Life & Times of Rio Grande Minnows. New Mexico Wildlife. 40(6):2-5.

Rosgen, D., 1996. *Applied River Morphology*, Pagosa Springs, CO, Wildland Hydrology. 360+p.

Sanchez, V. and D. Baird, 1997. River Channel Changes Downstream of Cochiti Dam. Middle Rio Grande, New Mexico. Sam S.Y. Wang, E.J. Langendoen and F.D. Shields Jr. Proceedings of the Conference on Management of Landscapes Disturbed by Channel Incision. The University of Mississippi, Oxford, Mississippi: The Center for Computational Hydroscience and Engineering. 6 pp.

Scurlock, D. 1998. From the Rio to the Sierra. An Environmental History of the Middle Rio Grande Basin. USDA, Forest Service, Rocky Mountain Research Station, Fort Collins. General Thechnical Report RMRS-GTR5. 440 p.

Schumm, S. A. 1969. *River Metamorphosis*. Journal of the Hydraulics Division. Vol 95, No. 1. pp. 255-273.

Schumm, S.A. and Khan, H.R. 1972. Experimental study of channel patterns. *Geological Society of America Bulletin,* 83, 1755-1770.

Simons, D.B and Albertson, M.L.1963. Uniform Water Conveyance Channels in Alluvial Material. Transactions of the American Society of Civil engineers. Paper No. 3399. Vol.128, PartI. pp. 65-107.

Stevens, H.H. and Yang, C.T. 1989. Summary and use of selected fluvial sediment-discharge formulas, USGS Water Resources Investigations Report 80-4026, 62 pp.

Taylor, J.P. and Mcdaniel, K.C. Accessed 2001. Restoration of Saltcedar Infested Flood Plains on the Bosque del Apache National Wildlife Refuge [Web page]. Available at : http://bhg.fws.gov/Literatur/newpage12.htm.

Thorne, C. R., R.D. Hey and M. D. Newson. 1997. *Applied Fluvial Geomorphology for River Engineering and Management*. John Wiley & Sons Ltd. 375 pp.

Tofaletti, F.B. 1969. Definitive computations of Sand Discharge in Rivers. *Journal of the Hydraulics Division*, 95, HY1, 225-246

US Army Corps of Engineers. 1998. Hydrologic Engineering Center-River Analysis System User's Manual. Version 2.2. Hydrologic Engineering Center, Davis, California, 227+p.

US Bureau of Reclamation. 1955. Step Method for Computing Total Sediment Load by the Modified Einstein Procedure. Prepared by the Sedimentation Section, Hydrology Branch. pp.18.

US Fish and Wildlife Service. 2000. http://pacific.fws.gov/vfwo/SpeciesAccount/birds/SWWF.htm

Van den Berg, J.H. 1995. Prediction of alluvial channel pattern of perennial rivers. *Geomorphology*. 12, 259-279.

Wargadalam, J. 1993. Hydraulic Geometry Equations of Alluvial Channels, Ph.D. Dissertation. Fort Collins, CO, Colorado State University, 203 pp.

Williams G. and G. Wolman. 1984. *Downstream Effects of Dams on Alluvial Rivers*. Geological Survey Professional Paper 1286, 83pp.

Woodson, R.C. 1961. Stabilization of the Middle Rio Grande in New Mexico. Journal of the Waterways and Harbors Division. Proceedings of the American Society of Civil Engineers. Vol.87, No. WW4. pp.1-15.

Woodson, R. C. and Martin, J. T. 1962. The Rio Grande comprehensive plan in New Mexico and its effects on the river regime through the middle valley, Control of Alluvial Rivers by Steel Jetties, *American Society of Civil Engineers Proceedings, Waterways and Harbors Division Journal 88,* E.J. Carlson and E.A. Dodge (eds.), NY, NY, American Society of Civil Engineers, 53-81.

# APPENDIX A – DATA LISTS

## TABLE A-1 AERIAL PHOTO
## (SOURCE: RICHARD ET AL. 2000)

Aerial Photos digitized in the Rio Grande Geomorphology Study, v. 1 by the USBR, Remote Sensing and Geographic Information Group, Denver, CO:

1) 1918 – Scale: 1:12,000, Hand drafted linens (39 sheets), USBR Albuquerque Area Office. Surveyed in 1918, published in 1922.

2) 1935 – Scale: 1:8,000. Black and white photography, USBR Albuquerque Area Office. Flown in 1935, published 1936.

3) 1949 – Scale 1:5,000. Photo-mosaic. J. Ammann Photogrammetric Engineers, San Antonio, TX. USBR Albuquerque Area Office.

4) March 15, 1962 – Scale: 1:4,800. Photo-mosaic. Abram Aerial Survey Corp. Lansing, MI. USBR Albuquerque Area Office.

5) April 1972 – Scale: 1:4,800. Photo-mosaic. Limbaugh Engineers, Inc., Albuquerque, NM. USBR Albuquerque Area Office.

6) March 31, 1985 – Scale: 1:4,800. Orthophoto. M&I Consulting Engineers, Fort Collins, CO. Aero-Metric Engineering, Sheboygan, MN. USBR Albuquerque Area Office.

7) February 24, 1992 – Scale: 1:4,800. Ratio-rectified photo-mosaic. Koogle and Poules Engineering, Albuquerque, NM. USBR Albuquerque Area Office.

8) Winter 2001 – Scale: 1:4,800. Photo-mosaic. USBR Albuquerque Area Office.

**Table A-2 Aerial photo dates and main daily discharge on those days.**

| Aerial Photo Dates | Mean Daily Discharge at Bernalillo (cfs) | Mean Daily Discharge at Albuquerque (cfs) |
|---|---|---|
| February 24, 1992 | No data | 159 |
| March 31, 1985 | No data | 109 |
| April 1972 | No data | Mean = 705<br>Max = 2540<br>Min = 116 |
| March 15, 1962 | 493 | No data |
| 1949 (unknown date) | Extreme low flow (from meta-data file) | No data |
| 1935 (unknown date) | Annual data from Otowi:<br>Mean = 1,520<br>Max = 7,490<br>Min = 350 | No data |
| 1918 (unknown date) | No data | No data |

# APPENDIX B – CROSS SECTION PLOTS

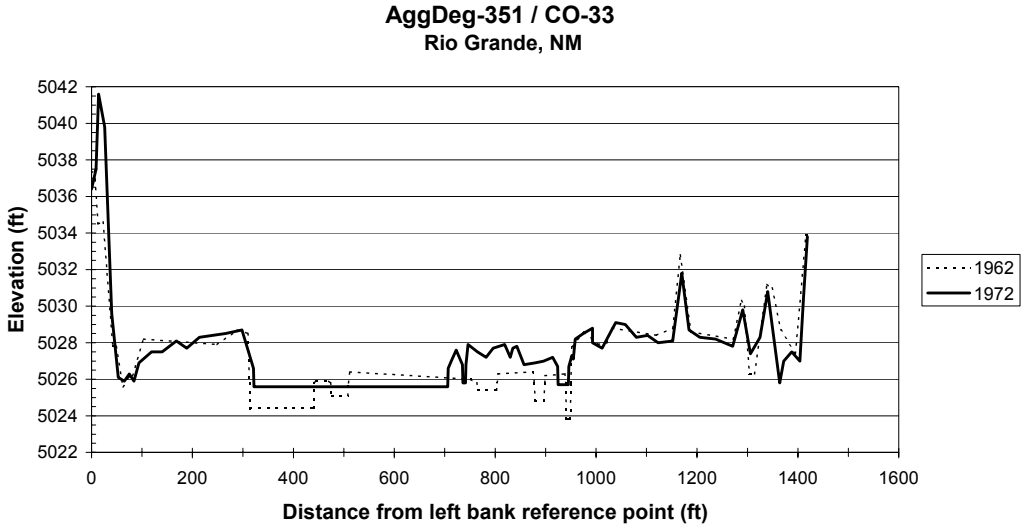


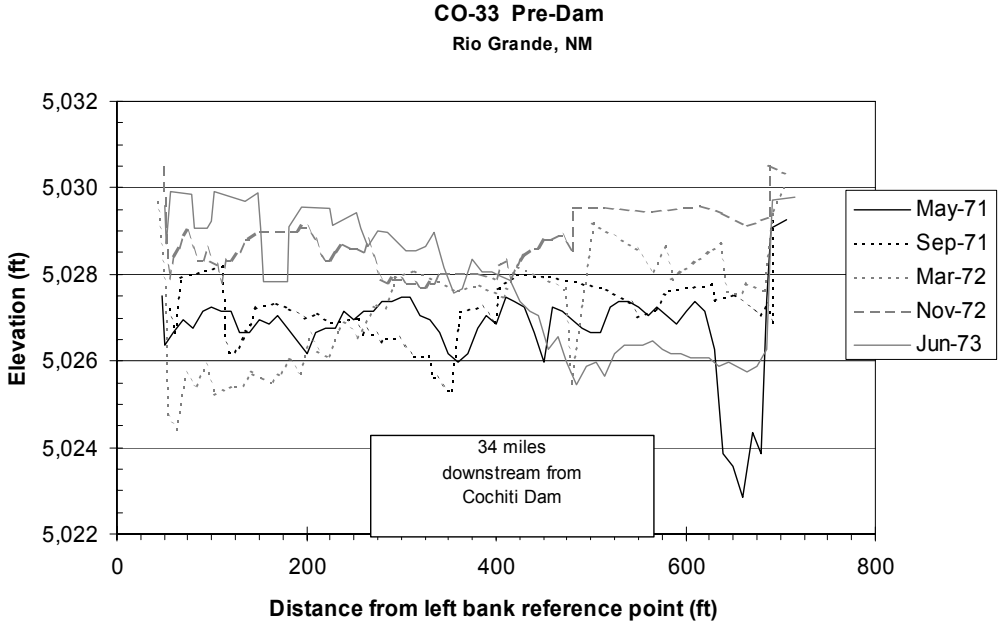

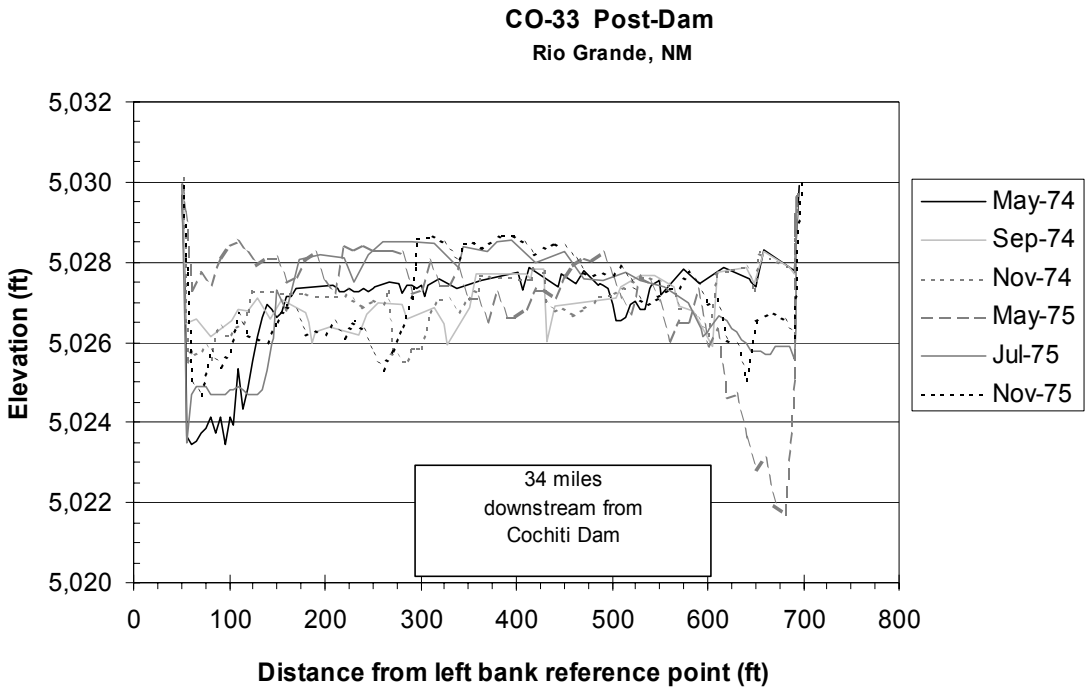
CO-33 Post-Dam
Rio Grande, NM
Elevation (ft)
5,032
5,030
5,028
5,026
5,024
5,022
5,020
0
100
200
300
400
500
600
700
800
Distance from left bank reference point (ft)
May-74
Sep-74
Nov-74
May-75
Jul-75
Nov-75
34 miles
downstream from
Cochiti Dam

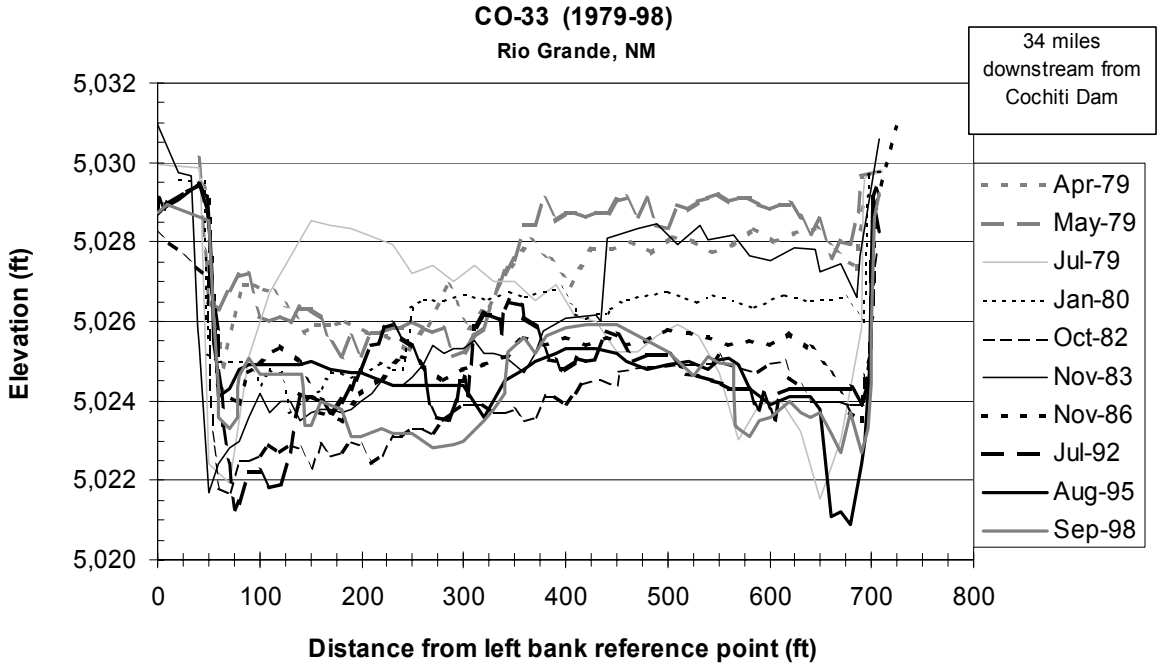
CO-33 (1979-98)
Rio Grande, NM
Elevation (ft)
5,032
5,030
5,028
5,026
5,024
5,022
5,020
0
100
200
300
400
500
600
700
800
Distance from left bank reference point (ft)
34 miles
downstream from
Cochiti Dam
Apr-79
May-79
Jul-79
Jan-80
Oct-82
Nov-83
Nov-86
Jul-92
Aug-95
Sep-98

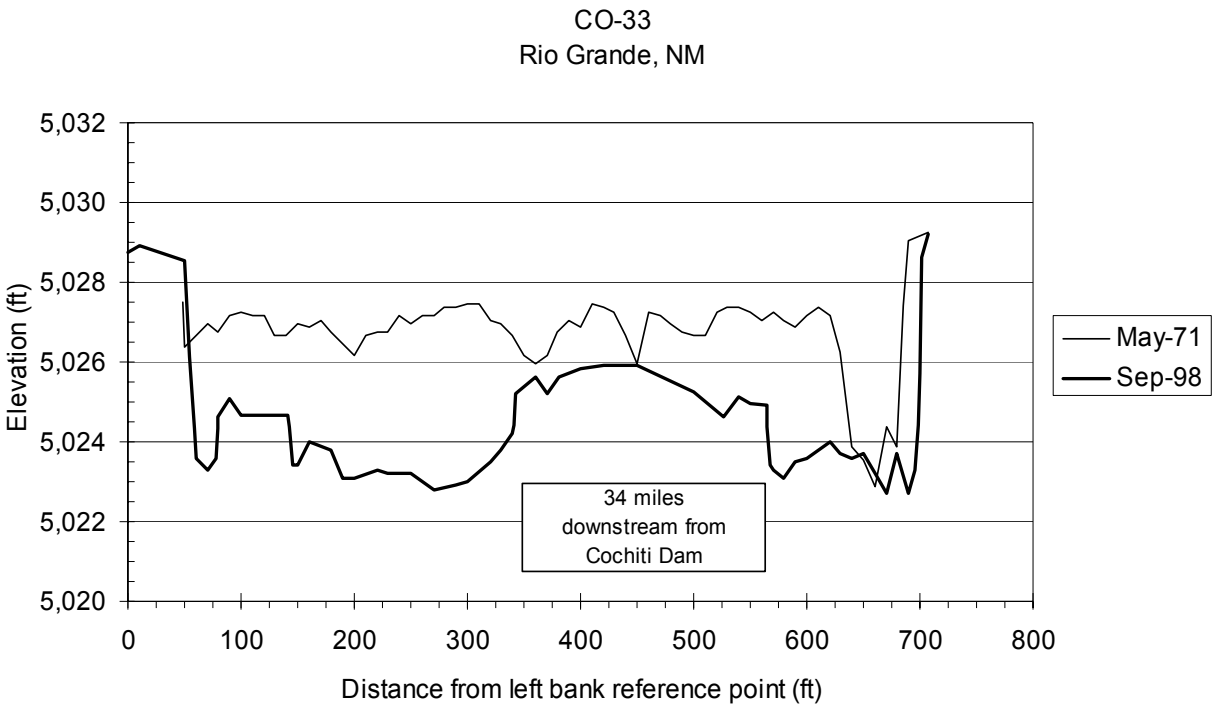
CO-33
Rio Grande, NM
5,032
5,030
5,028
5,026
5,024
5,022
5,020
Elevation (ft)
0
100
200
300
400
500
600
700
800
Distance from left bank reference point (ft)
34 miles
downstream from
Cochiti Dam
May-71
Sep-98

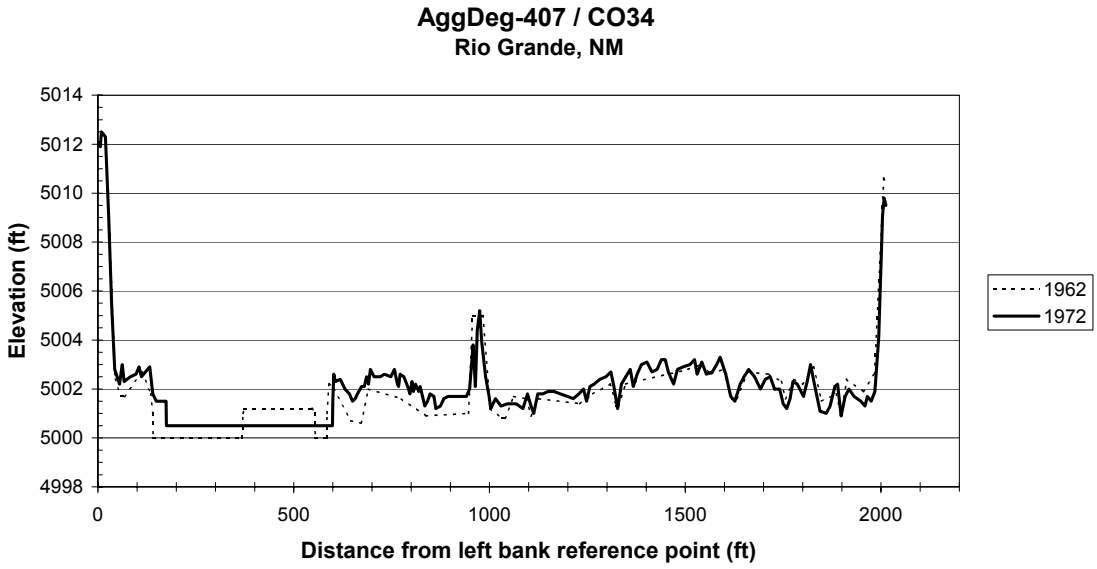
AggDeg-407 / CO34
Rio Grande, NM
Elevation (ft)
5014
5012
5010
5008
5006
5004
5002
5000
4998
0
500
1000
1500
2000
Distance from left bank reference point (ft)
1962
1972

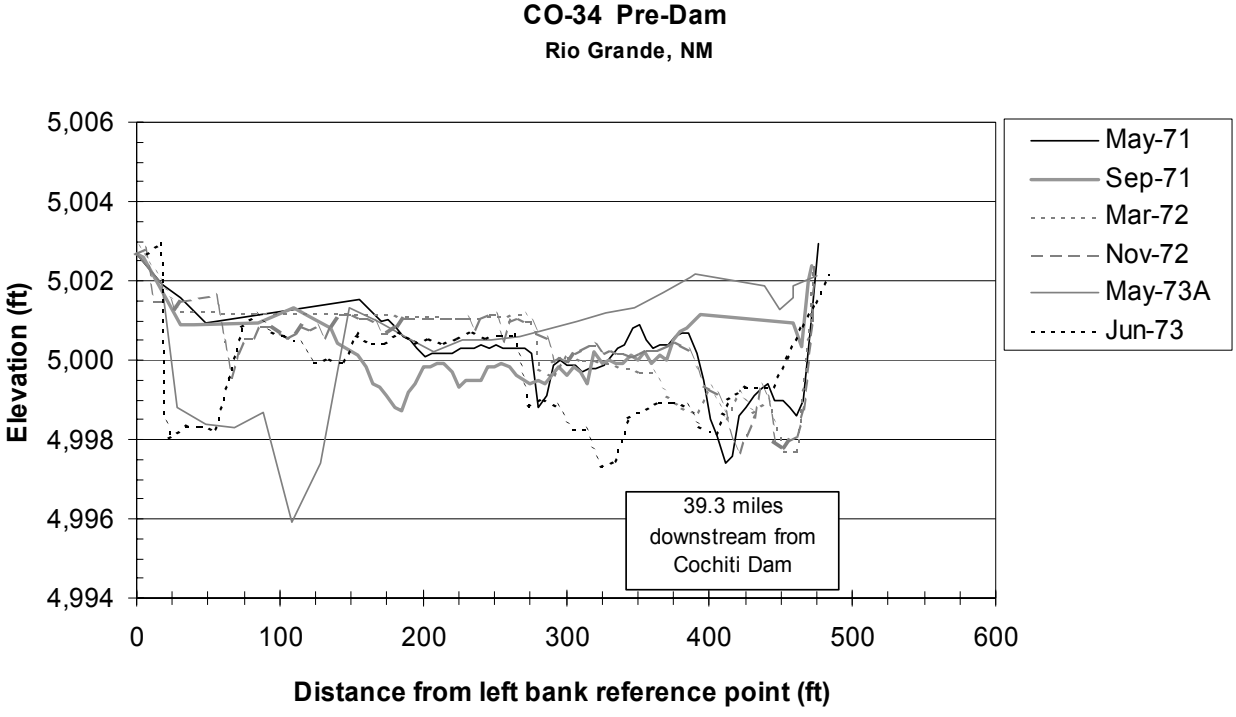
CO-34 Pre-Dam
Rio Grande, NM
Elevation (ft)
5,006
5,004
5,002
5,000
4,998
4,996
4,994
0
100
200
300
400
500
600
Distance from left bank reference point (ft)
May-71
Sep-71
Mar-72
Nov-72
May-73A
Jun-73
39.3 miles
downstream from
Cochiti Dam

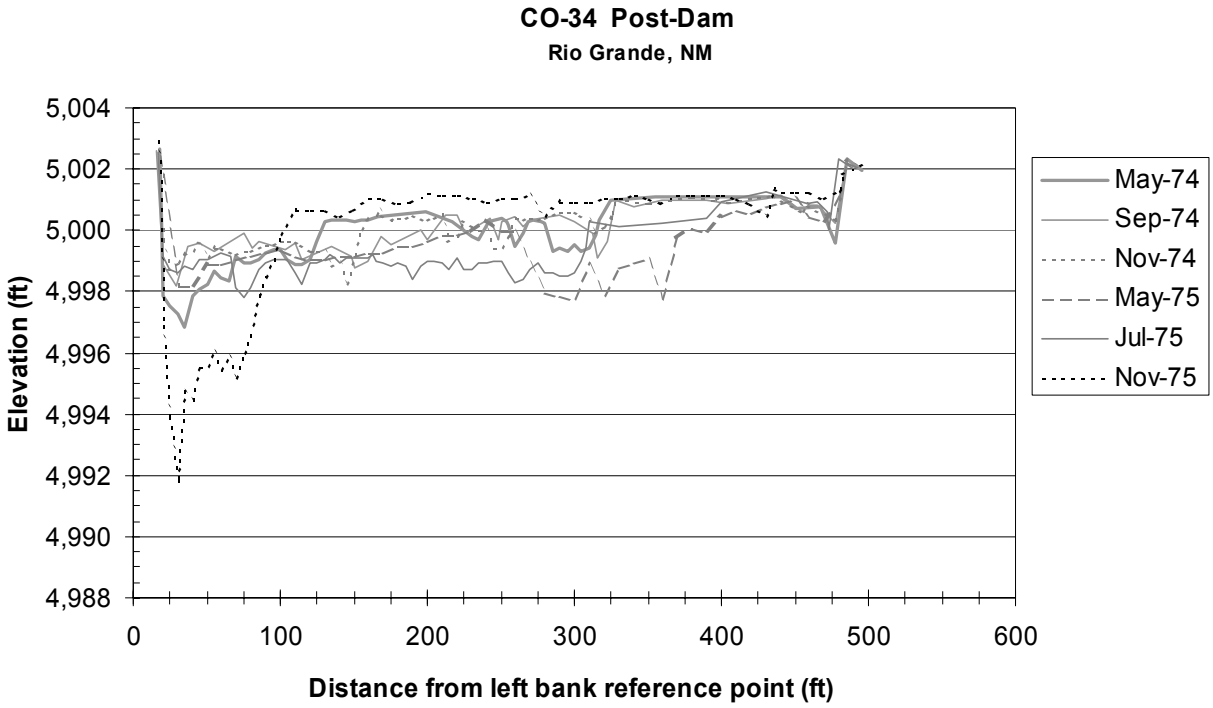
CO-34 Post-Dam
Rio Grande, NM
Elevation (ft)
5,004
5,002
5,000
4,998
4,996
4,994
4,992
4,990
4,988
0
100
200
300
400
500
600
Distance from left bank reference point (ft)
May-74
Sep-74
Nov-74
May-75
Jul-75
Nov-75

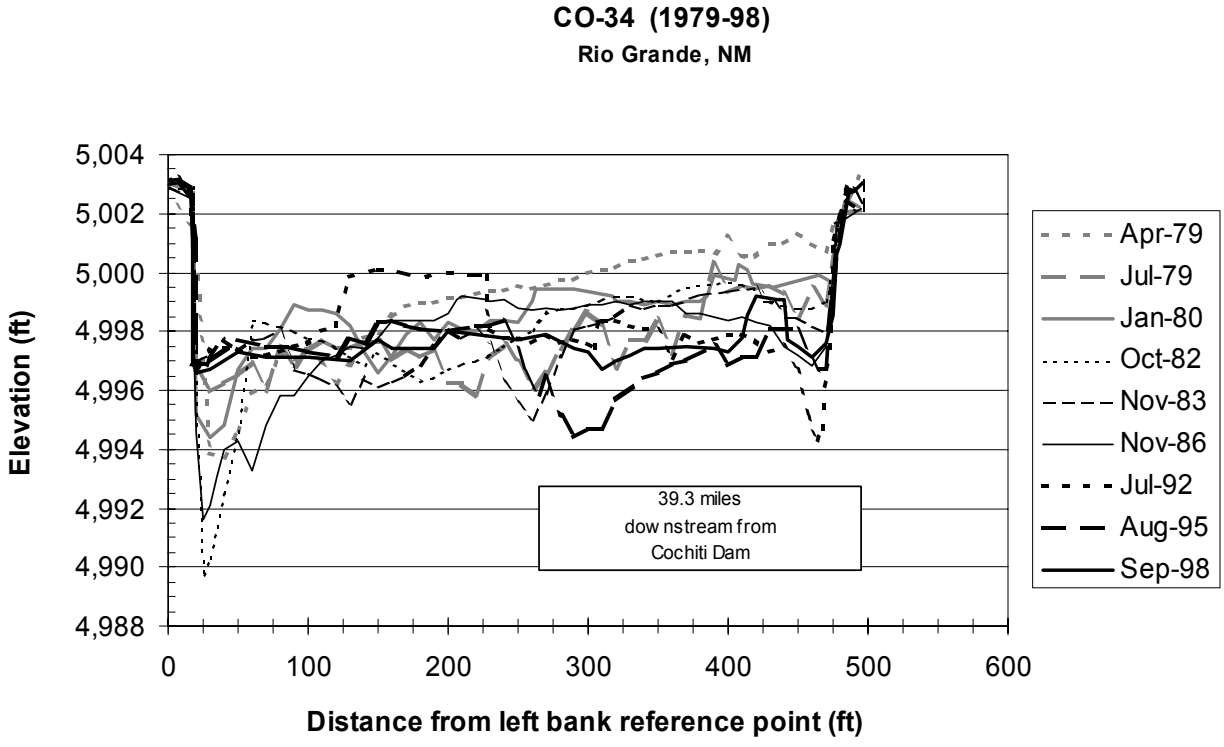
CO-34 (1979-98)
Rio Grande, NM
Elevation (ft)
5,004
5,002
5,000
4,998
4,996
4,994
4,992
4,990
4,988
0
100
200
300
400
500
600
Distance from left bank reference point (ft)
39.3 miles
dow nstream from
Cochiti Dam
Apr-79
Jul-79
Jan-80
Oct-82
Nov-83
Nov-86
Jul-92
Aug-95
Sep-98

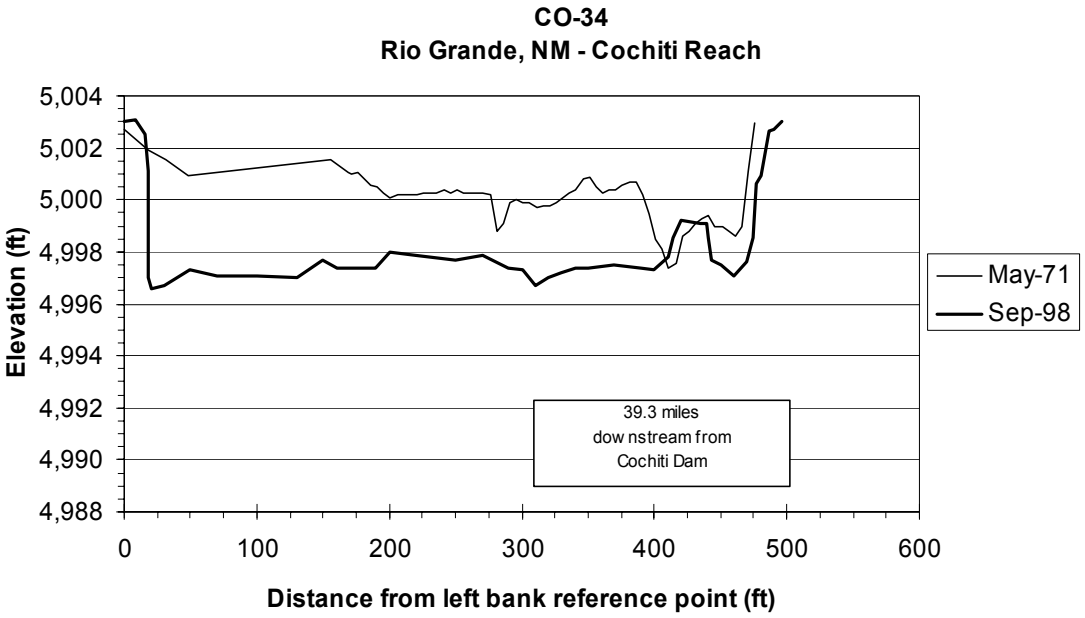
CO-34
Rio Grande, NM - Cochiti Reach
5,004
5,002
5,000
4,998
4,996
4,994
4,992
4,990
4,988
Elevation (ft)
0
100
200
300
400
500
600
Distance from left bank reference point (ft)
39.3 miles
dow nstream from
Cochiti Dam
May-71
Sep-98

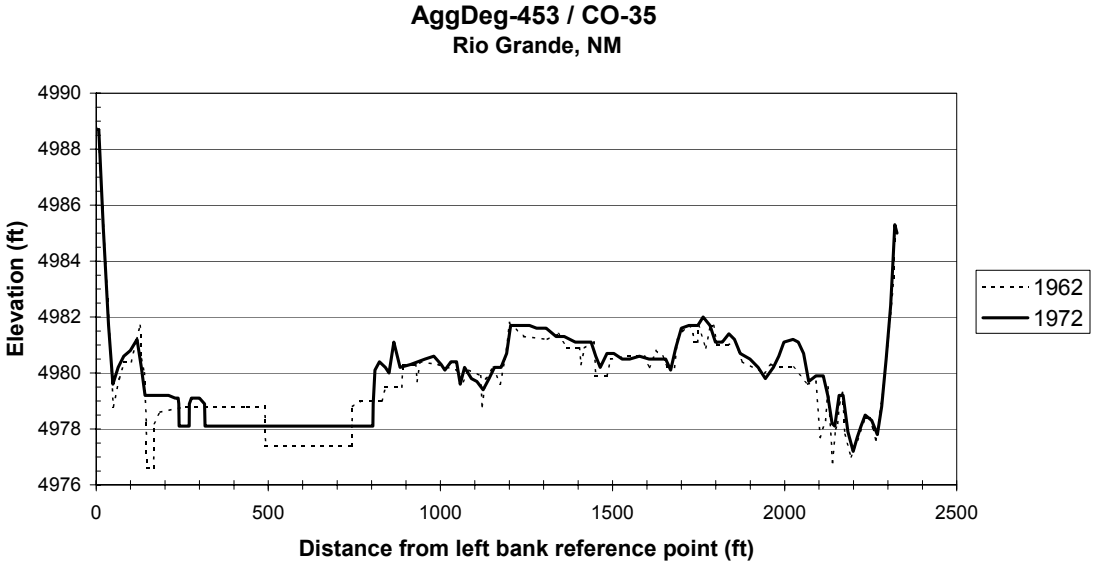
AggDeg-453 / CO-35
Rio Grande, NM
Elevation (ft)
4990
4988
4986
4984
4982
4980
4978
4976
0
500
1000
1500
2000
2500
Distance from left bank reference point (ft)
1962
1972

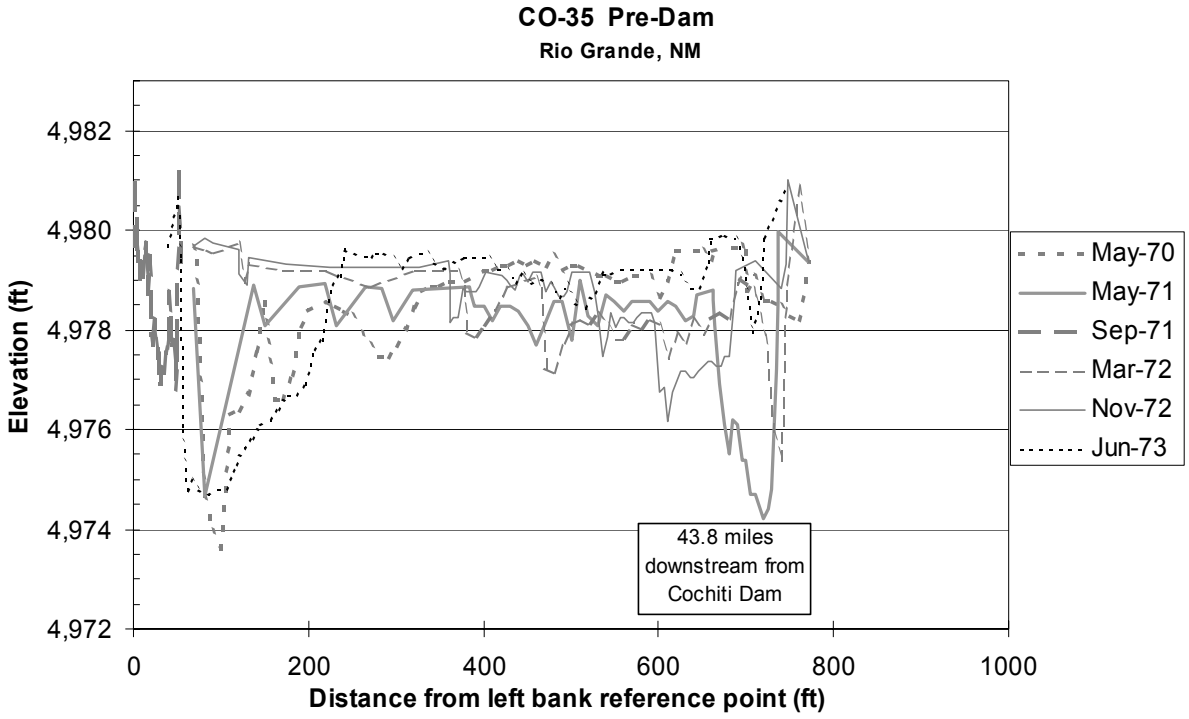
CO-35 Pre-Dam
Rio Grande, NM
Elevation (ft)
4,982
4,980
4,978
4,976
4,974
4,972
0
200
400
600
800
1000
Distance from left bank reference point (ft)
43.8 miles downstream from Cochiti Dam
May-70
May-71
Sep-71
Mar-72
Nov-72
Jun-73

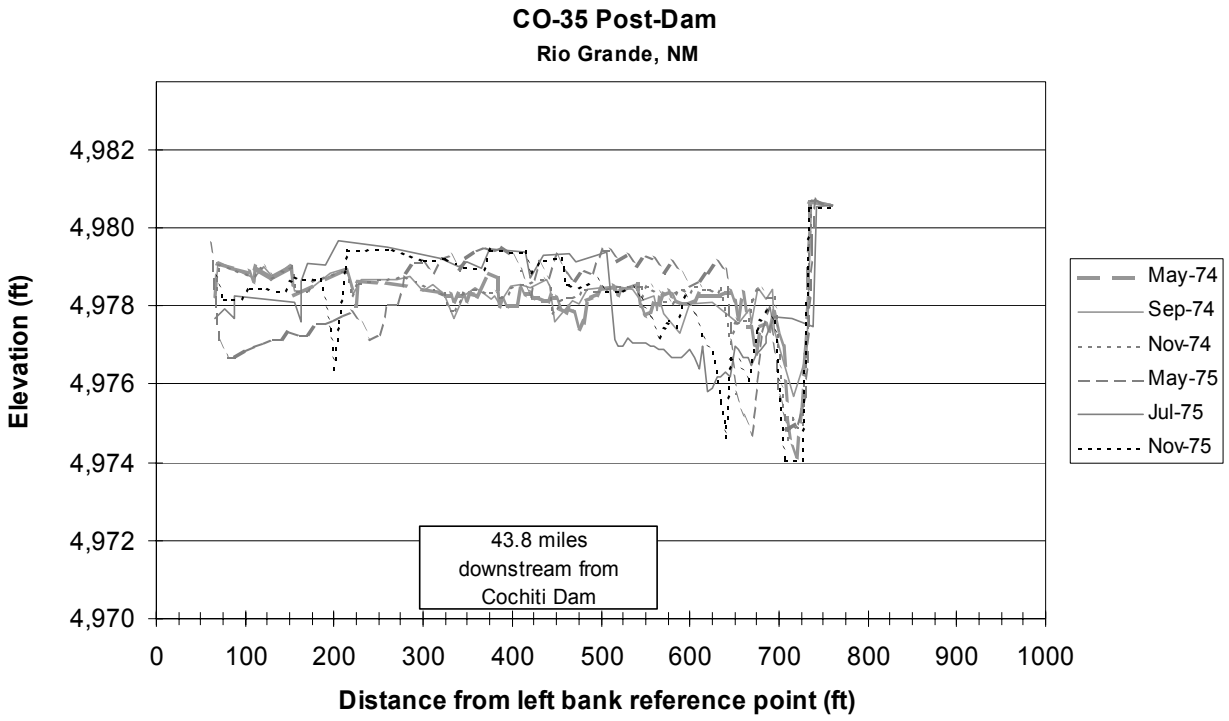
CO-35 Post-Dam
Rio Grande, NM
Elevation (ft)
4,982
4,980
4,978
4,976
4,974
4,972
4,970
0
100
200
300
400
500
600
700
800
900
1000
Distance from left bank reference point (ft)
43.8 miles
downstream from
Cochiti Dam
May-74
Sep-74
Nov-74
May-75
Jul-75
Nov-75

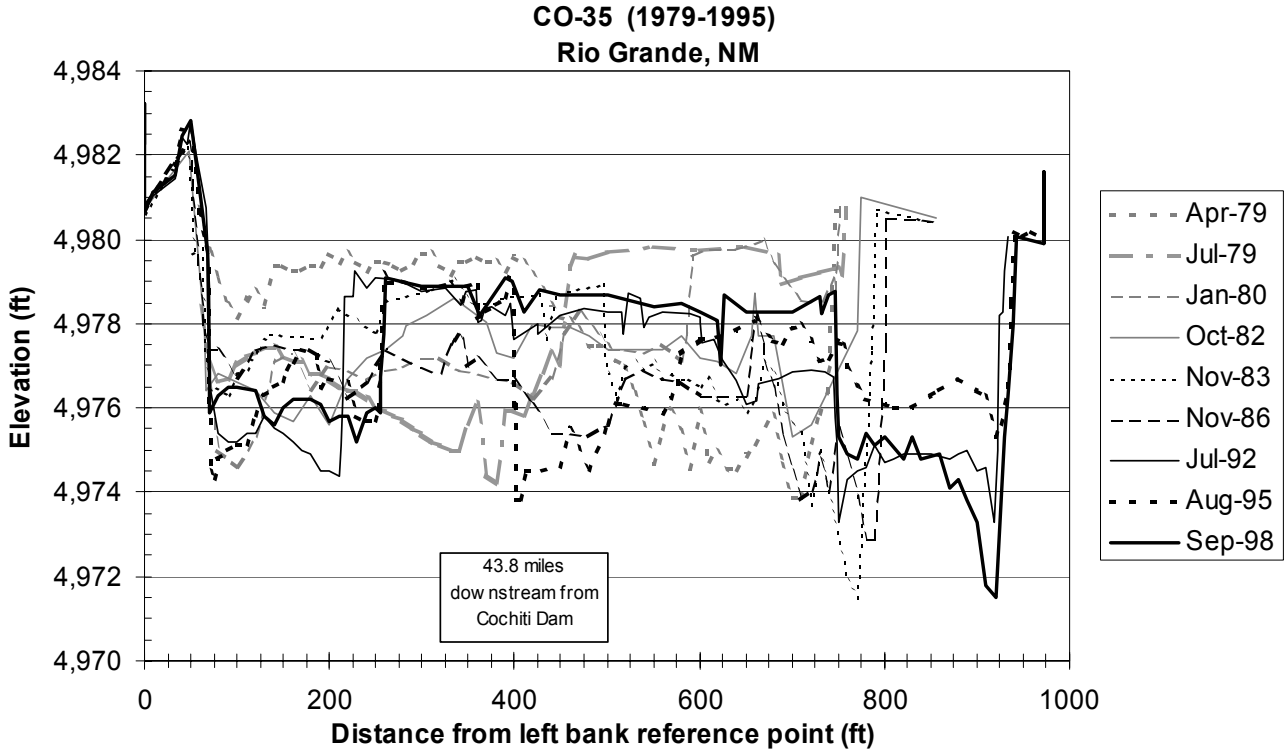
CO-35 (1979-1995)
Rio Grande, NM
Elevation (ft)
4,984
4,982
4,980
4,978
4,976
4,974
4,972
4,970
0
200
400
600
800
1000
Distance from left bank reference point (ft)
43.8 miles
dow nstream from
Cochiti Dam
Apr-79
Jul-79
Jan-80
Oct-82
Nov-83
Nov-86
Jul-92
Aug-95
Sep-98

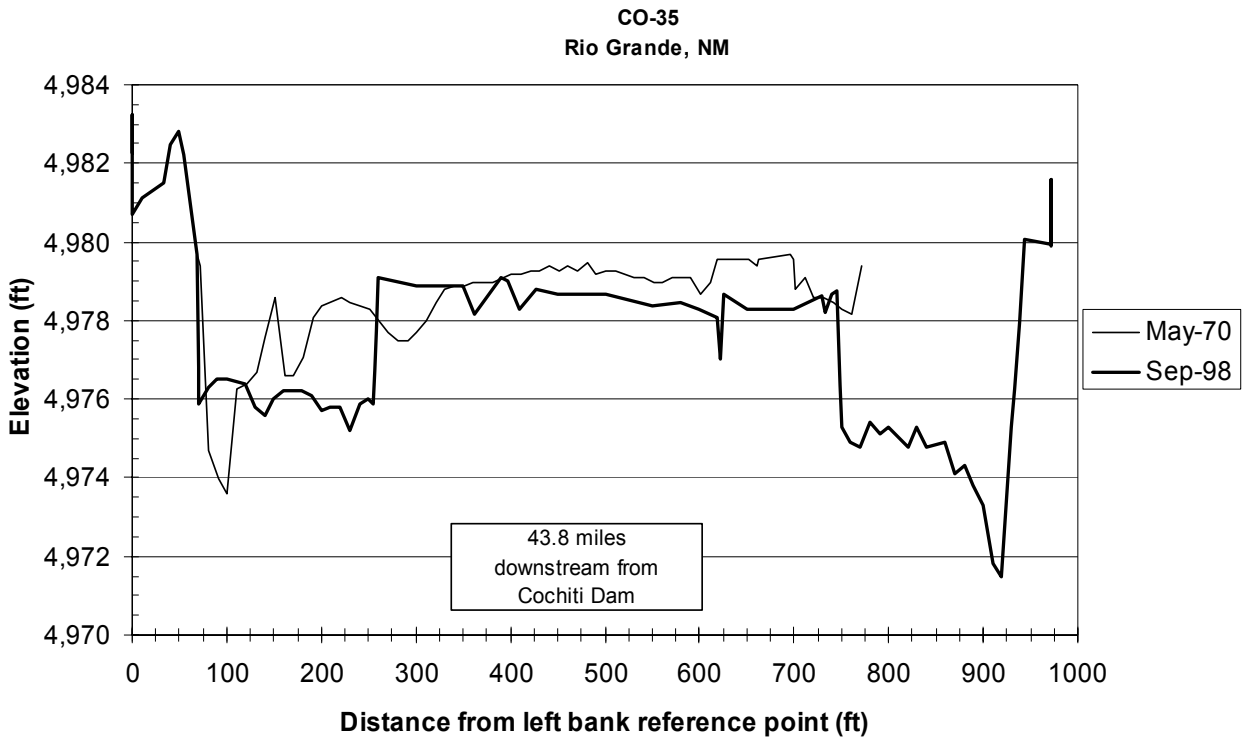
CO-35
Rio Grande, NM
4,984
4,982
4,980
4,978
4,976
4,974
4,972
4,970
Elevation (ft)
0
100
200
300
400
500
600
700
800
900
1000
Distance from left bank reference point (ft)
43.8 miles
downstream from
Cochiti Dam
May-70
Sep-98

# APPENDIX C – ANNUAL PEAK MEAN DISCHARGE PLOT

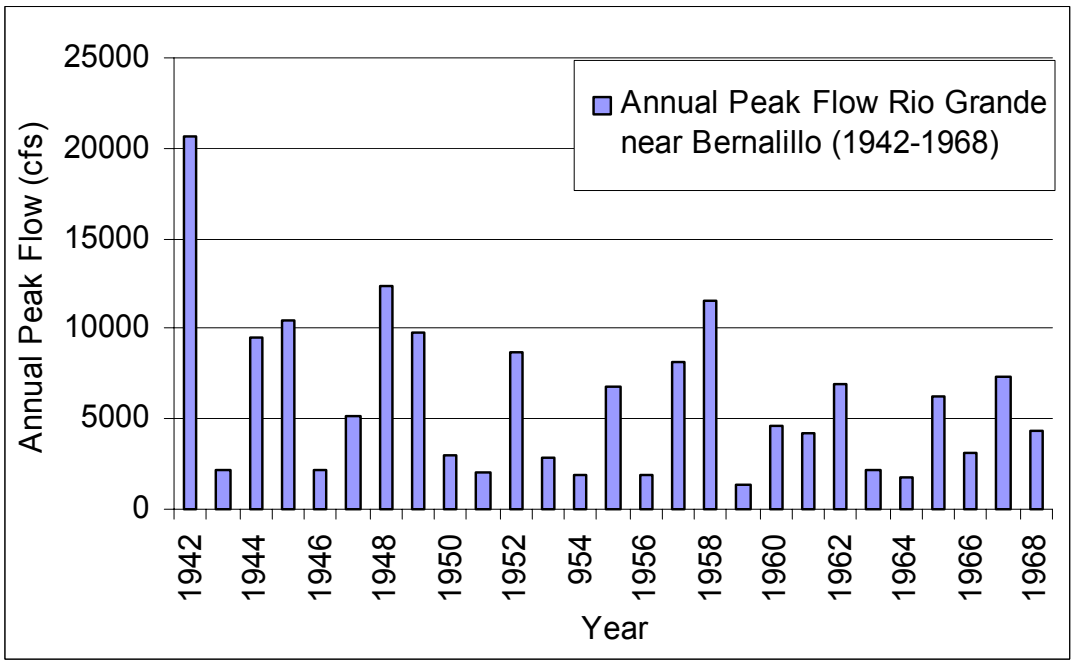

# APPENDIX D – BED MATERIAL HISTOGRAMS

**CO-34**

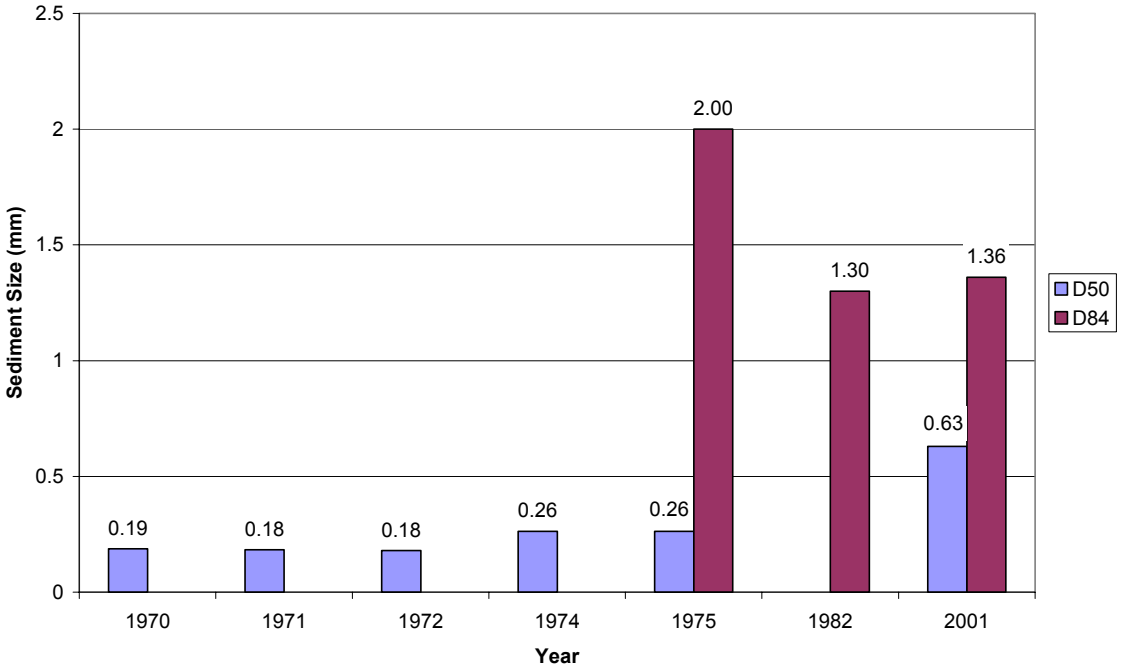


**CO-35**

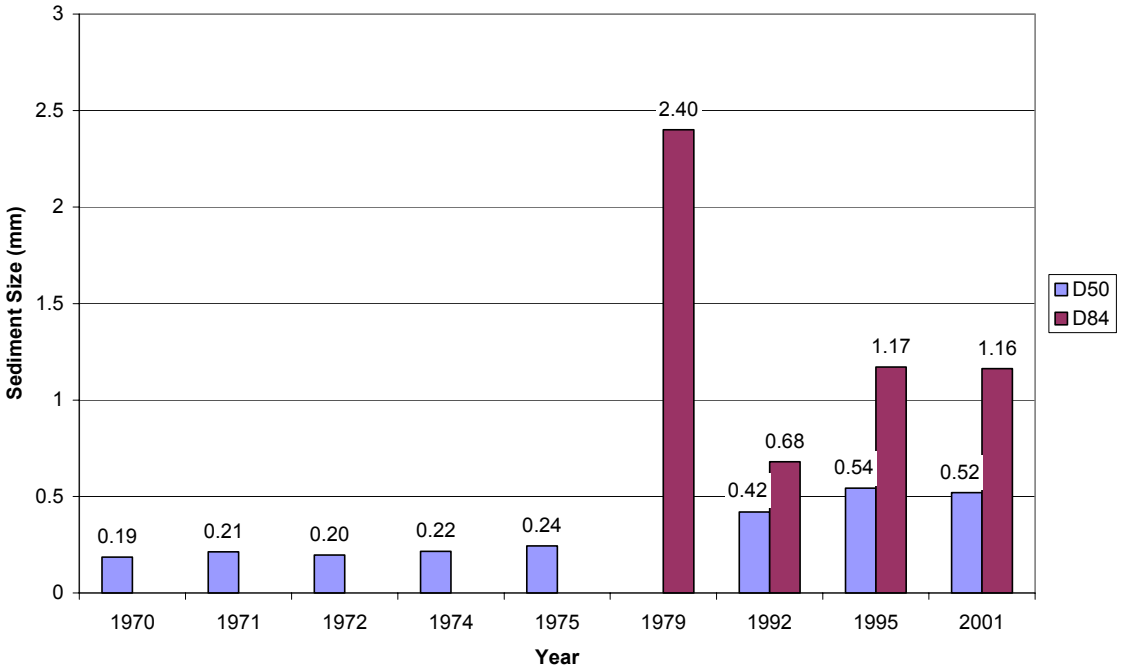

**CA-1**

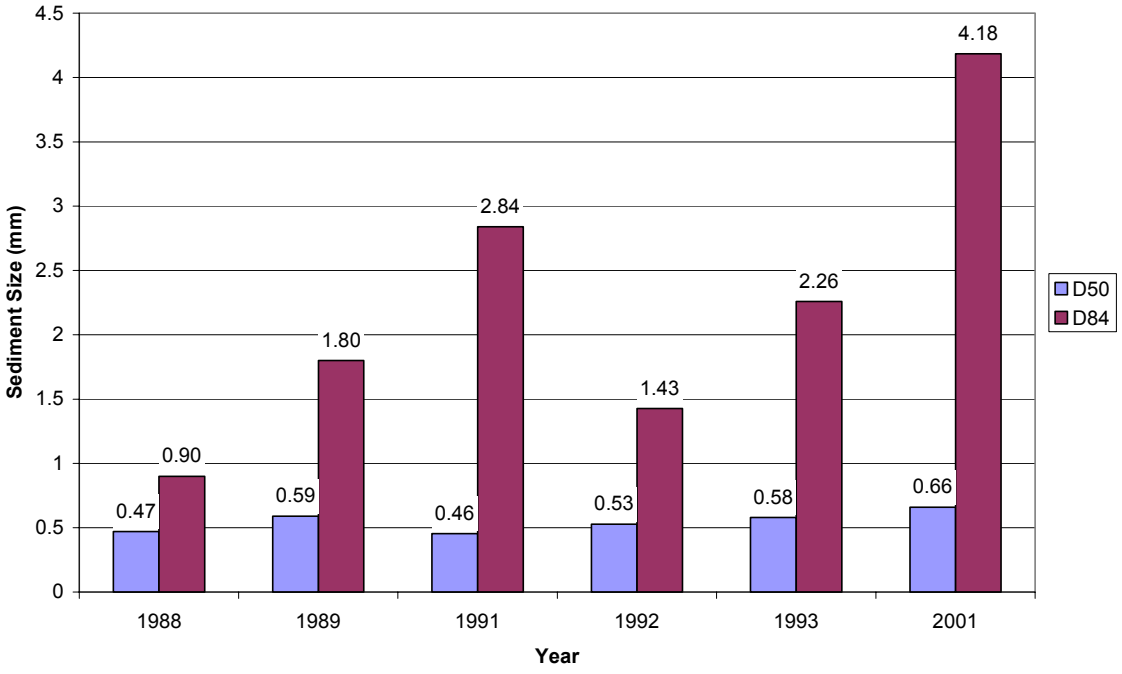
4.5
4
3.5
3
2.5
2
1.5
1
0.5
0
Sediment Size (mm)
0.47
0.90
0.59
1.80
0.46
2.84
0.53
1.43
0.58
2.26
0.66
4.18
1988
1989
1991
1992
1993
2001
Year
D50
D84

**CA-2**

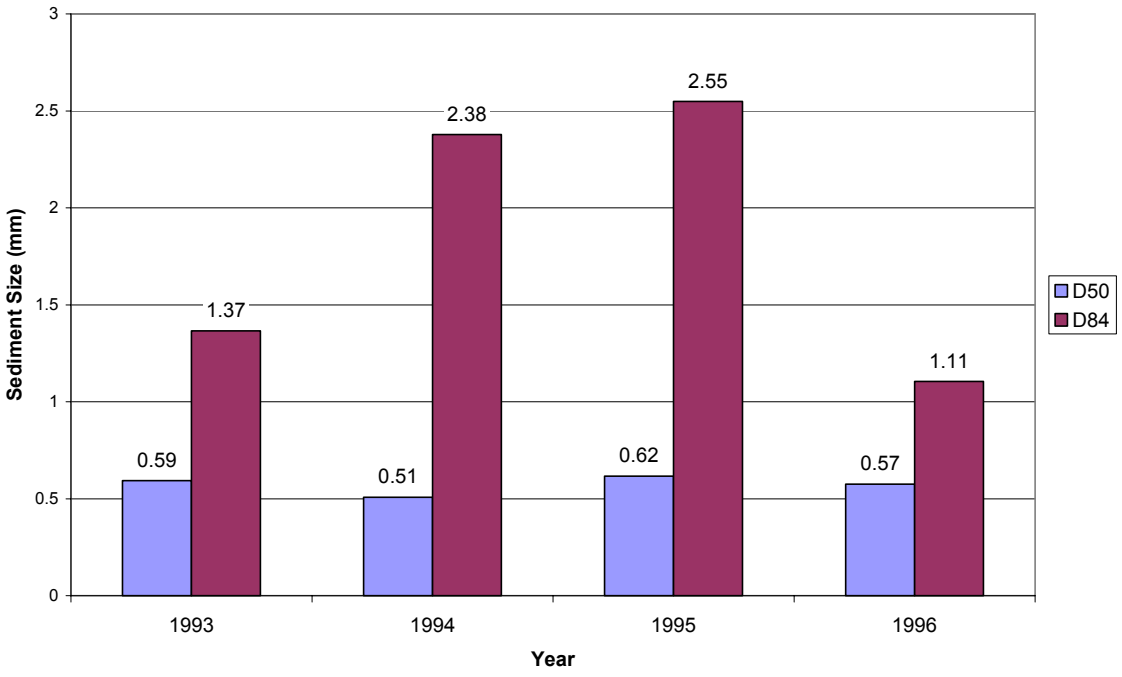
3
2.5
2
1.5
1
0.5
0
Sediment Size (mm)
0.59
1.37
0.51
2.38
0.62
2.55
0.57
1.11
1993
1994
1995
1996
Year
D50
D84

**CA-4**

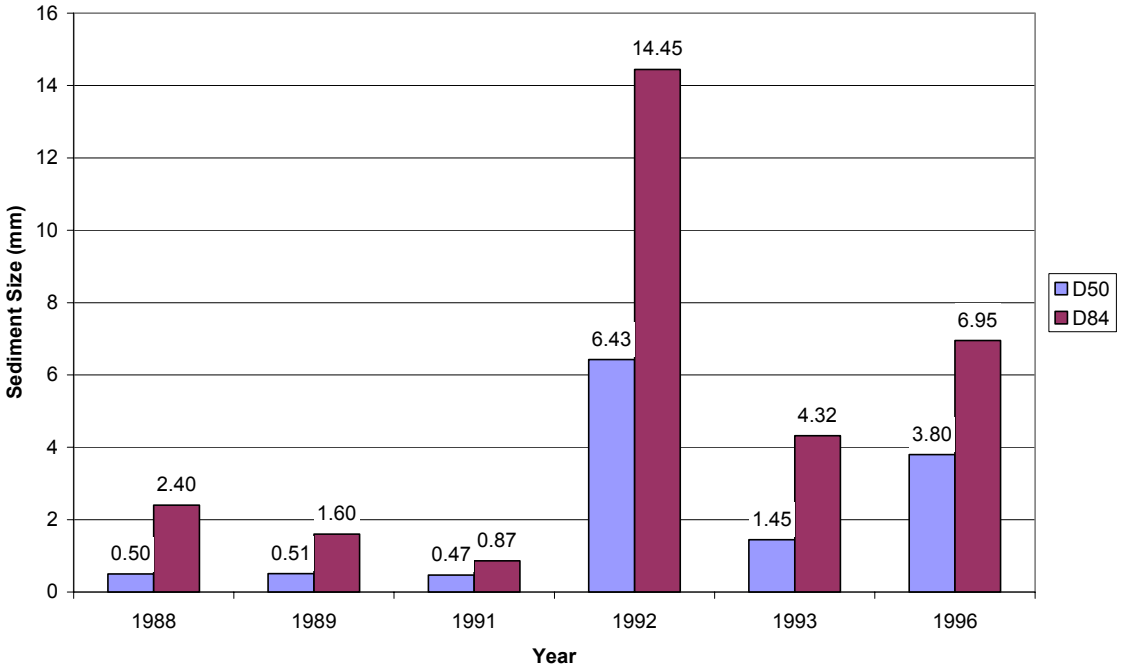
16
14
12
10
8
6
4
2
0
Sediment Size (mm)
14.45
6.43
6.95
4.32
3.80
2.40
1.60
0.87
1.45
0.50
0.51
0.47
1988
1989
1991
1992
1993
1996
Year
D50
D84

**CA-6**

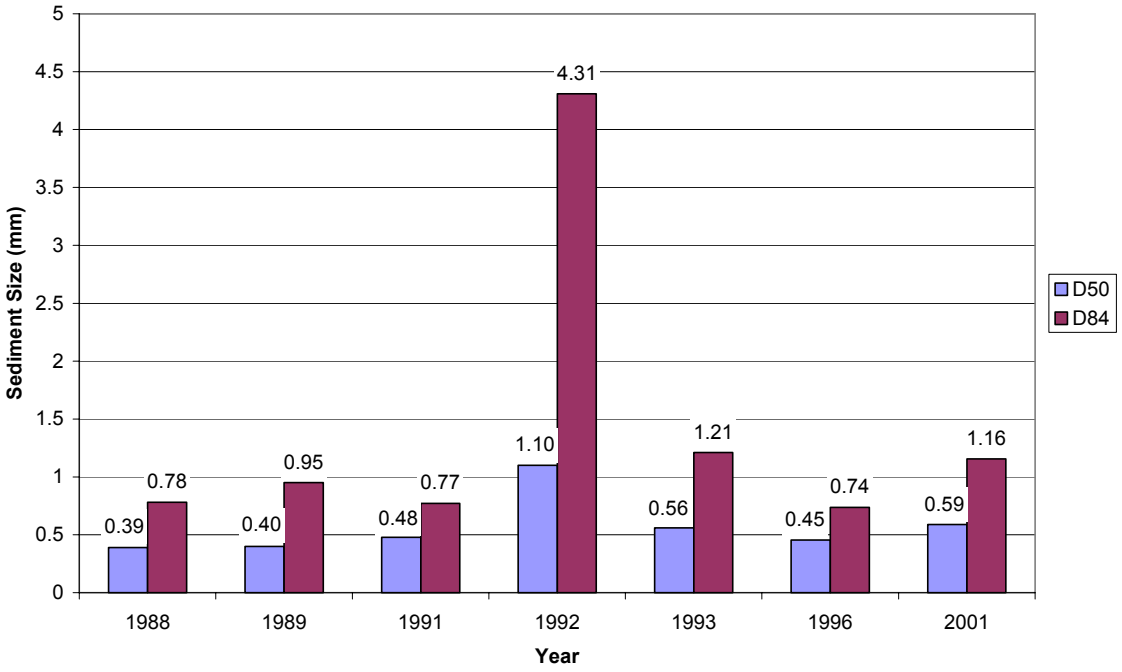
5
4.5
4
3.5
3
2.5
2
1.5
1
0.5
0
Sediment Size (mm)
4.31
1.10
1.21
1.16
0.95
0.78
0.77
0.74
0.56
0.59
0.40
0.48
0.45
0.39
1988
1989
1991
1992
1993
1996
2001
Year
D50
D84

**CA-8**

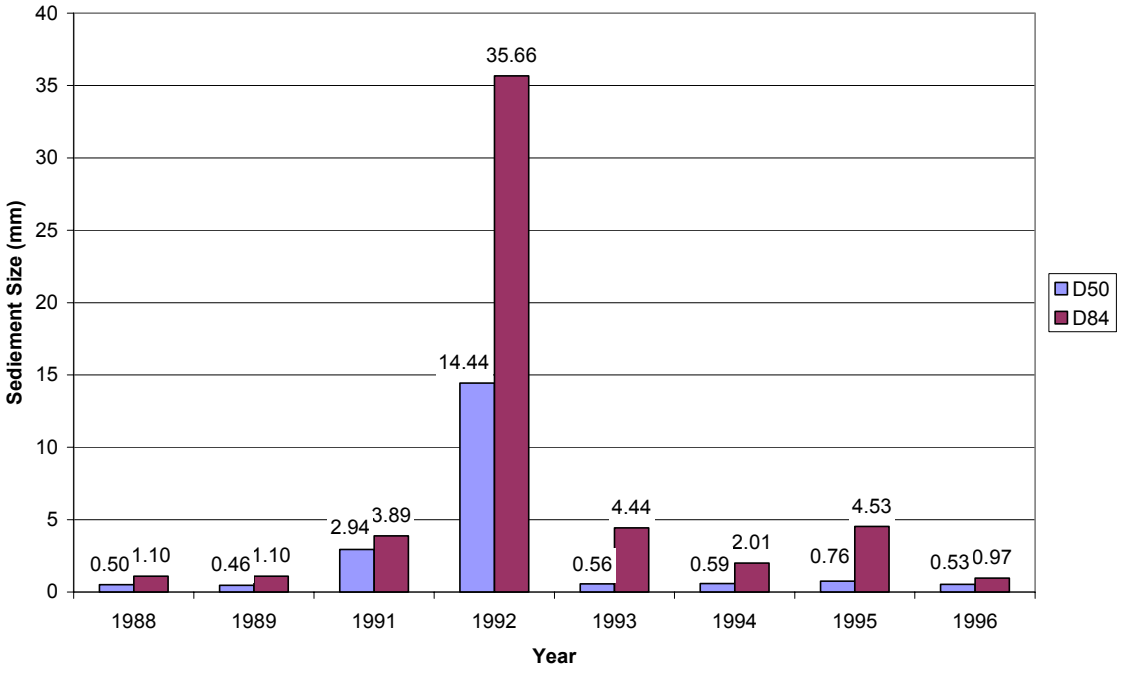
Sediment Size (mm)
40
35
30
25
20
15
10
5
0
35.66
14.44
4.44
4.53
3.89
2.94
2.01
1.10
1.10
0.97
0.50
0.46
0.56
0.59
0.76
0.53
1988
1989
1991
1992
1993
1994
1995
1996
Year
D50
D84

**CA-10**

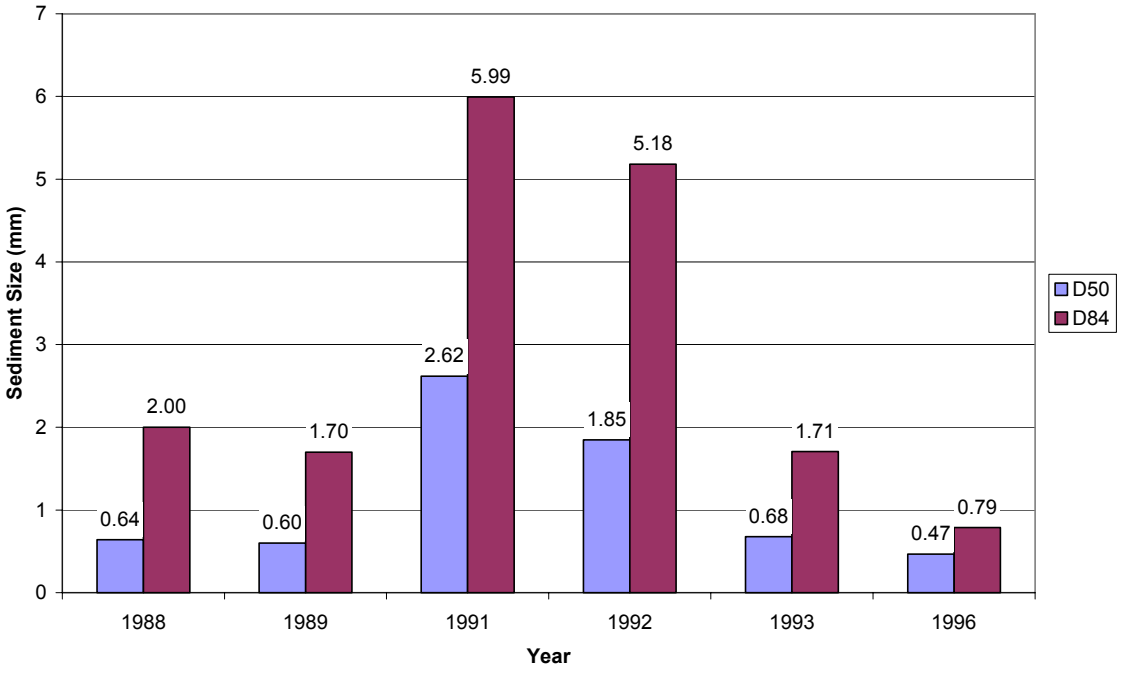
Sediment Size (mm)
7
6
5
4
3
2
1
0
5.99
5.18
2.62
2.00
1.70
1.85
1.71
0.79
0.64
0.60
0.68
0.47
1988
1989
1991
1992
1993
1996
Year
D50
D84

**CA-12**

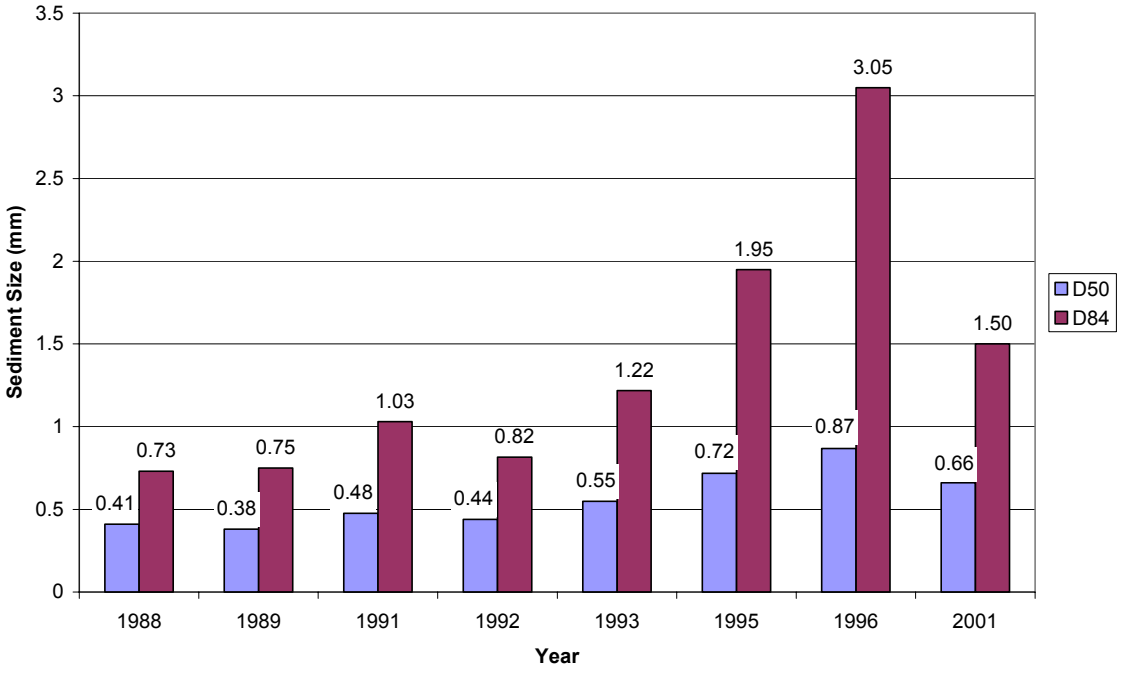
Sediment Size (mm)
3.5
3
2.5
2
1.5
1
0.5
0
0.41
0.73
0.38
0.75
0.48
1.03
0.44
0.82
0.55
1.22
0.72
1.95
0.87
3.05
0.66
1.50
1988
1989
1991
1992
1993
1995
1996
2001
Year
D50
D84

**CA-13**

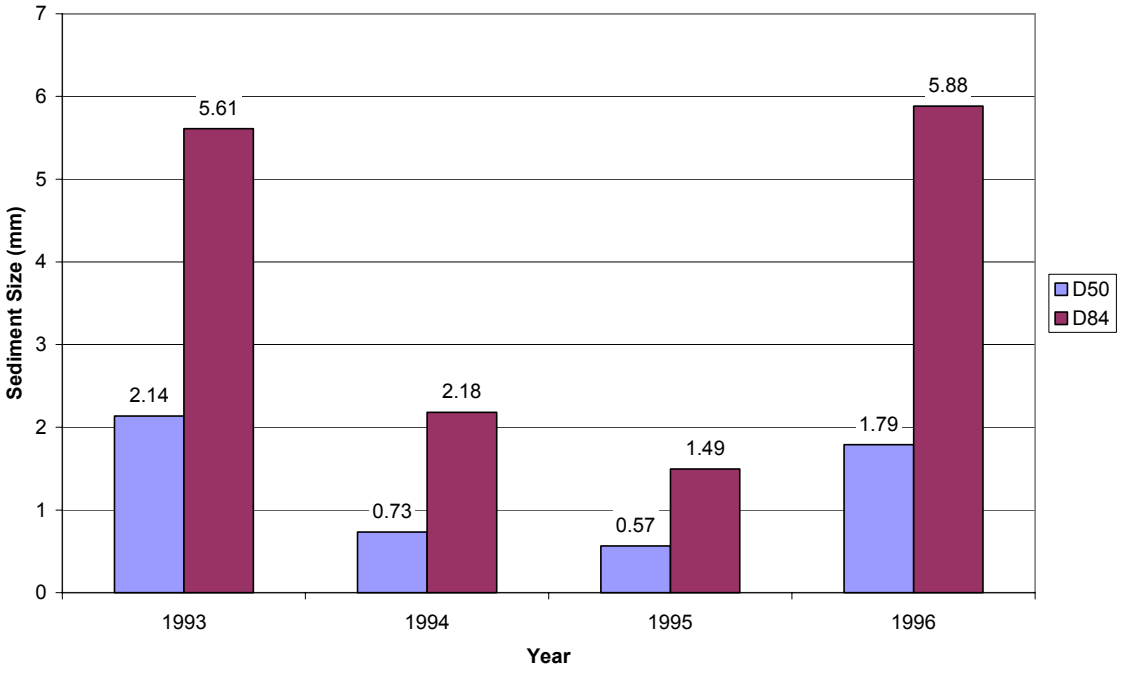
Sediment Size (mm)
7
6
5
4
3
2
1
0
2.14
5.61
0.73
2.18
0.57
1.49
1.79
5.88
1993
1994
1995
1996
Year
D50
D84

# APPENDIX E – REACH-AVERAGED RESULTS FROM HEC-RAS

| | Subreach 1 | | | | | | | | |
|---|---|---|---|---|---|---|---|---|---|
| **Year** | **Width** | **EG Slope** | **Velocity** | **Area** | **Depth** | **W/D** | **WP** | **WS slope** | **MBE** |
| **1962** | 641 | 0.0009 | 3.62 | 1395 | 2.24 | 306 | 645 | 0.0009 | 5016 |
| **1972** | 665 | 0.0008 | 5.28 | 978 | 1.52 | 472 | 668 | 0.0009 | 5016 |
| **1992** | 603 | 0.0010 | 3.85 | 1338 | 2.23 | 276 | 607 | 0.0010 | 5014 |
| **2001** | 524 | 0.0009 | 4.01 | 1252 | 2.41 | 222.3 | 529 | 0.0009 | 5013 |

| | Subreach 2 | | | | | | | | |
|---|---|---|---|---|---|---|---|---|---|
| **Year** | **Width** | **EG Slope** | **Velocity** | **Area** | **Depth** | **W/D** | **WP** | **WS slope** | **MBE** |
| **1962** | 692 | 0.0011 | 3.62 | 1420 | 2.14 | 358 | 695 | 0.0010 | 4998 |
| **1972** | 698 | 0.0008 | 5.27 | 1008 | 1.48 | 500 | 702 | 0.0010 | 4998 |
| **1992** | 640 | 0.0010 | 3.75 | 1389 | 2.21 | 303 | 644 | 0.0009 | 4996 |
| **2001** | 584 | 0.0009 | 3.86 | 1311 | 2.24 | 270.1 | 589 | 0.0009 | 4995 |

| | Subreach 3 | | | | | | | | |
|---|---|---|---|---|---|---|---|---|---|
| **Year** | **Width** | **EG Slope** | **Velocity** | **Area** | **Depth** | **W/D** | **WP** | **WS slope** | **MBE** |
| **1962** | 627 | 0.0011 | 3.97 | 1341 | 2.35 | 315 | 630 | 0.0010 | 4982 |
| **1972** | 653 | 0.0009 | 5.53 | 922 | 1.41 | 470 | 656 | 0.0010 | 4982 |
| **1992** | 599 | 0.0010 | 3.85 | 1332 | 2.25 | 276 | 604 | 0.0010 | 4980 |
| **2001** | 598 | 0.0012 | 4.03 | 1293 | 2.22 | 284.2 | 604 | 0.0010 | 4980 |

| | Total | | | | | | | | |
|---|---|---|---|---|---|---|---|---|---|
| **Year** | **Width** | **EG Slope** | **Velocity** | **Area** | **Depth** | **W/D** | **WP** | **WS slope** | **MBE** |
| **1962** | 652 | 0.0010 | 3.73 | 1384 | 2.24 | 325 | 656 | 0.0009 | |
| **1972** | 670 | 0.0009 | 5.35 | 969 | 1.47 | 479 | 674 | 0.0009 | |
| **1992** | 612 | 0.0010 | 3.84 | 1344 | 2.22 | 285 | 616 | 0.0010 | |
| **2001** | 563 | 0.0010 | 3.97 | 1281 | 2.30 | 254.3 | 568 | 0.0009 | |

# APPENDIX F – FLOW DISCHARGE DATA USED IN THE DEVELOPMENT OF THE EMPIRICAL WIDTH-DISCHARGE RELATIONSHIPS

| *Rio Grande at Otowi* | | | | *Rio Grande near Bernalillo* | | | |
|---|---|---|---|---|---|---|---|
| **Years** | **Annual Peak Flows (cfs)** | **Years** | **Annual Peak Flows (cfs)** | **Years** | **Annual Peak Flows (cfs)** | **Years** | **Annual Peak Flows (cfs)** |
| 1914 | 12500 | 1931 | 4600 | 1945 | 10500 | 1958 | 11600 |
| 1915 | 15600 | 1932 | 13500 | 1946 | 2200 | 1959 | 1400 |
| 1916 | 17200 | 1933 | 5570 | 1947 | 5190 | 1960 | 4670 |
| 1917 | 4440 | 1934 | 1880 | 1948 | 12400 | 1961 | 4270 |
| 1918 | 8410 | 1935 | 7490 | 1949 | 9760 | 1962 | 6900 |
| **1918 Average** | **11630** | **1935 Average** | **6608** | **1949 Average** | **8010** | **1962 Average** | **5768** |

| *Rio Grande at Albuquerque* | | | | | | | |
|---|---|---|---|---|---|---|---|
| **Years** | **Annual Peak Flows (cfs)** | **Years** | **Annual Peak Flows (cfs)** | **Years** | **Annual Peak Flows (cfs)** | **Years** | **Annual Peak** |
| 1968 | 4160 | 1981 | 2170 | 1988 | 3880 | 1997 | 5980 |
| 1969 | 5120 | 1982 | 4630 | 1989 | 3710 | 1998 | 3940 |
| 1970 | 3710 | 1983 | 7330 | 1990 | 2420 | 1999 | 4550 |
| 1971 | 2780 | 1984 | 8500 | 1991 | 4800 | 2000 | 1500 |
| 1972 | 1680 | 1985 | 8650 | 1992 | 5900 | 2001 | 4760 |
| **1972 Average** | **3490** | **1985 Average** | **6256** | **1992 Average** | **4142** | **2001 Average** | **4146** |

# APPENDIX G – EQUILIBRIUM CHANNEL WIDTH ANALYSIS. EXPONENTIAL MODEL DATA

| Subreach 1 | | | |
|---|---|---|---|
| Year | t (year) | Wt (ft) | Width change rate dW (ft/year) |
| 1935 | 0 | 935 | |
| 1949 | 14 | 787 | -10.6 |
| 1962 | 27 | 592 | -15.0 |
| 1972 | 37 | 668 | 7.6 |
| 1985 | 50 | 617 | -3.9 |
| 1992 | 57 | 615 | -0.4 |
| 2001 | 66 | 429 | -20.6 |

| Subreach 2 | | | |
|---|---|---|---|
| Year | t (year) | Wt (ft) | dW (ft/year) |
| 1918 | 0 | 1345 | |
| 1935 | 17 | 1088 | -15.12 |
| 1949 | 31 | 854 | -16.73 |
| 1962 | 44 | 679 | -13.46 |
| 1972 | 54 | 736 | 5.78 |
| 1985 | 67 | 690 | -3.57 |
| 1992 | 74 | 631 | -8.37 |
| 2001 | 66 | 516 | -12.81 |

| Subreach 3 | | | |
|---|---|---|---|
| Year | t (year) | Wt (ft) | dW (ft/year) |
| 1918 | 0 | 1722 | |
| 1935 | 0 | 1546 | -10.38 |
| 1949 | 14 | 1249 | -21.18 |
| 1962 | 27 | 672 | -44.40 |
| 1972 | 37 | 648 | -2.35 |
| 1985 | 50 | 644 | -0.36 |
| 1992 | 57 | 577 | -9.60 |
| 2001 | 66 | 492 | -9.35 |

| Corrales Reach | | | |
|---|---|---|---|
| Year | t (year) | Wt (ft) | dW (ft/year) |
| 1918 | 0 | 1275 | |
| 1935 | 17 | 1171 | -6.10 |
| 1949 | 31 | 948 | -15.92 |
| 1962 | 44 | 638 | -23.87 |
| 1972 | 54 | 682 | 4.35 |
| 1985 | 67 | 647 | -2.68 |
| 1992 | 74 | 607 | -5.65 |
| 2001 | 66 | 474 | -14.85 |

# APPENDIX H – MODIFIED EINSTEIN PROCEDURE INPUT DATA AND RESULTS

Table 1 - MEP input data for Albuquerque gage

| Year | Month | Day | Velocity (ft/s) | Temp (degrees) | Temp (F) | Depth (feet) | Inst. Discharge (cfs) | Computed Area (sq-ft) | Width (feet) | Concentration in ppm |
|---|---|---|---|---|---|---|---|---|---|---|
| 1978 | 4 | 10 | 1.9 | 9.5 | 49.1 | 1.2 | 326 | 181.2 | 151 | 408 |
| 1978 | 4 | 24 | 1.8 | 12.5 | 54.5 | 1.1 | 329 | 180.4 | 164 | 696 |
| 1978 | 5 | 8 | 2.3 | 16.5 | 61.7 | 2.3 | 1420 | 607.2 | 264 | 925 |
| 1978 | 5 | 22 | 4.4 | 18 | 64.4 | 3 | 4260 | 960 | 320 | 4020 |
| 1978 | 5 | 30 | 2.9 | 19 | 66.2 | 3.2 | 2520 | 864 | 270 | 942 |
| 1978 | 6 | 5 | 3.1 | 19 | 66.2 | 3.3 | 2810 | 920.7 | 279 | 1079 |
| 1978 | 6 | 26 | 2.4 | 20 | 68 | 2.2 | 1350 | 556.6 | 253 | 637 |
| 1978 | 7 | 24 | 2 | 25 | 77 | 1.7 | 1040 | 511.7 | 301 | 2526 |
| 1979 | 4 | 2 | 3 | 10 | 50 | 2.2 | 1840 | 605 | 275 | 781 |
| 1979 | 4 | 23 | 4.4 | 15 | 59 | 4 | 4980 | 1140 | 285 | 2107 |
| 1979 | 5 | 29 | 4.8 | 18 | 64.4 | 5 | 6610 | 1375 | 275 | 1997 |
| 1979 | 6 | 18 | 4.9 | 17.5 | 63.5 | 4.9 | 6920 | 1421 | 290 | 1818 |
| 1979 | 7 | 9 | 4.6 | 20 | 68 | 4.3 | 6040 | 1298.6 | 302 | 2027 |
| 1980 | 4 | 7 | 1.9 | 11 | 51.8 | 1.6 | 926 | 496 | 310 | 126 |
| 1980 | 4 | 28 | 4.7 | 12.5 | 54.5 | 3.2 | 4730 | 1008 | 315 | 2117 |
| 1980 | 5 | 12 | 4.5 | 13 | 55.4 | 4.7 | 6900 | 1527.5 | 325 | 1688 |
| 1980 | 6 | 9 | 4.8 | 17 | 62.6 | 4.3 | 6610 | 1376 | 320 | 1518 |
| 1981 | 4 | 20 | 1.9 | 17 | 62.6 | 1.4 | 641 | 336 | 240 | 68 |
| 1981 | 6 | 22 | 1.8 | 23 | 73.4 | 1.3 | 694 | 390 | 300 | 390 |
| 1981 | 7 | 27 | 1.8 | 27 | 80.6 | 1.1 | 584 | 308 | 280 | 685 |
| 1981 | 8 | 24 | 2 | 23 | 73.4 | 0.77 | 260 | 130.9 | 170 | 0 |
| 1982 | 4 | 26 | 2.6 | 12 | 53.6 | 2.4 | 1740 | 672 | 280 | 1658 |
| 1982 | 5 | 3 | 3.2 | 15 | 59 | 3.5 | 3350 | 1050 | 300 | 1129 |
| 1982 | 5 | 24 | 3.4 | 17.5 | 63.5 | 3.6 | 4280 | 1260 | 350 | 897 |
| 1982 | 6 | 7 | 3.7 | 13.5 | 56.3 | 3.6 | 4570 | 1224 | 340 | 678 |
| 1982 | 6 | 21 | 3.1 | 18 | 64.4 | 3.3 | 3480 | 1105.5 | 335 | 492 |
| 1982 | 7 | 7 | 2.3 | 21 | 69.8 | 2.5 | 1100 | 462.5 | 185 | 167 |
| 1982 | 7 | 26 | 1.5 | 24 | 75.2 | 1.6 | 159 | 102.4 | 64 | 69 |
| 1984 | 4 | 3 | 2.7 | 3 | 37.4 | 1.7 | 1350 | 493 | 290 | 107 |
| 1984 | 4 | 24 | 3.6 | 16 | 60.8 | 3.2 | 4270 | 1152 | 360 | 831 |

Table 1 - MEP input data for Albuquerque gage

| Year | Month | Day | Velocity (ft/s) | Temp (degrees) | Temp (F) | Depth (feet) | Inst. Discharge (cfs) | Computed Area (sq-ft) | Width (feet) | Concentration in ppm |
|---|---|---|---|---|---|---|---|---|---|---|
| 1984 | 5 | 8 | 4 | 12 | 53.6 | 3.2 | 4440 | 1088 | 340 | 904 |
| 1984 | 7 | 10 | 1.7 | 23.5 | 74.3 | 1.6 | 396 | 232 | 145 | 144 |
| 1985 | 5 | 15 | 5 | 15 | 59 | 3.8 | 7170 | 1444 | 380 | 434 |
| 1985 | 6 | 17 | 3.2 | 20.5 | 68.9 | 3 | 3620 | 1110 | 370 | 84 |
| 1986 | 5 | 6 | 3.1 | 15 | 59 | 2.1 | 2430 | 787.5 | 375 | 241 |
| 1986 | 5 | 20 | 3 | 16.5 | 61.7 | 2.1 | 2300 | 774.9 | 369 | 223 |
| 1986 | 6 | 3 | 3.6 | 12 | 53.6 | 2.6 | 3440 | 954.2 | 367 | 387 |
| 1988 | 5 | 11 | 2.53 | 20.5 | 68.9 | 1.9 | 1800 | 712.5 | 375 | 337 |
| 1990 | 5 | 8 | 2.77 | 16.5 | 61.7 | 2.3 | 1950 | 713 | 310 | 142 |
| 1990 | 7 | 2 | 2.05 | 24.5 | 76.1 | 1.1 | 570 | 270.6 | 246 | 102 |
| 1991 | 4 | 4 | 2.89 | 10 | 50 | 2.3 | 1490 | 506 | 220 | 262 |
| 1991 | 4 | 10 | 3.33 | 12 | 53.6 | 2.4 | 2130 | 650.4 | 271 | 2157 |
| 1991 | 4 | 22 | 3.44 | 13.5 | 56.3 | 2.6 | 3060 | 878.8 | 338 | 174 |
| 1991 | 6 | 3 | 3.79 | -999999 |  | 3.1 | 3590 | 957.9 | 309 | 669 |
| 1991 | 7 | 2 | 3.32 | 15 | 59 | 2.1 | 2470 | 756 | 360 | 300 |
| 1991 | 7 | 10 | 1.44 | -999999 |  | 0.99 | 401 | 280.17 | 283 | 218 |
| 1992 | 6 | 18 | 2.93 | 19.5 | 67.1 | 2.9 | 2610 | 899 | 310 | 550 |
| 1992 | 6 | 29 | 1.64 | 24 | 75.2 | 1.9 | 853 | 535.8 | 282 | 851 |
| 1992 | 7 | 31 | 2.03 | 23.5 | 74.3 | 1.4 | 801 | 397.6 | 284 | 1299 |
| 1994 | 4 | 1 | 2.47 | 9.5 | 49.1 | 1.9 | 1370 | 551 | 290 | 151 |
| 1994 | 5 | 2 | 3.36 | -999999 |  | 3.1 | 3300 | 985.8 | 318 | 317 |
| 1994 | 6 | 13 | 3.67 | 17.9 | 64.22 | 4.2 | 5030 | 1386 | 330 | 143 |
| 1994 | 6 | 27 | 3.68 | 22.9 | 73.22 | 4 | 4860 | 1308 | 327 | 382 |
| 1995 | 5 | 5 | 3.26 | 13.5 | 56.3 | 3.8 | 3980 | 1204.6 | 317 | 641 |
| 1995 | 5 | 24 | 4.13 | 17 | 62.6 | 4.8 | 6400 | 1540.8 | 321 | 668 |
| 1995 | 6 | 6 | 3.94 | -999999 |  | 3.8 | 4960 | 1261.6 | 332 | 682 |
| 1995 | 7 | 3 | 3.99 | 16.5 | 61.7 | 4.4 | 5620 | 1416.8 | 322 | 992 |
| 1996 | 4 | 5 | 1.95 | 8.3 | 46.94 | 1.7 | 437 | 219.3 | 129 | 919 |
| 1996 | 5 | 3 | 1.99 | 15.4 | 59.72 | 2 | 471 | 238 | 119 | 367 |
| 1996 | 6 | 20 | 1.78 | 19.2 | 66.56 | 1.2 | 572 | 319.2 | 266 | 86 |
| 1997 | 4 | 4 | 2.87 | 10 | 50 | 2.2 | 2090 | 721.6 | 328 | 1498 |

Table 1 - MEP input data for Albuquerque gage

| Year | Month | Day | Velocity (ft/s) | Temp (degrees) | Temp (F) | Depth (feet) | Inst. Discharge (cfs) | Computed Area (sq-ft) | Width (feet) | Concentration in ppm |
|---|---|---|---|---|---|---|---|---|---|---|
| 1997 | 6 | 3 | 3.52 | 16.5 | 61.7 | 4.2 | 5040 | 1411.2 | 336 | 1818 |
| 1998 | 5 | 5 | 3.25 | 13.5 | 56.3 | 3 | 3180 | 990 | 330 | 534 |
| 1998 | 6 | 3 | 3.13 | 18 | 64.4 | 3.4 | 3540 | 1118.6 | 329 | 2177 |
| 1999 | 4 | 27 | 2.23 | 12 | 53.6 | 1.6 | 969 | 428.8 | 268 | 164 |
| 1999 | 5 | 24 | 3.49 | 15.5 | 59.9 | 3.4 | 4080 | 1166.2 | 343 | 648 |
| 1978 | 8 | 7 | 1.9 | 22.5 | 72.5 | 1.4 | 817 | 421.4 | 301 | 785 |
| 1978 | 8 | 22 | 1.8 | 21 | 69.8 | 1.1 | 559 | 304.7 | 277 | 476 |
| 1979 | 8 | 13 | 1.9 | 21.5 | 70.7 | 1.4 | 588 | 308 | 220 | 514 |
| 1979 | 9 | 10 | 2.3 | 20 | 68 | 1.3 | 521 | 234 | 180 | 137 |
| 1980 | 8 | 18 | 1.4 | 22.5 | 72.5 | 0.89 | 377 | 267 | 300 | 436 |
| 1980 | 9 | 15 | 1.6 | 21.5 | 70.7 | 0.96 | 447 | 279.36 | 291 | 229 |
| 1990 | 8 | 6 | 1.6 | 18 | 64.4 | 1 | 415 | 258 | 258 | 157 |
| 1990 | 9 | 4 | 1.4 | 17.5 | 63.5 | 0.8 | 267 | 189.6 | 237 | 79 |
| 1992 | 8 | 31 | 2.1 | 21.5 | 70.7 | 1.8 | 1070 | 514.8 | 286 | 343 |
| 1993 | 8 | 13 | 2.08 | 20 | 68 | 1.6 | 536 | 262.4 | 164 | 179 |
| 1994 | 8 | 4 | 1.64 | 22.2 | 71.96 | 1.8 | 588 | 358.2 | 199 | 1658 |
| 1994 | 9 | 30 | 1.73 | 17.2 | 62.96 | 1.4 | 383 | 225.4 | 161 | 108 |
| 1997 | 9 | 2 | 1.95 | 20.5 | 68.9 | 1.5 | 774 | 381 | 254 | 445 |
| 1999 | 9 | 17 | 2.32 | 19 | 66.2 | 1.8 | 1080 | 477 | 265 | 152 |

Table 1 - MEP input data for Albuquerque gage

| Year | Month | Day | Avr. Depth of SS sampler |
|---|---|---|---|
| 1978 | 4 | 10 | 0.9 |
| 1978 | 4 | 24 | 0.8 |
| 1978 | 5 | 8 | 2 |
| 1978 | 5 | 22 | 2.7 |
| 1978 | 5 | 30 | 2.9 |
| 1978 | 6 | 5 | 3 |
| 1978 | 6 | 26 | 1.9 |
| 1978 | 7 | 24 | 1.4 |
| 1979 | 4 | 2 | 1.9 |
| 1979 | 4 | 23 | 3.7 |
| 1979 | 5 | 29 | 4.7 |
| 1979 | 6 | 18 | 4.6 |
| 1979 | 7 | 9 | 4 |
| 1980 | 4 | 7 | 1.3 |
| 1980 | 4 | 28 | 2.9 |
| 1980 | 5 | 12 | 4.4 |
| 1980 | 6 | 9 | 4 |
| 1981 | 4 | 20 | 1.1 |
| 1981 | 6 | 22 | 1 |
| 1981 | 7 | 27 | 0.8 |
| 1981 | 8 | 24 | 0.47 |
| 1982 | 4 | 26 | 2.1 |
| 1982 | 5 | 3 | 3.2 |
| 1982 | 5 | 24 | 3.3 |
| 1982 | 6 | 7 | 3.3 |
| 1982 | 6 | 21 | 3 |
| 1982 | 7 | 7 | 2.2 |
| 1982 | 7 | 26 | 1.3 |
| 1984 | 4 | 3 | 1.4 |
| 1984 | 4 | 24 | 2.9 |

Table 1 - MEP input data for Albuquerque gage

| Year | Month | Day | Avr. Depth of SS sampler |
|---|---|---|---|
| 1984 | 5 | 8 | 2.9 |
| 1984 | 7 | 10 | 1.3 |
| 1985 | 5 | 15 | 3.5 |
| 1985 | 6 | 17 | 2.7 |
| 1986 | 5 | 6 | 1.8 |
| 1986 | 5 | 20 | 1.8 |
| 1986 | 6 | 3 | 2.3 |
| 1988 | 5 | 11 | 1.6 |
| 1990 | 5 | 8 | 2 |
| 1990 | 7 | 2 | 0.8 |
| 1991 | 4 | 4 | 2 |
| 1991 | 4 | 10 | 2.1 |
| 1991 | 4 | 22 | 2.3 |
| 1991 | 6 | 3 | 2.8 |
| 1991 | 7 | 2 | 1.8 |
| 1991 | 7 | 10 | 0.69 |
| 1992 | 6 | 18 | 2.6 |
| 1992 | 6 | 29 | 1.6 |
| 1992 | 7 | 31 | 1.1 |
| 1994 | 4 | 1 | 1.6 |
| 1994 | 5 | 2 | 2.8 |
| 1994 | 6 | 13 | 3.9 |
| 1994 | 6 | 27 | 3.7 |
| 1995 | 5 | 5 | 3.5 |
| 1995 | 5 | 24 | 4.5 |
| 1995 | 6 | 6 | 3.5 |
| 1995 | 7 | 3 | 4.1 |
| 1996 | 4 | 5 | 1.4 |
| 1996 | 5 | 3 | 1.7 |
| 1996 | 6 | 20 | 0.9 |
| 1997 | 4 | 4 | 1.9 |

Table 1 - MEP input data for Albuquerque gage

| Year | Month | Day | Avr. Depth of SS sampler |
|---|---|---|---|
| 1997 | 6 | 3 | 3.9 |
| 1998 | 5 | 5 | 2.7 |
| 1998 | 6 | 3 | 3.1 |
| 1999 | 4 | 27 | 1.3 |
| 1999 | 5 | 24 | 3.1 |
| 1978 | 8 | 7 | 1.1 |
| 1978 | 8 | 22 | 0.8 |
| 1979 | 8 | 13 | 1.1 |
| 1979 | 9 | 10 | 1 |
| 1980 | 8 | 18 | 0.59 |
| 1980 | 9 | 15 | 0.66 |
| 1990 | 8 | 6 | 0.7 |
| 1990 | 9 | 4 | 0.5 |
| 1992 | 8 | 31 | 1.5 |
| 1993 | 8 | 13 | 1.3 |
| 1994 | 8 | 4 | 1.5 |
| 1994 | 9 | 30 | 1.1 |
| 1997 | 9 | 2 | 1.2 |
| 1999 | 9 | 17 | 1.5 |

Table 1 - MEP input data for Albuquerque gage

| Year | Month | Day | SED-BED-SIEVE- % <0.062 mm | SED-BED-SIEVE- % <0.125 mm | SED-BED-SIEVE- % <0.25 mm | SED-BED-SIEVE- % <0.5 mm | SED-BED-SIEVE- % <1 mm | SED-BED-SIEVE- % <2 mm | SED-BED-SIEVE-% < 4 mm | SED-BED-SIEVE-% < 8 mm | SED-BED-SIEVE-%< 16 mm | SED-BED-SIEVE-% < 32 mm |
|---|---|---|---|---|---|---|---|---|---|---|---|---|
| 1978 | 4 | 10 | | | | | 92 | 95 | 97 | 98 | 100 | |
| 1978 | 4 | 24 | | | | | | | | | | |
| 1978 | 5 | 8 | 1 | 3 | 36 | 84 | 98 | 100 | | | | |
| 1978 | 5 | 22 | 1 | 3 | 36 | 90 | 100 | | | | | |
| 1978 | 5 | 30 | 0 | 4 | 45 | 90 | 99 | 100 | | | | |
| 1978 | 6 | 5 | 0 | 1 | 28 | 86 | 98 | 100 | | | | |
| 1978 | 6 | 26 | | | | | 64 | 67 | 72 | 82 | 96 | 100 |
| 1978 | 7 | 24 | 1 | 3 | 49 | 88 | 95 | 100 | | | | |
| 1979 | 4 | 2 | 0 | 2 | 44 | 89 | 97 | 100 | | | | |
| 1979 | 4 | 23 | | | | | 81 | 86 | 88 | 91 | 95 | 100 |
| 1979 | 5 | 29 | | | | | 70 | 82 | 87 | 89 | 92 | 100 |
| 1979 | 6 | 18 | | | | | 66 | 72 | 76 | 80 | 84 | 100 |
| 1979 | 7 | 9 | | | | | 82 | 90 | 93 | 95 | 98 | 100 |
| 1980 | 4 | 7 | | | | | 86 | 91 | 93 | 95 | 97 | 100 |
| 1980 | 4 | 28 | | | | | 79 | 85 | 88 | 91 | 97 | 100 |
| 1980 | 5 | 12 | | | | | 79 | 82 | 84 | 85 | 91 | 100 |
| 1980 | 6 | 9 | | | | | 77 | 81 | 83 | 86 | 89 | 100 |
| 1981 | 4 | 20 | | | | | 90 | 93 | 96 | 98 | 100 | |
| 1981 | 6 | 22 | | | | | 88 | 91 | 92 | 94 | 96 | 100 |
| 1981 | 7 | 27 | | | | | 97 | 99 | 99 | 99 | 100 | |
| 1981 | 8 | 24 | | | | | 96 | 98 | 99 | 100 | | |
| 1982 | 4 | 26 | | | | | 97 | 99 | 99 | 100 | | |
| 1982 | 5 | 3 | | | | | 99 | 100 | | | | |
| 1982 | 5 | 24 | | | | | 89 | 97 | 99 | 100 | | |
| 1982 | 6 | 7 | | | | | 86 | 91 | 94 | 96 | 99 | 100 |
| 1982 | 6 | 21 | | | | | 86 | 94 | 96 | 96 | 96 | 100 |
| 1982 | 7 | 7 | | | | | 87 | 93 | 97 | 99 | 100 | |
| 1982 | 7 | 26 | | | | | 82 | 93 | 97 | 100 | | |
| 1984 | 4 | 3 | | | | | 68 | 72 | 75 | 80 | 91 | 100 |
| 1984 | 4 | 24 | 0 | 1 | 55 | 99 | 100 | | | | | |

Table 1 - MEP input data for Albuquerque gage

| Year | Month | Day | SED-BED-SIEVE- % <0.062 mm | SED-BED-SIEVE- % <0.125 mm | SED-BED-SIEVE- % <0.25 mm | SED-BED-SIEVE- % <0.5 mm | SED-BED-SIEVE- % <1 mm | SED-BED-SIEVE- % <2 mm | SED-BED-SIEVE-% < 4 mm | SED-BED-SIEVE-% < 8 mm | SED-BED-SIEVE- %< 16 mm | SED-BED-SIEVE-% < 32 mm |
|---|---|---|---|---|---|---|---|---|---|---|---|---|
| 1984 | 5 | 8 | | | | | 98 | 99 | 99 | 99 | 100 | |
| 1984 | 7 | 10 | | | | | 79 | 92 | 97 | 100 | | |
| 1985 | 5 | 15 | 15 | 57 | 96 | 100 | | | | | | |
| 1985 | 6 | 17 | | | | | 98 | 98 | 98 | 99 | 100 | |
| 1986 | 5 | 6 | | | | | 85 | 87 | 89 | 91 | 94 | 100 |
| 1986 | 5 | 20 | | | | | 73 | 83 | 90 | 97 | 100 | |
| 1986 | 6 | 3 | | | | | 97 | 98 | 99 | 100 | | |
| 1988 | 5 | 11 | 19 | 40 | 54 | 86 | 99 | 100 | | | | |
| 1990 | 5 | 8 | 9 | 18 | 28 | 66 | 93 | 98 | 99 | 100 | | |
| 1990 | 7 | 2 | 0 | 1 | 17 | 82 | 97 | 99 | 100 | 100 | | |
| 1991 | 4 | 4 | 0 | 1 | 20 | 77 | 96 | 99 | 99 | 100 | | |
| 1991 | 4 | 10 | | 0 | 2 | 39 | 90 | 98 | 100 | | | |
| 1991 | 4 | 22 | 8 | 11 | 22 | 81 | 98 | 99 | 100 | | | |
| 1991 | 6 | 3 | 0 | 3 | 23 | 77 | 97 | 100 | 100 | | | |
| 1991 | 7 | 2 | 1 | 4 | 16 | 72 | 97 | 100 | | | | |
| 1991 | 7 | 10 | | 0 | 11 | 60 | 94 | 99 | 100 | | | |
| 1992 | 6 | 18 | 23 | 75 | 97 | 100 | | | | | | |
| 1992 | 6 | 29 | | 0 | 12 | 68 | 91 | 99 | 100 | | | |
| 1992 | 7 | 31 | 0 | 3 | 17 | 44 | 70 | 79 | 83 | 88 | 100 | |
| 1994 | 4 | 1 | | 0 | 6 | 40 | 72 | 87 | 96 | 99 | 100 | |
| 1994 | 5 | 2 | 0 | 1 | 10 | 48 | 79 | 92 | 97 | 99 | 100 | |
| 1994 | 6 | 13 | 3 | 35 | 99 | 100 | | | | | | |
| 1994 | 6 | 27 | 0 | 1 | 14 | 63 | 94 | 99 | 100 | | | |
| 1995 | 5 | 5 | | 0 | 7 | 67 | 92 | 96 | 97 | 99 | 100 | |
| 1995 | 5 | 24 | | 0 | 8 | 60 | 89 | 97 | 99 | 100 | | |
| 1995 | 6 | 6 | | 0 | 4 | 39 | 71 | 78 | 82 | 86 | 90 | 100 |
| 1995 | 7 | 3 | | 0 | 10 | 86 | 99 | 100 | 100 | | | |
| 1996 | 4 | 5 | 0 | 1 | 12 | 56 | 87 | 92 | 93 | 94 | 94 | 100 |
| 1996 | 5 | 3 | 1 | 4 | 15 | 61 | 92 | 98 | 100 | | | |
| 1996 | 6 | 20 | | 0 | 12 | 60 | 82 | 88 | 90 | 92 | 98 | 100 |
| 1997 | 4 | 4 | 4 | 7 | 16 | 69 | 95 | 99 | 99 | 100 | | |

Table 1 - MEP input data for Albuquerque gage

| Year | Month | Day | SED-BED-SIEVE- % <0.062 mm | SED-BED-SIEVE- % <0.125 mm | SED-BED-SIEVE- % <0.25 mm | SED-BED-SIEVE- % <0.5 mm | SED-BED-SIEVE- % <1 mm | SED-BED-SIEVE- % <2 mm | SED-BED-SIEVE-% < 4 mm | SED-BED-SIEVE-% < 8 mm | SED-BED-SIEVE- %< 16 mm | SED-BED-SIEVE-% < 32 mm |
|---|---|---|---|---|---|---|---|---|---|---|---|---|
| 1997 | 6 | 3 | | 0 | 7 | 49 | 80 | 89 | 100 | 96 | 97 | 100 |
| 1998 | 5 | 5 | 1 | 3 | 13 | 66 | 92 | 97 | 98 | 99 | 100 | |
| 1998 | 6 | 3 | 0 | 1 | 10 | 58 | 89 | 95 | 98 | 100 | | |
| 1999 | 4 | 27 | | 0 | 7 | 56 | 91 | 99 | 100 | | | |
| 1999 | 5 | 24 | | 0 | 12 | 60 | 88 | 95 | 98 | 100 | | |
| 1978 | 8 | 7 | | | | | 97 | 99 | 100 | | | |
| 1978 | 8 | 22 | | | | | 94 | 98 | 100 | | | |
| 1979 | 8 | 13 | | | 30 | 79 | 97 | 98 | 100 | | | |
| 1979 | 9 | 10 | 0 | 1 | 34 | 85 | 97 | 98 | | 99 | 99 | 100 |
| 1980 | 8 | 18 | 1 | 1 | 27 | 66 | 72 | 74 | | 79 | 85 | 100 |
| 1980 | 9 | 15 | | | | | 85 | 90 | 93 | 95 | 97 | 100 |
| 1990 | 8 | 6 | 0 | 1 | 10 | 57 | 78 | 89 | 95 | 99 | 100 | |
| 1990 | 9 | 4 | 0 | 1 | 17 | 65 | 91 | 98 | 99 | 100 | | |
| 1992 | 8 | 31 | 0 | 1 | 13 | 73 | 96 | 99 | 99 | 100 | | |
| 1993 | 8 | 13 | 0 | 1 | 10 | 54 | 83 | 87 | 90 | 94 | 100 | |
| 1994 | 8 | 4 | 1 | 3 | 18 | 68 | 93 | 98 | 100 | | | |
| 1994 | 9 | 30 | | 0 | 11 | 56 | 84 | 93 | 98 | 100 | | |
| 1997 | 9 | 2 | 0 | 1 | 6 | 53 | 85 | 93 | 96 | 97 | 100 | |
| 1999 | 9 | 17 | 0 | 1 | 6 | 48 | 84 | 95 | 98 | 98 | 100 | |

Table 1 - MEP input data for Albuquerque gage

| | | | 0.002 | 0.004 | 0.008 | 0.016 | 0.062 | 0.125 | 0.25 | 0.5 | 1 | 2 |
|---|---|---|---|---|---|---|---|---|---|---|---|---|
| Year | Month | Day | SED-SUSP-FALL-D-% <.002mm | SED-SUSP-FALL-D-% <0.004 mm | SED-SUSP-FALL-D-% <0.008 mm | SED-SUSP-FALL-D-%<0.016 mm | SED-SUSP-FALL-D-% <0.062m m | SED-SUSP-FALL-D-% <0.125 mm | SED-SUSP-FALL-D-% <0.25 mm | SED-SUSP-FALL-D-% <0.500 mm | SED-SUSP-FALL-D-% <1 mm | SED-SUSP-Sieve-D-% <2 mm |
| 1978 | 4 | 10 | 55 | 63 | | 74 | 85 | 88 | 98 | 100 | | |
| 1978 | 4 | 24 | 15 | 17 | | 20 | 24 | 26 | 56 | 94 | 96 | 96 |
| 1978 | 5 | 8 | 32 | 34 | | 39 | 59 | 69 | 87 | 100 | | |
| 1978 | 5 | 22 | 9 | 10 | | 13 | 24 | 33 | 53 | 83 | 98 | |
| 1978 | 5 | 30 | 19 | 21 | | 25 | 44 | 56 | 89 | 100 | | |
| 1978 | 6 | 5 | 11 | 12 | | 16 | 32 | 42 | 76 | 100 | | |
| 1978 | 6 | 26 | | | | | 31 | 45 | 79 | 95 | 100 | |
| 1978 | 7 | 24 | 40 | 48 | | 85 | 94 | 96 | 100 | | | |
| 1979 | 4 | 2 | | | | | 29 | 48 | 90 | 100 | | |
| 1979 | 4 | 23 | 6 | 7 | | 9 | 22 | 42 | 82 | 100 | | |
| 1979 | 5 | 29 | 7 | 8 | | 10 | 17 | 32 | 77 | 100 | | |
| 1979 | 6 | 18 | 4 | 5 | | 6 | 13 | 27 | 72 | 96 | 100 | |
| 1979 | 7 | 9 | 1 | 1 | | 2 | 6 | 19 | 78 | 98 | 100 | |
| 1980 | 4 | 7 | | | | | 29 | 38 | 84 | 100 | | |
| 1980 | 4 | 28 | 4 | 5 | | 5 | 12 | 19 | 53 | 83 | 99 | |
| 1980 | 5 | 12 | 8 | 8 | | 10 | 17 | 28 | 70 | 96 | 100 | |
| 1980 | 6 | 9 | 3 | 4 | 4 | 5 | 9 | 16 | 68 | 94 | 100 | |
| 1981 | 4 | 20 | 22 | 26 | 30 | 35 | 50 | 59 | 82 | 99 | 100 | |
| 1981 | 6 | 22 | 18 | 22 | | 38 | 53 | 56 | 65 | 96 | 100 | |
| 1981 | 7 | 27 | 39 | 48 | | 76 | 90 | 92 | 97 | 100 | | |
| 1981 | 8 | 24 | 44 | 55 | | 74 | 94 | 94 | 98 | 100 | | |
| 1982 | 4 | 26 | 3 | 4 | | 5 | 13 | 15 | 33 | 87 | 100 | |
| 1982 | 5 | 3 | 9 | 13 | | 17 | 48 | 61 | 81 | 97 | 100 | |
| 1982 | 5 | 24 | 6 | 8 | | 11 | 35 | 48 | 81 | 99 | 100 | |
| 1982 | 6 | 7 | 5 | 7 | | 9 | 27 | 43 | 79 | 98 | 100 | |
| 1982 | 6 | 21 | 4 | 6 | | 8 | 22 | 39 | 81 | 100 | | |
| 1982 | 7 | 7 | | | | | 38 | 41 | 88 | 98 | 100 | |
| 1982 | 7 | 26 | | | | | 76 | 85 | 94 | 100 | | |
| 1984 | 4 | 3 | | | | | 51 | 58 | 79 | 100 | | |
| 1984 | 4 | 24 | | | | | 31 | 53 | 86 | 100 | | |

Table 1 - MEP input data for Albuquerque gage

| Year | Month | Day | SED-SUSP-FALL-D-% <.002mm | SED-SUSP-FALL-D-% <0.004 mm | SED-SUSP-FALL-D-% <0.008 mm | SED-SUSP-FALL-D-%<0.016 mm | SED-SUSP-FALL-D-% <0.062m m | SED-SUSP-FALL-D-% <0.125 mm | SED-SUSP-FALL-D-% <0.25 mm | SED-SUSP-FALL-D-% <0.500 mm | SED-SUSP-FALL-D-% <1 mm | SED-SUSP-Sieve-D-% <2 mm |
|---|---|---|---|---|---|---|---|---|---|---|---|---|
| 1984 | 5 | 8 | | | | | 25 | 39 | 77 | 98 | 100 | |
| 1984 | 7 | 10 | | | | | 80 | 81 | 87 | 98 | 100 | |
| 1985 | 5 | 15 | | | | | 42 | 75 | 100 | | | |
| 1985 | 6 | 17 | | | | | 58 | 87 | 99 | 100 | | |
| 1986 | 5 | 6 | | | | | 20 | 31 | 77 | 100 | | |
| 1986 | 5 | 20 | | | | | 21 | 33 | 74 | 98 | 100 | |
| 1986 | 6 | 3 | | | | | 16 | 27 | 85 | 100 | | |
| 1988 | 5 | 11 | 58 | 71 | | 88 | 96 | 100 | | | | |
| 1990 | 5 | 8 | | | | | 74 | 91 | 100 | | | |
| 1990 | 7 | 2 | | | | | 81 | 93 | 99 | 100 | | |
| 1991 | 4 | 4 | | | | | 41 | 50 | 86 | 100 | | |
| 1991 | 4 | 10 | | | | | 10 | 13 | 19 | 78 | 100 | |
| 1991 | 4 | 22 | | | | | 77 | 90 | 96 | 100 | | |
| 1991 | 6 | 3 | | | | | 23 | 37 | 67 | 92 | 94 | 96 |
| 1991 | 7 | 2 | | | | | 67 | 79 | 93 | 100 | | |
| 1991 | 7 | 10 | | | | | 47 | 48 | 54 | 85 | 100 | |
| 1992 | 6 | 18 | | | | | 11 | 22 | 41 | 78 | 84 | 92 |
| 1992 | 6 | 29 | | | | | 7 | 8 | 20 | 84 | 93 | 100 |
| 1992 | 7 | 31 | | | | | 12 | 12 | 20 | 79 | 96 | 100 |
| 1994 | 4 | 1 | | | | | 41 | 52 | 82 | 100 | | |
| 1994 | 5 | 2 | | | | | 38 | 47 | 70 | 99 | 100 | |
| 1994 | 6 | 13 | | | | | 57 | 94 | 97 | 100 | | |
| 1994 | 6 | 27 | | | | | 21 | 34 | 66 | 100 | | |
| 1995 | 5 | 5 | | | | | 29 | 41 | 64 | 100 | | |
| 1995 | 5 | 24 | | | | | 25 | 40 | 64 | 95 | 100 | |
| 1995 | 6 | 6 | | | | | 14 | 17 | 44 | 75 | 100 | |
| 1995 | 7 | 3 | | | | | 12 | 15 | 30 | 68 | 83 | 95 |
| 1996 | 4 | 5 | | | | | 3 | 4 | 9 | 54 | 90 | 100 |
| 1996 | 5 | 3 | | | | | 9 | 10 | 13 | 74 | 100 | |
| 1996 | 6 | 20 | | | | | 64 | 66 | 83 | 100 | | |
| 1997 | 4 | 4 | | | | | 22 | 23 | 35 | 74 | 100 | |

Table 1 - MEP input data for Albuquerque gage

| Year | Month | Day | SED-SUSP-FALL-D-% <.002mm | SED-SUSP-FALL-D-% <0.004 mm | SED-SUSP-FALL-D-% <0.008 mm | SED-SUSP-FALL-D-%<0.016 mm | SED-SUSP-FALL-D-% <0.062m m | SED-SUSP-FALL-D-% <0.125 mm | SED-SUSP-FALL-D-% <0.25 mm | SED-SUSP-FALL-D-% <0.500 mm | SED-SUSP-FALL-D-% <1 mm | SED-SUSP-Sieve-D-% <2 mm |
|---|---|---|---|---|---|---|---|---|---|---|---|---|
| 1997 | 6 | 3 | | | | | 9 | 13 | 29 | 81 | 95 | 99 |
| 1998 | 5 | 5 | | | | | 31 | 45 | 68 | 97 | 98 | 100 |
| 1998 | 6 | 3 | | | | | 5 | 15 | 48 | 82 | 97 | 100 |
| 1999 | 4 | 27 | 31 | 36 | 42 | 49 | 61 | 72 | 93 | 100 | | |
| 1999 | 5 | 24 | 12 | 14 | 17 | 19 | 28 | 36 | 65 | 99 | 100 | |
| 1978 | 8 | 7 | 36 | 52 | | 70 | 84 | 88 | 99 | 100 | | |
| 1978 | 8 | 22 | 42 | 53 | | 75 | | | | | | |
| 1979 | 8 | 13 | 34 | 44 | | 59 | 65 | 67 | 74 | 81 | 99 | |
| 1979 | 9 | 10 | | | | | 77 | 82 | 98 | 100 | | |
| 1980 | 8 | 18 | 16 | 18 | | 22 | 27 | 27 | 36 | 96 | 100 | |
| 1980 | 9 | 15 | 46 | 57 | | 79 | 91 | 93 | 98 | 100 | | |
| 1990 | 8 | 6 | | | | | 74 | 86 | 97 | 100 | | |
| 1990 | 9 | 4 | | | | | 84 | 90 | 96 | 100 | | |
| 1992 | 8 | 31 | | | | | 81 | 89 | 95 | 100 | | |
| 1993 | 8 | 13 | | | | | 82 | 83 | 94 | 100 | | |
| 1994 | 8 | 4 | 60 | 76 | 89 | 94 | 98 | 99 | 99 | 100 | | |
| 1994 | 9 | 30 | | | | | 85 | 88 | 96 | 100 | | |
| 1997 | 9 | 2 | | | | | 94 | 95 | 98 | 100 | | |
| 1999 | 9 | 17 | | | | | 74 | 77 | 90 | 100 | | |
| | | | | | | | | | **66** | | | |

Table 2 - MEP results for Albuquerque gage and bed-material load estimations

| | | MEP results | | | | | | |
|---|---|---|---|---|---|---|---|---|
| Date | Inst. Discharge (cfs) | Total load | Sand load | Gravel load | d10 bed material | % washload | % bed material load | Bed material load (t/day) |
| 4/10/1978 | 326 | 498 | 177.8 | 0 | 0.16 | 92 | 8 | 40 |
| 4/24/1978 | 329 | 1319.9 | 1075.3 | 71.7 | 0.15 | 31 | 69 | 911 |
| 5/8/1978 | 1420 | 5186.7 | 2984.6 | 0 | 0.14 | 71 | 29 | 1504 |
| 5/22/1978 | 4260 | 69638.5 | 58057.7 | 0 | 0.15 | 36 | 64 | 44569 |
| 5/30/1978 | 2520 | 9891.2 | 6931.3 | 0 | 0.14 | 60 | 40 | 3956 |
| 6/5/1978 | 2810 | 12581.3 | 9882.1 | 0 | 0.17 | 51 | 49 | 6165 |
| 6/26/1978 | 1350 | 3967.6 | 3206.7 | 6.9 | 0.14 | 50 | 50 | 1984 |
| 7/24/1978 | 1040 | 7854.2 | 1099.4 | 0 | 0.14 | 96 | 4 | 314 |
| 4/2/1979 | 1840 | 7402.1 | 6199.2 | 0 | 0.14 | 54 | 46 | 3405 |
| 4/23/1979 | 4980 | 46703.6 | 32668.3 | 63.2 | 0.14 | 47 | 53 | 24753 |
| 5/29/1979 | 6610 | 56805.4 | 45329.2 | 589.6 | 0.17 | 50 | 50 | 28403 |
| 6/18/1979 | 6920 | 47923.7 | 42714.1 | 718 | 0.17 | 42 | 58 | 27796 |
| 7/9/1979 | 6040 | 50108.4 | 47521.4 | 465.8 | 0.15 | 31 | 69 | 34575 |
| 4/7/1980 | 926 | 632.5 | 535 | 0 | 0.18 | 60 | 40 | 253 |
| 4/28/1980 | 4730 | 44563.5 | 40624.3 | 586 | 0.2 | 41 | 59 | 26292 |
| 5/12/1980 | 6900 | 101837.1 | 39079.1 | 130.8 | 0.13 | 32 | 68 | 69249 |
| 6/9/1980 | 6610 | 94407.8 | 36004.9 | 170.2 | 0.14 | 22 | 78 | 73638 |
| 4/20/1981 | 641 | 382.7 | 311.3 | 0 | 0.15 | 62 | 38 | 145 |
| 6/22/1981 | 694 | 1223 | 813.7 | 0 | 0.15 | 58 | 42 | 514 |
| 7/27/1981 | 584 | 1527.7 | 506.4 | 0 | 0.15 | 94 | 6 | 92 |
| 4/26/1982 | 1740 | 12907.8 | 11471.2 | 0 | 0.16 | 21 | 79 | 10197 |
| 5/3/1982 | 3350 | 15377.6 | 10182.8 | 0 | 0.13 | 62 | 38 | 5843 |
| 5/24/1982 | 4280 | 15493.5 | 11800.8 | 15 | 0.12 | 47 | 53 | 8212 |
| 6/7/1982 | 4570 | 14722.7 | 12313.3 | 52 | 0.17 | 55 | 45 | 6625 |
| 6/21/1982 | 3480 | 7363.3 | 6331.5 | 6.8 | 0.25 | 81 | 19 | 1399 |
| 7/7/1982 | 1100 | 944.3 | 746.8 | 0.2 | 0.18 | 60 | 40 | 378 |
| 7/26/1982 | 159 | 42.4 | 18 | 0 | 0.19 | 90 | 10 | 4 |
| 4/3/1984 | 1350 | 1600.6 | 1250.6 | 12 | 0.048 | | 100 | 1601 |
| 4/24/1984 | 4270 | 16901.2 | 13834.9 | 0 | 0.12 | 52 | 48 | 8113 |
| 5/8/1984 | 4440 | 20624.1 | 17745.6 | 0 | 0.14 | 43 | 57 | 11756 |
| 7/10/1984 | 396 | 232.4 | 93.8 | 0 | 0.19 | 84 | 16 | 37 |
| 5/15/1985 | 7170 | 21145.9 | 15792.6 | 0 | 0.039 | | 100 | 21146 |
| 6/17/1985 | 3620 | 2060 | 1568.9 | 0 | 0.26 | 99 | 1 | 21 |
| 5/6/1986 | 2430 | 4713.4 | 4334.6 | 10.2 | 0.16 | 41 | 59 | 2781 |
| 5/20/1986 | 2300 | 3625.9 | 3274 | 37.7 | 0.2 | 60 | 40 | 1450 |
| 6/3/1986 | 3440 | 9018.5 | 8383 | 11.4 | 0.15 | 40 | 60 | 5411 |
| 6/30/1986 | 3320 | 5074.7 | 3089.8 | 0 | 0.24 | 95 | 5 | 254 |
| 5/11/1988 | 1800 | 6156.2 | 2448.1 | 0 | 0.046 | 94 | 6 | 369 |
| 5/8/1990 | 1950 | 2721.4 | 2022.2 | 1.7 | 0.065 | 74 | 26 | 708 |

Table 2 - MEP results for Albuquerque gage and bed-material load estimations

| | | MEP results | | | | | | |
|---|---|---|---|---|---|---|---|---|
| Date | Inst. Discharge (cfs) | Total load | Sand load | Gravel load | d10 bed material | % washload | % bed material load | Bed material load (t/day) |
| 7/2/1990 | 570 | 380 | 240.4 | 0 | 0.19 | 95 | 5 | 19 |
| 4/4/1991 | 1490 | 2590.6 | 2128.5 | 0 | 0.18 | 69 | 31 | 803 |
| 4/10/1991 | 2130 | 18967.7 | 17698 | 20.9 | 0.3 | 35 | 65 | 12329 |
| 4/22/1991 | 3060 | 4027 | 2628.7 | 9 | 0.1 | 86 | 14 | 564 |
| 6/3/1991 | 3590 | 15609.6 | 11825 | 2152 | 0.16 | 45 | 55 | 8585 |
| 7/2/1991 | 2470 | 4588.4 | 3182.9 | 0 | 0.18 | 85 | 15 | 688 |
| 7/10/1991 | 401 | 335.8 | 220.7 | 0 | 0.24 | 53 | 47 | 158 |
| 6/18/1992 | 2610 | 9164.3 | 7276.8 | 985.4 | 0.042 | | 100 | 9164 |
| 6/29/1992 | 853 | 2162.6 | 2024.2 | 0 | 0.24 | 19 | 81 | 1752 |
| 7/31/1992 | 801 | 3884.5 | 3509.8 | 1.5 | 0.18 | 15 | 85 | 3302 |
| 4/1/1994 | 1370 | 1191.1 | 947.9 | 7.6 | 0.29 | 84 | 16 | 191 |
| 5/2/1994 | 3300 | 5670.8 | 4495.7 | 48.1 | 0.25 | 70 | 30 | 1701 |
| 6/13/1994 | 5030 | 4493.5 | 3129.8 | 0 | 0.074 | 67 | 33 | 1483 |
| 6/27/1994 | 4860 | 11452.3 | 10331.9 | 18 | 0.2 | 54 | 46 | 5268 |
| 5/5/1995 | 3980 | 11194 | 9148.1 | 6.1 | 0.26 | 65 | 35 | 3918 |
| 5/24/1995 | 6400 | 19248.6 | 16235 | 63.7 | 0.26 | 65 | 35 | 6737 |
| 6/6/1995 | 4960 | 16225.7 | 14723.8 | 200.5 | 0.29 | 45 | 55 | 8924 |
| 7/3/1995 | 5620 | 25603.1 | 21572.6 | 2069.4 | 0.26 | 31 | 69 | 17666 |
| 4/5/1996 | 437 | 1494.9 | 1454.8 | 0 | 0.21 | 6 | 94 | 1405 |
| 5/3/1996 | 471 | 734.3 | 691.2 | 0 | 0.19 | 12 | 88 | 646 |
| 6/20/1996 | 572 | 282.8 | 189.4 | 0 | 0.22 | 80 | 20 | 57 |
| 4/4/1997 | 2090 | 14852.7 | 12854.9 | 0 | 0.16 | 28 | 72 | 10694 |
| 6/3/1997 | 5040 | 54393.6 | 34813.5 | 247.4 | 0.26 | 30 | 70 | 38076 |
| 5/5/1998 | 3180 | 8875.1 | 7447.3 | 6.5 | 0.20 | 62 | 38 | 3373 |
| 6/3/1998 | 3540 | 27598 | 26510.6 | 47 | 0.25 | 48 | 52 | 14351 |
| 4/27/1999 | 969 | 1031.9 | 669.6 | 0.1 | 0.25 | 93 | 7 | 72 |
| 5/24/1999 | 4080 | 14002.3 | 11851 | 152.6 | 0.21 | 60 | 40 | 5601 |
| 8/7/1978 | 817 | 2504.4 | 902.9 | 0 | 0.13 | 90 | 10 | 250 |
| 8/22/1978 | 559 | 1075.7 | 397.8 | 0 | 0.14 | 94 | 6 | 65 |
| 8/13/1979 | 588 | 1160.1 | 549.9 | 0 | 0.16 | 69 | 31 | 360 |
| 9/10/1979 | 521 | 539.3 | 362.4 | 0 | 0.16 | 87 | 13 | 70 |
| 8/18/1980 | 377 | 633.5 | 483.1 | 0 | 0.16 | 30 | 70 | 443 |
| 9/15/1980 | 447 | 393.6 | 126.2 | 0 | | | | |
| 8/24/1981 | 260 | 1484.8 | 421.6 | 0 | 0.14 | 95 | 5 | 74 |
| 8/6/1990 | 415 | 220.6 | 89.1 | 0 | 0.25 | 97 | 3 | 7 |
| 9/4/1990 | 267 | 84.8 | 34.4 | 0 | 0.18 | | | |
| 8/31/1992 | 1070 | 1153.8 | 333.8 | 0 | 0.21 | 94 | 6 | 69 |
| 8/13/1993 | 536 | 413.4 | 191.6 | 0 | 0.25 | 94 | 6 | 25 |
| 8/4/1994 | 588 | 2807.3 | 179.4 | 0 | 0.18 | 99 | 1 | 28 |
| 9/30/1994 | 383 | 155.1 | 55 | 0 | 0.12 | 87 | 13 | 20 |

Table 2 - MEP results for Albuqueruqe gage and bed-material load estimations

| | | MEP results | | | | | | |
|---|---|---|---|---|---|---|---|---|
| Date | Inst. Discharge (cfs) | Total load | Sand load | Gravel load | d10 bed material | % washload | % bed material load | Bed material load (t/day) |
| 9/2/1997 | 774 | 1355.1 | 335.1 | 0 | 0.27 | 98 | 2 | 27 |
| 9/17/1999 | 1080 | 980.3 | 615.3 | 0.7 | 0.27 | 91 | 9 | 88 |
| | | | Average (spring) | | 0.175 | 57 | | |
| | | | Average (summer) | | 0.187 | 87 | | |